

NCDOT
2011-09



Final Report

**Recommendations for Placement of Cable
Median Barriers on 6:1 and 4:1 Sloped
Medians with Horizontal Curvatures**

Prepared By

Howie Fang
Ning Li
Matthew DiSogra
Matthew Gutowski

Department of Mechanical Engineering & Engineering Science

and

David C. Weggel

Department of Civil and Environmental Engineering

The University of North Carolina at Charlotte
Charlotte, NC 28223-0001

September 15, 2012

Technical Report Documentation Page

1. Report No. FHWA/NC/2011-09	2. Government Accession No.	3. Recipient's Catalog No.	
4. Title and Subtitle Recommendations for Placement of Cable Median Barriers on 6:1 and 4:1 Sloped Medians with Horizontal Curvatures		5. Report Date September 15, 2012	
		6. Performing Organization Code	
7. Author(s) Howie Fang, David Weggel, Ning Li, Matt DiSogra, Matt Gutowski		8. Performing Organization Report No.	
9. Performing Organization Name and Address The University of North Carolina at Charlotte 9201 University City Boulevard Charlotte, NC 28223-0001		10. Work Unit No. (TRAIS)	
		11. Contract or Grant No.	
12. Sponsoring Agency Name and Address North Carolina Department of Transportation Research and Analysis Group 1 South Wilmington Street Raleigh, North Carolina 27601		13. Type of Report and Period Covered Final Report 08/16/2010 – 08/15/2012	
		14. Sponsoring Agency Code 2011-09	
Supplementary Notes:			
16. Abstract <i>This report summarizes the research efforts of using finite element modeling and simulations to evaluate the performance of generic low-tension cable median barriers (CMBs) on four-lane and six-lane freeways with a 46-foot median, horizontal curvature, and 6:1 and 4:1 median slopes. A literature review is included on the performance evaluation of CMBs and applications of finite element modeling and simulations in roadside safety research. The modeling and simulation work is presented on a CMB with vehicular impacts of a 1996 Dodge Neon and a 2006 Ford F250 at 62.1 mph (100 km/hr). The placement of CMB at 4, 6, and 8 ft (1.22, 1.83, and 2.44 m) from the median centerline was evaluated under vehicular impacts at three departure angles (20°, 25°, and 30°).</i> <i>The simulation results show that the current NCDOT CMB meets the Test Level 3 (TL-3) requirements of MASH when placed at 4 ft (1.22 m) from the median centerline on the 6:1 slope of a four-lane freeway. The backside impacts to the CMB placed at 8 ft (2.44 m) from the median centerline on the 6:1 slope of a four-lane freeway only partially engages the vehicle, which allows the vehicle to enter the opposing travel lane before being redirected or stopped.</i> <i>Compared to the CMB on a four-lane freeway, the CMB placement at 8 ft (2.44 m) from the median centerline on a six-lane freeway has reduced performance in both the front-side and backside impacts by the Ford F250 for TL-3 requirements of MASH. For the tested impacts with a Dodge Neon, the CMB on the 6:1 slope of the six-lane freeway has similar performance to that of a four-lane freeway on the 6:1 slope.</i> <i>Based on the simulation results, placing the CMB at 6 ft (1.83 m) from the median centerline on a 4:1 slope of a six-lane freeway is not recommended.</i> <i>The use of finite element simulations in this project is shown to be both effective and efficient and thus recommended for future investigations of other research topics.</i>			
17. Key Words <i>Cable barrier; Median barrier; Horizontal curvature; Roadside safety; Highway safety; Finite element method</i>		18. Distribution Statement	
19. Security Classif. (of this report) Unclassified	20. Security Classif. (of this page) Unclassified	21. No. of Pages 108	22. Price

DISCLAIMER

The contents of this report reflect the views of the authors and not necessarily the views of the university. The authors are responsible for the facts and the accuracy of the data presented herein. The contents do not necessarily reflect the official views or policies of either the North Carolina Department of Transportation or the Federal Highway Administration. This report does not constitute a standard, specification, or regulation.

ACKNOWLEDGMENTS

This study was supported by the North Carolina Department of Transportation (NCDOT) under Research Project No. 2011-09. The authors greatly appreciate the support of NCDOT personnel from the *Roadway Design Unit, Division of Transportation Mobility & Safety, Highway Division 5, FHWA – NC Division*, and the *Research and Development Unit* for their support and cooperation during the grant period.

The authors would like to thank the undergraduate students at UNC Charlotte, Sean Cary, Matthew McClelland, and Caitlin Nicolas who helped with generating the plots, figures, and animation videos of the simulation results. These three students were offered undergraduate research assistantships using the research funds of this project.

EXECUTIVE SUMMARY

This report summarizes the research efforts of using finite element modeling and simulations to evaluate the performance of generic low-tension cable median barriers (CMBs) on four-lane and six-lane freeways with a 46-foot median, horizontal curvature, and 6:1 and 4:1 median slopes. A literature review is included on the performance evaluation of CMBs and applications of finite element modeling and simulations in roadside safety research. The modeling and simulation work is presented on a CMB with vehicular impacts of a 1996 Dodge Neon and a 2006 Ford F250 at 62.1 mph (100 km/hr). The placement of CMB at 4, 6, and 8 ft (1.22, 1.83, and 2.44 m) from the median centerline was evaluated under vehicular impacts at three departure angles (20°, 25°, and 30°).

The simulation results show that the current NCDOT CMB meets the Test Level 3 (TL-3) requirements of MASH when placed at 4 ft (1.22 m) from the median centerline on the 6:1 slope of a four-lane freeway. The backside impacts to the CMB placed at 8 ft (2.44 m) from the median centerline on the 6:1 slope of a four-lane freeway only partially engages the vehicle, which allows the vehicle to enter the opposing travel lane before being redirected or stopped.

Compared to the CMB on a four-lane freeway, the CMB placement at 8 ft (2.44 m) from the median centerline on a six-lane freeway has reduced performance in both the front-side and backside impacts by the Ford F250 for TL-3 requirements of MASH. For the tested impacts with a Dodge Neon, the CMB on the 6:1 slope of the six-lane freeway has similar performance to that of a four-lane freeway on the 6:1 slope.

Based on the simulation results, placing the CMB at 6 ft (1.83 m) from the median centerline on a 4:1 slope of a six-lane freeway is not recommended.

The use of finite element simulations in this project is shown to be both effective and efficient and thus recommended for future investigations of other research topics.

TABLE OF CONTENTS

Title Page	i
Technical Report Documentation Page	ii
Disclaimer	iii
Acknowledgments	iv
Executive Summary	v
Table of Contents	vi
List of Tables	vii
List of Figures	viii
1. Introduction	1
1.1 Background	2
1.2 Research Objectives and Tasks	3
2. Literature Review	6
2.1 Performance Evaluation of Cable Barriers	6
2.2 Crash Modeling and Simulations	11
3. Finite Element Modeling of Vehicles and the CMB	18
3.1 FE Models of a Passenger Car and Pick-up Truck	18
3.2 FE Model of the CMB on Curved Median	18
3.3 Simulation Setup	20
4. Simulation Results and Analysis	22
4.1 Case 1: CMB on 6:1 Slope of Four-lane Freeway	22
4.2 Case 2: CMB on 6:1 Slope of Four-lane Freeway – Retrofit Design	34
4.3 Case 3: CMB on 6:1 Slope of Six-lane Freeway	37
4.4 Case 4: CMB on 4:1 Slope of Six-lane Freeway	52
5. Findings and Conclusions	55
6. Recommendations	57
7. Implementation and Technology Transfer Plan	58
References	59
Appendix A. Time history of vehicle traversal velocity	66

List of Tables

Table 2.1: Some major changes from NCHRP Report 350 to MASH

Table 3.1: Categories of simulation work

Table 4.1: Simulation results of Dodge Neon impacting the NCDOT CMB on a four-lane freeway

Table 4.2: Simulation results of a Ford F250 impacting the NCDOT CMB on a four-lane freeway

Table 4.3: Simulation results of vehicle impacting the retrofit CMB on a four-lane freeway

Table 4.4: Simulation results of Dodge Neon impacting the NCDOT CMB on a six-lane freeway

Table 4.5: Simulation results of Ford F250 impacting the NCDOT CMB on a six-lane freeway

Table 4.6: Simulation results of vehicle impacting the NCDOT CMB on a six-lane freeway

List of Figures

- Fig. 1.1: In-service three-strand, low-tension cable median barriers in North Carolina
- Fig. 1.2: Vehicles impacting a CMB at different angles on a median with horizontal curvature
- Fig. 1.3: FE model of a CMB placed on a median with horizontal curvature
- Fig. 1.4: Finite element models of a CMB and test vehicles
- Fig. 1.5: Cable heights in the current NCDOT CMB design
- Fig. 1.6: Median configuration for a CMB placed on the sloped median of a four-lane freeway
- Fig. 1.7: Median configuration for a CMB placed on the sloped median of a six-lane freeway
-
- Fig. 3.1: FE simulations of a Dodge Neon and a Ford F250 crossing a sloped median
- Fig. 3.2: Post geometry and cable positions of the CMB in the current NCDOT design
- Fig. 3.3: Placement of a CMB on a four-lane divided freeway with horizontal curvature
- Fig. 3.4: Definitions of departure and impact angles
- Fig. 3.5: A Ford F250 impacting the CMB by first knocking down the post
-
- Fig. 4.1: A Dodge Neon impacting the CMB placed at 6 ft from the median centerline, 30° backside impact
- Fig. 4.2: A Dodge Neon impacting the CMB placed at 8 ft from the median centerline, 25° backside impact
- Fig. 4.3: A Dodge Neon impacting the CMB placed at 4 ft from the median centerline on the 6:1 slope of a four-lane freeway
- Fig. 4.4: A Dodge Neon impacting the CMB placed at 6 ft from the median centerline on the 6:1 slope of a four-lane freeway
- Fig. 4.5: A Dodge Neon impacting the CMB placed at 8 ft from median centerline on the 6:1 slope of a four-lane freeway
- Fig. 4.6: A Ford F250 impacting the CMB placed at 4 ft from the median centerline, 30° front-side impact
- Fig. 4.7: A Ford F250 impacting the CMB placed at 8 ft from the median centerline, 30° front-side impact
- Fig. 4.8: A Ford F250 impacting the CMB placed at 8 ft from the median centerline, 25° backside impact
- Fig. 4.9: A Ford F250 impacting the CMB placed at 8 ft from the median centerline, 30° backside impact
- Fig. 4.10: A Ford F250 impacting the CMB placed at 4 ft from the median centerline, 30° backside impact

- Fig. 4.11: A Ford F250 impacting the CMB placed at 6 ft from the median centerline, 30° backside impact
- Fig. 4.12: A Ford F250 impacting the CMB placed at 4 ft from the median centerline on the 6:1 slope of a four-lane freeway
- Fig. 4.13: A Ford F250 impacting the CMB placed at 6 ft from the median centerline on the 6:1 slope of a four-lane freeway
- Fig. 4.14: A Ford F250 impacting the CMB placed at 8 ft from the median centerline on the 6:1 slope of a four-lane freeway
- Fig. 4.15: Front-side impact at 25° by a Dodge Neon with the CMB (retrofit) on a four-lane freeway
- Fig. 4.16: Backside impact at 25° by a Dodge Neon with the CMB (retrofit) on a four-lane freeway
- Fig. 4.17: A Ford F250 impacting the CMB (retrofit) at 6 ft from the median centerline, 25° front-side impact
- Fig. 4.18: A Ford F250 impacting the CMB (retrofit) at 8 ft from the median centerline, 25° front-side impact
- Fig. 4.19: A Ford F250 impacting the CMB (retrofit) at 8 ft from the median centerline, 25° backside impact
- Fig. 4.20: Front-side impact at 25° by a Ford F250 with the CMB (retrofit) on a four-lane freeway
- Fig. 4.21: Backside impact at 25° by a Ford F250 with the CMB (retrofit) on a four-lane freeway
- Fig. 4.22: A Dodge Neon impacting the CMB placed at 4 ft from the median centerline, 25° backside impact
- Fig. 4.23: A Dodge Neon impacting the CMB placed at 8 ft from the median centerline, 30° backside impact
- Fig. 4.24: Dodge Neon impacting the CMB placed at 4 ft from the median centerline on the 6:1 slope of a six-lane freeway
- Fig. 4.25: Dodge Neon impacting the CMB placed at 6 ft from the median centerline on the 6:1 slope of a six-lane freeway
- Fig. 4.26: Dodge Neon impacting the CMB placed at 8 ft from the median centerline on the 6:1 slope of a six-lane freeway
- Fig. 4.27: A Ford F250 impacting the CMB placed at 4 ft from the median centerline, 25° front-side impact
- Fig. 4.28: A Ford F250 impacting the CMB placed at 4 ft from the median centerline, 30° front-side impact
- Fig. 4.29: A Ford F250 impacting the CMB placed at 6 ft from the median centerline, 30° front-side impact
- Fig. 4.30: A Ford F250 impacting the CMB placed at 4 ft from the median centerline, 30° backside impact

- Fig. 4.31: A Ford F250 impacting the CMB placed at 6 ft from the median centerline, 20° backside impact
- Fig. 4.32: A Ford F250 impacting the CMB placed at 6 ft from the median centerline, 25° backside impact
- Fig. 4.33: A Ford F250 impacting the CMB placed at 6 ft from the median centerline, 30° backside impact
- Fig. 4.34: A Ford F250 impacting the CMB placed at 8 ft from the median centerline, 20° backside impact
- Fig. 4.35: A Ford F250 impacting the CMB placed at 8 ft from the median centerline, 25° backside impact
- Fig. 4.36: A Ford F250 impacting the CMB placed at 8 ft from the median centerline, 30° backside impact
- Fig. 4.37: A Ford F250 impacting the CMB placed at 4 ft from the median centerline on the 6:1 slope of a six-lane freeway
- Fig. 4.38: Ford F250 impacting the CMB placed at 6 ft from the median centerline on the 6:1 slope of a six-lane freeway
- Fig. 4.39: Ford F250 impacting the CMB placed at 8 ft from the median centerline on the 6:1 slope of a six-lane freeway
- Fig. 4.40: A Ford F250 impacting the CMB placed at 6 ft from the median centerline, 25° front-side impact
- Fig. 4.41: A Ford F250 impacting the CMB placed at 6 ft from the median centerline, 25° backside impact
- Fig. 4.42: A Dodge Neon impacting the CMB placed at 6 ft from the median centerline on the 4:1 slope of a six-lane freeway
- Fig. 4.43: A Ford F250 impacting the CMB placed at 6 ft from the median centerline on the 4:1 slope of a six-lane freeway
-
- Fig. A.1: Front-side impacts by a Dodge Neon on the CMB placed at 4 ft from the median centerline on the outer 6:1 slope of a four-lane freeway
- Fig. A.2: Front-side impacts by a Dodge Neon on the CMB placed at 6 ft from the median centerline on the outer 6:1 slope of a four-lane freeway
- Fig. A.3: Front-side impacts by a Dodge Neon on the CMB placed at 8 ft from the median centerline on the outer 6:1 slope of a four-lane freeway
- Fig. A.4: Backside impacts by a Dodge Neon on the CMB placed at 4 ft from the median centerline on the outer 6:1 slope of a four-lane freeway
- Fig. A.5: Backside impacts by a Dodge Neon on the CMB placed at 6 ft from the median centerline on the outer 6:1 slope of a four-lane freeway
- Fig. A.6: Backside impacts by a Dodge Neon on the CMB placed at 8 ft from the median centerline on the outer 6:1 slope of a four-lane freeway

- Fig. A.7: Front-side impacts by a Ford F250 on the CMB placed at 4 ft from the median centerline on the outer 6:1 slope of a four-lane freeway
- Fig. A.8: Front-side impacts by a Ford F250 on the CMB placed at 6 ft from the median centerline on the outer 6:1 slope of a four-lane freeway
- Fig. A.9: Front-side impacts by a Ford F250 on the CMB placed at 8 ft from the median centerline on the outer 6:1 slope of a four-lane freeway
- Fig. A.10: Backside impacts by a Ford F250 on the CMB placed at 4 ft from the median centerline on the outer 6:1 slope of a four-lane freeway
- Fig. A.11: Backside impacts by a Ford F250 on the CMB placed at 6 ft from the median centerline on the outer 6:1 slope of a four-lane freeway
- Fig. A.12: Backside impacts by a Ford F250 on the CMB placed at 8 ft from the median centerline on the outer 6:1 slope of a four-lane freeway
- Fig. A.13: Front-side impact by a Dodge Neon on the retrofit CMB placed at 6 ft from the median centerline on the outer 6:1 slope of a four-lane freeway
- Fig. A.14: Front-side impact by a Dodge Neon on the retrofit CMB placed at 8 ft from the median centerline on the outer 6:1 slope of a four-lane freeway
- Fig. A.15: Backside impact by a Dodge Neon on the retrofit CMB placed at 6 ft from the median centerline on the outer 6:1 slope of a four-lane freeway
- Fig. A.16: Backside impact by a Dodge Neon on the retrofit CMB placed at 8 ft from the median centerline on the outer 6:1 slope of a four-lane freeway
- Fig. A.17: Front-side impact by a Ford F250 on the retrofit CMB placed at 6 ft from the median centerline on the outer 6:1 slope of a four-lane freeway
- Fig. A.18: Front-side impact by a Ford F250 on the retrofit CMB placed at 8 ft from the median centerline on the outer 6:1 slope of a four-lane freeway
- Fig. A.19: Backside impact by a Ford F250 on the retrofit CMB placed at 6 ft from the median centerline on the outer 6:1 slope of a four-lane freeway
- Fig. A.20: Backside impact by a Ford F250 on the retrofit CMB placed at 8 ft from the median centerline on the outer 6:1 slope of a four-lane freeway
- Fig. A.21: Front-side impacts by a Dodge Neon on the CMB placed at 4 ft from the median centerline on the outer 6:1 slope of a six-lane freeway
- Fig. A.22: Front-side impacts by a Dodge Neon on the CMB placed at 6 ft from the median centerline on the outer 6:1 slope of a six-lane freeway
- Fig. A.23: Front-side impacts by a Dodge Neon on the CMB placed at 8 ft from the median centerline on the outer 6:1 slope of a six-lane freeway
- Fig. A.24: Backside impacts by a Dodge Neon on the CMB placed at 4 ft from the median centerline on the outer 6:1 slope of a six-lane freeway
- Fig. A.25: Backside impacts by a Dodge Neon on the CMB placed at 6 ft from the median centerline on the outer 6:1 slope of a six-lane freeway
- Fig. A.26: Backside impacts by a Dodge Neon on the CMB placed at 8 ft from the median centerline on the outer 6:1 slope of a six-lane freeway
- Fig. A.27: Front-side impacts by a Ford F250 on the CMB placed at 4 ft from the median centerline on the outer 6:1 slope of a six-lane freeway

- Fig. A.28: Front-side impacts by a Ford F250 on the CMB placed at 6 ft from the median centerline on the outer 6:1 slope of a six-lane freeway
- Fig. A.29: Front-side impacts by a Ford F250 on the CMB placed at 8 ft from the median centerline on the outer 6:1 slope of a six-lane freeway
- Fig. A.30: Backside impacts by a Ford F250 on the CMB placed at 4 ft from the median centerline on the outer 6:1 slope of a six-lane freeway
- Fig. A.31: Backside impacts by a Ford F250 on the CMB placed at 6 ft from the median centerline on the outer 6:1 slope of a six-lane freeway
- Fig. A.32: Backside impacts by a Ford F250 on the CMB placed at 8 ft from the median centerline on the outer 6:1 slope of a six-lane freeway
- Fig. A.33: Front-side impact by a Dodge Neon on the CMB placed at 6 ft from the median centerline on the inner 4:1 slope of a six-lane freeway
- Fig. A.34: Backside impact by a Dodge Neon on the CMB placed at 6 ft from the median centerline on the inner 4:1 slope of a six-lane freeway
- Fig. A.35: Front-side impact by a Ford F250 on the CMB placed at 6 ft from the median centerline on the inner 4:1 slope of a six-lane freeway
- Fig. A.36: Backside impact by a Ford F250 on the CMB placed at 6 ft from the median centerline on the inner 4:1 slope of a six-lane freeway

1. Introduction

Roadside barrier systems are important devices to ensure transportation safety. Different types of barriers have been developed over the years including rigid, semi-rigid, and flexible systems. These barriers serve the purpose of safely redirecting vehicles leaving the roadway and/or preventing run-out-of-way vehicles from intruding into oncoming traffic. All barriers used on U.S. highways must be designed and tested to satisfy the requirements specified by the Manual for Assessing Safety Hardware (MASH 2009). Commonly used barrier systems include concrete barriers, W-beam guardrails, and cable barriers. Concrete barriers are rigid systems that have high initial cost yet require less maintenance; however, they are less forgiving in severe crashes. The commonly used W-beam guardrails consist of steel rails mounted on wood or steel posts with end treatments and transitions. The W-beam guardrails are less rigid than concrete barriers and are intended to be sacrificial; therefore, substantial replacement and/or repairs are required after major vehicle crashes. Even low-energy impacts can bend and damage the steel rails and displace posts enough for the barrier to perform poorly in a subsequent crash event. Besides the high cost of maintaining these systems, there are always safety risks to motorists and highway workers.

Cable barriers are flexible and cost-effective barrier systems that are ideal for retrofit designs in existing, relatively wide medians to prevent cross-median crashes. Cable barriers differ from concrete barriers and W-beam guardrails in that they can be installed on sloped terrain and still perform effectively. They are more forgiving when struck by an off-roadway vehicle, because the cables deflect laterally and reduce impact forces transmitted to the vehicle and occupants. The high flexibility of cable barriers, however, requires that the median has sufficient width to allow for lateral cable deflections. For a single-run cable median barrier (CMB), the median is required to have a minimum width of 24 ft, with 12 ft on each side of the cable barrier.

Cross-median collisions are the most severe highway crashes because of their typically high relative velocities (BMI-SG 2004). In the safety studies by Hunter et al. (2001) of the North Carolina Department of Transportation (NCDOT), the investigators performed a before-after comparison by developing several regression models that used a reference population, e.g., freeway locations without CMBs, to predict the number of accidents at locations with CMB treatments. The predicted number of accidents was then compared to the actual number of collisions at sites with CMBs. Although a statistically significant increase was found in the total number of crashes on sections after installing the CMBs, a significant reduction was also found in the number of serious and fatal collisions. These safety studies by NCDOT led to the installation of more CMBs in North Carolina with three-strand CMBs (Fig. 1) the most commonly used. By 2006, cross-median penetrations on CMBs in North Carolina were found to be only 3.6% (Troy 2007).



Fig. 1.1: In-service three-strand, low-tension cable median barriers in North Carolina

In a previously-conducted study (Bi et al. 2010), the generic low-tension CMBs installed on a 6:1 sloped median were evaluated using finite element (FE) simulations. The results of this study confirmed the CMB performance from crash data collected by NCDOT engineers (Troy 2007). The CMB performance on medians with horizontal curvatures and steeper slopes, however, has not been fully investigated. In current practice, CMBs on 4:1 sloped medians are installed eight feet from the ditch centerline. With the presence of superelevation and horizontal curvature, such installation has raised concern. In a previous NCDOT project, the CMB performance on a 4:1 sloped median was evaluated. However, due to time and resource restrictions, horizontal curvatures were not explicitly included in the simulation models. In addition, the CMB performance on 6:1 sloped medians with horizontal curvatures has not been fully evaluated and warrants further investigation. Furthermore, the ongoing project does not investigate the best locations to place the CMBs on such medians.

In this study, full-scale FE simulations were utilized to evaluate the CMB performance on 6:1 and 4:1 sloped medians with horizontal curvatures. Several key factors considered in this investigation include: horizontal curvatures to be explicitly included in FE models, CMB locations (i.e., distance from ditch centerline), vehicle impact speeds and angles, and cable placement on the posts. The effects of median curvatures were investigated for both front- and backside hits. Recommendations for placing CMBs on such medians were made based on evaluation of CMB performance under the above mentioned conditions.

1.1 Background

The CMB performance largely depends on the interaction of cables with the impacting vehicle and is affected by several factors such as the impact angle, impact speed, median slope, and impact side (i.e., front or back). Horizontal curvatures and median slopes strongly affect the vehicle-cable interaction and could dramatically change the CMB performance if it is not properly installed with due consideration given to these factors. The situation is further complicated when consideration is given to vehicle impacts occurring on both sides of the CMB.

One of the major issues with horizontal curvature is that the angle of an errant vehicle impacting the CMB could be very different from the angle at which the vehicle leaves the roadway. Figure 2 schematically illustrates this situation in which two vehicles leave the roadway at the same angle with respect to the normal travel directions. The impact angle of Vehicle 1 is typically larger than the angle at which the vehicle leaves the roadway, while the impact angle of Vehicle 2 is typically smaller. In this case, the impact severity of Vehicle 1 would be greater than that of Vehicle 2, and the placement of the CMB in the median should take into account this difference. The situation is further complicated when different impact velocities and angles are considered. These issues

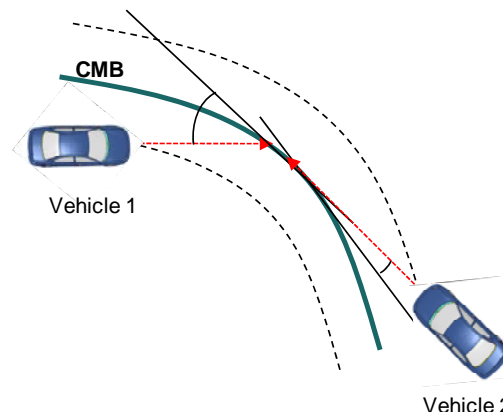


Fig. 1.2: Vehicles impacting a CMB at different angles on a median with horizontal curvature

need to be fully researched before an appropriate installation can be decided. Recommendations for CMB placement on sloped medians with horizontal curvatures are of practical importance in transportation safety.

1.2 Research Objectives and Tasks

The objective of the proposed research is to use full-scale FE simulations to: 1) investigate the CMB performance under different impact conditions on 6:1 and 4:1 sloped medians with horizontal curvatures; and 2) based on the performance evaluations, develop guidelines for placing CMBs on 6:1 and 4:1 sloped medians with horizontal curvatures.

In this study, full-scale FE simulations were utilized to develop guidelines for placing CMBs on 6:1 and 4:1 sloped medians with horizontal curvatures. Available crash data were collected and used to validate the simulation models. Factors considered in the simulations include:

- 1) CMB location on the median;
- 2) the vehicle's initial impact speed;
- 3) the vehicle's impact angle or the angle of the vehicle leaving the roadway;
- 4) impact side (front-side or backside).

Figure 1.3 shows the CMB model placed on a 4:1 sloped median with a horizontal curvature. A computer program was developed to generate the CMB models with other median slopes and CMB placements.

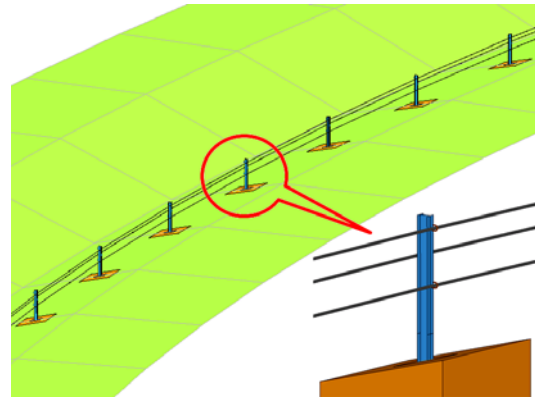


Fig. 1.3: FE model of a CMB placed on a median with horizontal curvature

Task 1: Literature Review and Data Collection

The objective of this task is to review literature on crash testing, modeling, and simulations that are particularly related to CMBs to assist model validation and crash simulations. Literature on median barrier placement with horizontal curvature was searched, collected, and reviewed. The FE models of vehicles and the NCDOT CMB were obtained from previous NCDOT research projects, as shown in Fig. 1.4 These models were modified and combined for simulations on 6:1 and 4:1 sloped medians with horizontal curvatures.

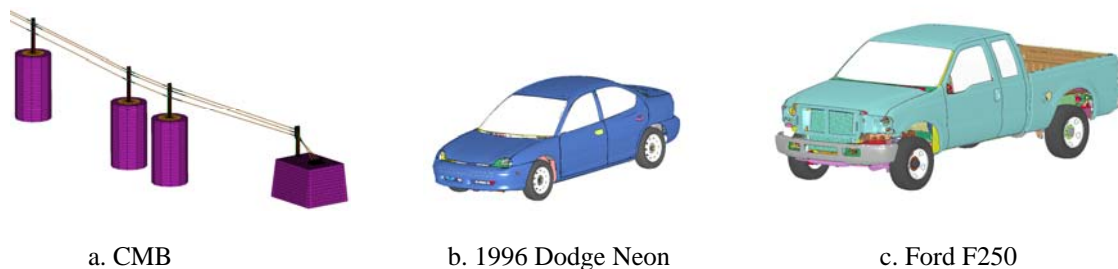
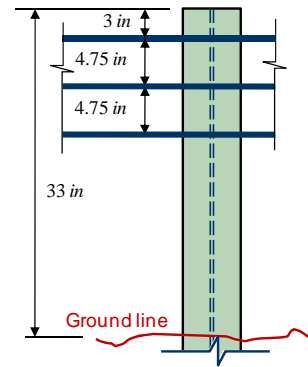


Fig. 1.4: Finite element models of the CMB and test vehicles

Task 2: Development of CMB Models for 6:1 and 4:1 Medians with Horizontal Curvatures

In this task, the FE model of the CMB was generated for both 6:1 and 4:1 sloped medians with horizontal curvatures. The current NCDOT CMB design, as shown in Fig. 1.5, was adopted in all the simulation models. FE models of the curved CMB on a curved median and an impacting vehicle were combined to form the simulation models.

In this study, one initial impact velocity, (62.1 mph or 100 km/hr) and three impact angles (20°, 25°, and 30°) were used. Both the Dodge Neon and Ford F250 models were used in the impact velocity-angle matrix of simulations. Several locations to place the CMB were determined on both the 6:1 and 4:1 sloped medians.



Current NCDOT CMB design

Fig. 1.5: Cable heights in the current NCDOT CMB design

Task 3: Investigation of CMB Performance under Different Impact and Median Conditions

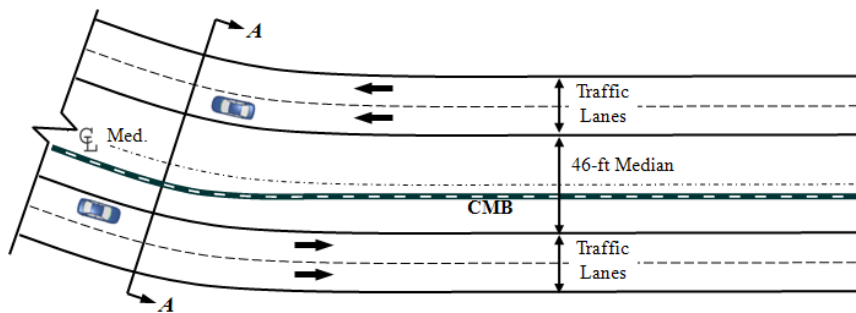
In this task, CMB performance on 6:1 and 4:1 sloped medians with horizontal curvatures was investigated for both front-side and backside impacts. Figures 1.6 and 1.7 schematically illustrate the configurations of the 6:1 and 4:1 sloped medians, respectively.

Task 4: Development of Guidelines for CMB Placement

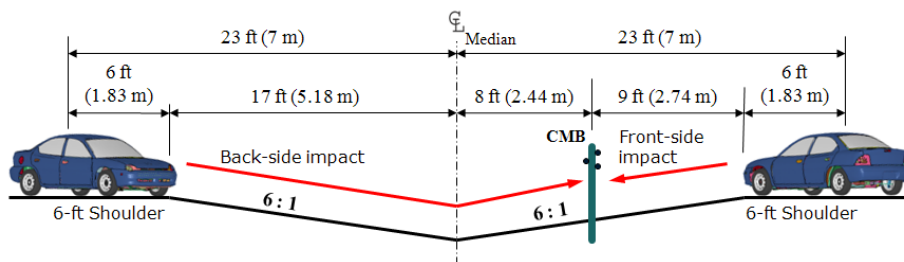
The results of the FE simulations in Task 3 were analyzed to thoroughly understand the CMB performance on 6:1 and 4:1 sloped medians with horizontal curvatures. Recommendations were made to help determine the best installation strategy on such medians with consideration given to a range of impact angles, types of vehicles and both sides of barrier impact.

Task 5: Final Report

The final project report provides a comprehensive summary of research activities, findings, and outcomes of this project. It synthesizes literature review, FE modeling efforts, simulation results, and will provide guidance for the placement of CMBs on medians with horizontal curvatures.

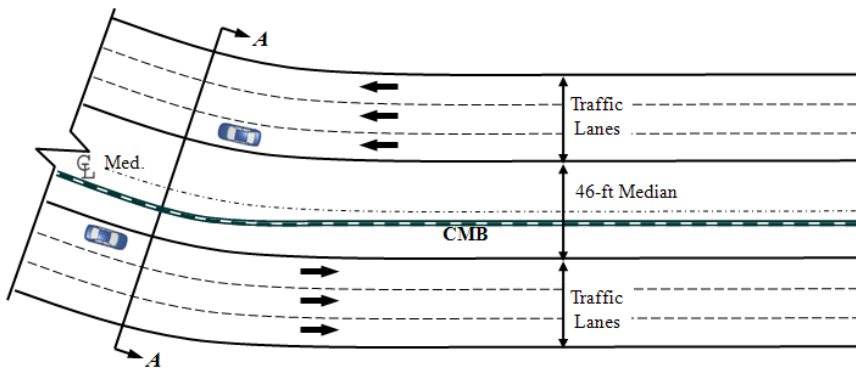


a. 46-ft median of a four-lane freeway

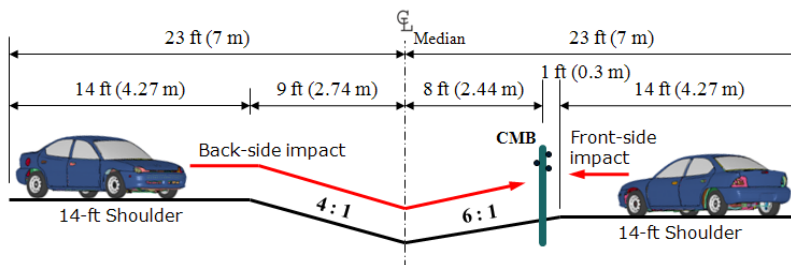


b. Section A-A.

Fig. 1.6: Median configuration for a CMB placed on the sloped median of a four-lane freeway



a. 46-ft median of a six-lane freeway



b. Section A-A

Fig. 1.7: Median configuration for a CMB placed on the sloped median of a six-lane freeway

2. Literature Review

Cable barriers have been used since the 1960s for vehicle containment. In the 1980s, some state DOTs started using modified cable rails as median barriers. Today, the majority of U.S. states have installed cable barriers in highway medians. In this section, a comprehensive summary is provided on studies related to CMBs and other guardrail systems. The topics cover performance evaluation (in-service and crash testing) and the application of finite element analysis (FEA) to highway safety research.

2.1 Performance Evaluation of Cable Barriers

Early in the 1960s, New York State pioneered the development of weak-post barrier systems through analytical models and full-scale vehicle crash testing. In 1965, the state guardrail and median barrier standards were changed to include only weak-post barriers. In the early 1970s, a study was performed to evaluate the field performance of the older strong-post barriers and newly developed weak-post barriers based on accident data collected in New York State from 1967 to 1970 (Zweden and Bryden 1977). Statistical analysis was performed to compare the performance of the investigated barriers based on occupant injury, vehicular responses, and after-impact maintenances. This study generated a number of significant conclusions on the performance of weak- and strong-post barriers. Although there was no significant difference in fatality rates between the two barriers, weak-post barriers exhibited a combined fatality/serious injury rate significantly lower than the strong-post barriers. The resulting occupant injury appeared to be linked to barrier stiffness since the cable barriers (both strong and weak post versions) had lower injury severity rates, while the stiffer median barriers had the highest injury rates. With respect to barrier penetration, the weak-post barriers demonstrated a lower penetration rate than the strong-post barriers (with the exception of the W-beam), which may be due to the lack of consistency between early strong-post barrier designs. The study also indicated that barrier penetrations for the weak-post systems typically resulted from low cable heights. Barrier end terminals (the first or last 50 ft of the barrier) were observed to have higher penetration rates than their midsection counterparts and resulted in higher serious injury rates. Barrier damages were linked to their stiffness; however, weak-post barriers on average were less expensive to repair than strong-post barriers despite the former's longer damage lengths.

In the early 1980's, there were significant changes in vehicle designs with smaller and lighter vehicles constituting a large portion of road traffic. A study was initiated by the New York State DOT in 1983 to determine how impact severity on traffic barriers was affected by vehicle sizes and weights, barrier types and mounting heights, and roadway features (Hiss and Bryden 1992). Several conclusions were drawn regarding the performance of cable barriers, W-beams, and box-beam guardrails. For example, injuries were found to be insensitive for cable barriers with rail heights over 24 in. (0.61 m). For cable and W-beam median barriers, however, the sample sizes were too small to assess their performance due to their limited use and exposure to possible accidents.

Ross et al. (1984) investigated the performance of longitudinal barriers placed on sloped terrain using both crash tests and computer simulations by the highway vehicle object

simulation model (HVOSM). In the study, they determined typical conditions to place longitudinal barriers on sloped terrain and evaluated the behavior of widely used barrier systems. Guidelines were developed for the selection and placement of barriers on sloped terrain. It was found from the study that W-beam and thrie-beam guardrails were more sensitive to the terrain slopes than cable barriers. In the study conducted by Ross et al. (1993), uniform procedures were developed for evaluating the safety performance of candidate roadside hardware systems, including longitudinal barriers, crash cushions, breakaway supports, truck-mounted attenuators, and work zone traffic control devices. The report from this study, the NCHRP Report 350, was adopted as the standard guideline for evaluating the safety performance of roadside safety devices. The evaluation of safety devices was facilitated through three main criteria: 1) structural adequacy; 2) occupant risk; and 3) post-impact trajectory. Structural adequacy refers to how well the device performed its intended tasks (i.e., a guardrail preventing a vehicle from striking a shielded object). The occupant risk criteria attempted to quantify the potential for severe occupant injury. The post-impact vehicle trajectory ensured that the device would not cause subsequent harm (i.e., a vehicle being redirected back into the travel lane). The guideline recognized the infinite number of roadside hardware installations and crash configurations; therefore, standardized installations and practically representative impact scenarios were used to provide a basis for comparing the performance of similar devices. Of particular note was the multi-service-level concept that provides six different test levels to allow for more or less stringent performance evaluations (ideally depending on the ultimate usage/placement of the hardware).

With respect to cross-median crashes, the Manual for Assessing Safety Hardware (MASH) (MASH-1 2009) is currently the standard for testing median barriers. MASH originated from the NCHRP Project 22-14(02) in which NCHRP Report 350 was revised on test vehicles, impact conditions, and the evaluation criteria. Table 2.1 shows some major updates in MASH compared to NCHRP Report 350.

Table 2.1: Some major changes from NCHRP Report 350 to MASH

Item	NCHRP 350	MASH
Small test vehicle	820C (1,800 lbs.)	1100C (2,420 lbs.)
Impact angle for small test vehicle	20°	25°
Light pick-up truck test vehicle	2000P (4,400 lbs.)	2270P (5,000 lbs.)
Single unit truck	8000 kg	10,000 kg
Impact speed for TL-4 single unit truck	80 km/hr	90 km/hr
Impact angle for gating terminals & crash cushions	15°	5°
Maximum roll and pitch angles	N/A	75°
Cable tension	N/A	Recommended at 37.8°C (100°F)

Although six different test levels are specified in the report, the warrants for devices meeting an individual test level is outside the scope of the document and left to the judgment of the transportation agency implementing the hardware. Generally, however, devices tested to the lower test levels (1 and 2) are used on lower volume, lower speed roadways, while devices tested to higher levels (3 to 6) are typically used on larger volume, higher speed roadways.

In the early 1990's, the Traffic Engineering Branch of NCDOT conducted a study (Lynch et al. 1993) of accidents on North Carolina's interstate highways in which vehicles crossed

medians and entered opposing travel lanes. The study analyzed accidents that occurred during the period from April 1, 1988 to October 31, 1991. The objectives of this study were to identify interstate locations with unusually high cross-median accidents, to determine possible safety improvements, to develop a priority listing of these locations with recommended improvements, and to develop a model for identifying potentially dangerous locations on North Carolina interstate highways. Data collected in the study showed that 751 cross-median crashes took place in North Carolina and resulted in 105 fatalities. These crashes represented three percent of the total crashes but 32 percent of the total fatalities on interstate highways during the study period. One of the outcomes of this study was the recommendation to construct median barriers along 24 sections of interstate highways in North Carolina.

In a subsequent safety study, Hunter et al. (2001) evaluated three-strand CMBs installed on a nine-mile stretch on interstate freeway I-40 in North Carolina. Data extracted from the Highway Safety Information System was from 1990 to 1997 and a before-after comparison was made by developing several regression models that used a reference population (e.g., all freeway locations without CMBs) to predict the number of accidents at locations with CMB treatments. The predicted number of accidents was then compared to the actual number of collisions at sites with CMBs. Although a statistically significant increase was found in the total number of crashes on sections after the installation of CMBs, a significant reduction was also found in the number of serious and fatal collisions. These safety studies by NCDOT “provided a great deal of momentum” towards the installation of more barriers in North Carolina (Stasburg and Crawley 2005), with three-strand CMBs the most commonly used median barriers. North Carolina had approximately 550 miles (885 km) of low-tension CMBs by year 2006, with only 3.6% of the impacts resulting in cross-median penetrations (Troy 2007).

In 2010, Hu and Donnell (2010) utilized a nested logit model to estimate crash severity using crash data from rural divided highways in North Carolina. Vehicle, driver, roadway, barrier placement and median cross-section were considered in the model. The research results showed that the collision with a CMB reduced the possibility of severe crashes, and that steeper median slopes increased the possibility of severe crashes. Stine et al. (2010) ran thousands of simulations using CarSIM to investigate the safety of earth-divided rural highway medians without barriers. They claimed that flatter median slopes decreased the possibility of vehicle rollovers, but increased the possibility of crossing the medians.

A similar conclusion on the effectiveness of CMBs was also reported by Oregon DOT. Following three fatalities from a cross-median accident in 1996, the Oregon DOT installed CMBs along a section of I-5 to reduce the potential of future occurrences. Sposito and Johnston (1999) evaluated the cost-effectiveness of this system in preventing cross-median crashes. By comparing frequency/severity data from pre- and post-installations, the CMBs were found to reduce both the fatality rate and susceptibility of cross-median collisions. The study also indicated that the number of accidents with minor injuries increased from 0.7 to 3.8 per year since the barrier installation. Based on a cost-analysis including maintenance cost, the annual cost of CMBs was found to always be less than those of concrete median barriers. The report showed that the cost-effectiveness of CMBs in reducing cross-median

crashes was in agreement with similar studies performed in North Carolina, Iowa, and New York.

In the early 1990's, the Washington State DOT (WSDOT) started installing the U.S. generic low-tension CMBs on medians wider than 32 ft (9.75 m). Subsequently, the WSDOT sponsored crash tests to evaluate the performance of this barrier system in accordance with the NCHRP Report 350. In the two crash tests (Bullard and Menges 1996, 2000), the vehicles were contained by the cables and brought to a stop with relatively minor damages and the occupant risk values were within the preferred limits set by the NCHRP Report 350 (Albin et al. 2001).

Cable barriers in Washington State successfully restrained 95 percent of errant vehicles without involving a second vehicle (WSDOT 2006). By comparison, W-beam guardrails and concrete barriers only restrained 67 to 75 percent of errant vehicles without involving a second vehicle in the crash. From 1990 to 2008, WSDOT had installed 181 miles of cable barriers on Washington's highways. Despite the overall increased number of collisions, serious injuries from highway crashes were reduced by nearly 59 percent while the vehicle miles increased by 29 percent. It was also reported that the annual cross-median collisions decreased by 61 percent. Based on WSDOT's data, CMBs were more likely to contain vehicles than concrete barriers. In addition, CMBs reduced the rollover collisions by approximately 28 percent.

Despite the statewide success of CMBs, the public had strong concerns about the increasing number of crashes and cross-median collisions on I-5 in Marysville, WA. As a result, the WSDOT (2006) conducted a comprehensive review of traffic safety on I-5 in Marysville from 1999 through 2004. This study showed that the cross-median penetrations occurred where the CMB was placed within five feet from the bottom of the ditch, which caused the vehicle's suspension to be compressed right after crossing the bottom of the ditch. Consequently, the vehicle was not able to engage with the cables, particularly the bottom cable, and thus under-rode the CMB. While recommending the continuous use of CMBs, a few suggestions were also made for future research including placement of CMBs on sloped medians and CMB anchor designs (MacDonald and Batiste 2007).

Ray and McGinnis (1997) provided a synthesis of information regarding the use of guardrails and median barriers in the U.S. and their performance with respect to the testing standards specified by the NCHRP Report 350. Comprehensive background information was provided for the evolution of testing procedures, selection and placement procedures, and in-service evaluation of longitudinal and median barriers. The notable advantages of steel-post cable barriers, as indicated in the report, were their compliance to the TL-3 of NCHRP Report 350, inexpensive installation, minimized sight distance problems, reduced occupant forces in the event of a collision, and reduced snow drifting and accumulation. Disadvantages of this system included periodic monitoring of cable tensions, a large clear area for barrier deflections, and increased barrier damage in the event of a collision.

Using data collected in Connecticut, Iowa, and North Carolina from 1997 to 1999, Ray and Weir (2001) performed an in-service performance evaluation of four guardrail systems: the

G1 cable barriers, G2 weak-post W-beams, and the G4-1S and G4-1W strong-post W-beams. The study particularly focused on estimating the number of unreported collisions and the true distribution of occupant injuries. The performance was evaluated in terms of collision characteristics, occupant injury, and barrier damage. With the limited data samples collected in the study, no statistically significant difference was found on performance of the guardrails in the three states, and there was no significant performance difference between the G1 and G2 and between the G1 and G4-1W. However, occupant injuries were less common in collisions with a G1 cable guardrail than with G4-1S or both G4 types combined.

Based on a review of previous research and testing of CMBs, Alberson et al. (2003) developed a new terminal to improve the lateral deflection, maintenance, and crash performance of the generic low-tension CMBs. By replacing the single, large concrete anchorage block with three specially designed posts, the new terminal eliminated spring connectors and was expected to withstand higher tensile loads. Full-scale crash testing on the new terminal showed reduced lateral cable deflections and suggested a performance improvement. This newly developed cable barrier system was expected to (partially) address the issue of cable heights in backside hits by changing the cable heights in the terminal section. A recommendation was made for further investigation of cable heights in the length-of-need sections in relation to vehicle profiles.

Recently, Alberson et al. (2007) completed a study in which a preliminary guideline was developed for the selection of CMB systems. The project reviewed cable barrier installations in the U.S. and overseas including the generic low-tension CMBs and five proprietary high tension cable systems. A survey was also conducted in the study to identify experiences, practices, and design and construction standards for cable barrier systems in various states. The study indicated a continuously increased usage of CMBs with a total of 1,645 miles of installation. As expected, the severity of accidents was found to decrease at locations where CMBs were installed, while the total number of accidents was found to increase. The study indicated that the placement of CMBs was critical to minimizing the number of fatal accidents and maximizing the performance of the systems, and that these issues were sometimes at odds and deserved further research.

In a project funded by the New Jersey DOT, Gabler et al. (2005) evaluated the post-impact performance of two median barrier systems in New Jersey: a three-strand CMB and a modified thrie-beam guardrail. FE modeling was used as a major tool for the investigation. The project also included field investigation of crashes involving the subject barriers and a survey of median barrier experiences of other state DOTs. This study concluded that three-strand cable barriers were capable of containing and redirecting passenger vehicles, that cable barriers were effective at reducing the incidence of cross-median collisions in wider medians, and that cable barriers reduced the overall collision severity despite the typically increased total number of accidents. In the work of Gabauer and Gabler (2009), they performed a statistical study on the risk of vehicle rollovers. Factors investigated were barrier and vehicle types. Observations from limited crash data showed that concrete barriers were less likely to cause rollovers than other types of barrier systems, and that SUVs were more likely (more than three times) to roll over than pickup trucks and passenger cars. Note that this study only focused on the vehicle rollovers and did not consider crash severity.

Nevertheless, the study clearly indicates that the current full-scale tests, which utilize a pickup truck as the test vehicle, do not fully address safety issues such as vehicle rollover. Furthermore, despite being more forgiving, CMBs were shown to have a higher percentage of vehicle rollover which remains to be a concern and warrants future research in this area.

The effects of horizontal curvature on highway accidents have been known and studied for decades. Most of the studies were focused on the causal effects of horizontal curves on traffic accidents, with few studies on the effects on CMB performance. Zegeer et al. (1992) analyzed 10,900 horizontal curves in Washington State with corresponding accident, geometric, traffic, and roadway data variables. Using a statistical model, they found that sharper curves and narrower pavement width were associated with significantly higher curve accidents. Based on the finding, they recommended a variety of improvements for horizontal curves. Miaou et al. (1992) studied the relationship between truck accidents and highway geometric design using the Poisson regression approach and reached a similar conclusion: horizontal curvatures had a strong correlation with truck accident involvement. In the work of Mohamedshah et al. (1993), they developed models for truck accidents on interstate highways and two-lane rural roads using data from HSIS. Both the interstate and rural-road models indicated that the horizontal curvature was a primary factor causing truck accidents. A number of subsequent studies, including those of recent years, all confirmed that horizontal curvatures increased the frequency and/or severity of vehicle crashes (Abdel-Aty et al. 2006; Mussa and Chimba 2006; Caliendo et al. 2007; Pandea and Abdel-Aty 2009; Choi et al. 2010; Lu et al. 2010; Venkataraman et al. 2011).

As for the effects of horizontal curvatures on the performance of CMBs and other barriers, there are no studies available in the literature, mainly due to the difficulty in conducting such research using experiments or crash data. In the study of Sheikh et al. (2008), they reviewed the state's practice related to CMBs on the benefits, available guidelines, policies, and procedures for barrier placement, in-service performance, and maintenance. One of the observations of the study was that there was a significant effect of horizontal curvature on cable deflections: a significant difference existed on cable deflections between impacts from the concave side and the convex sides.

2.2 Crash Modeling and Simulations

Most publically available FE models of vehicles and roadside safety structures were developed at the National Crash Analysis Center (NCAC), George Washington University. Since the 1990's, significant effort has been placed on the development of FE crash models that are available as LS-DYNA input files from NCAC's website (NCAC web1). A list of references of these modeling efforts and simulation work performed at NCAC is also available from NCAC's website (NCAC web2).

The modeling and simulation efforts at NCAC can be found in several representative works. Marzougui et al. (2000) developed the FE model of an F-shaped portable concrete barrier (PCB) and validated the model with full-scale crash test data. With the proven fidelity and accuracy of the modeling methodology, the models of two modified PCB designs were created and used in FE simulations to evaluate their safety performance. A third design was then developed based on the simulation results and its performance was analyzed. In the

work by Zaouk et al. (2000a, 2000b), a detailed FE model of a 1996 Dodge Neon was developed. The three dimensional geometric data of each component was obtained by using a passive digitizing arm and then imported into a preprocessor for mesh generation, parts connection, and material properties. Tensile tests were conducted on specimens to obtain the material properties of the various sheet metal components. The body-in-white model was used in the simulation of a frontal impact and the results were compared with test data to evaluate the accuracy and validity of the model. Kan et al. (2001) developed an integrated FE model that included the vehicular structure, interior components, an occupant (Hybrid III dummy), and an airbag for crashworthiness evaluation. The integrated model was then used in a case study to demonstrate the potential benefit of the integrated simulation and analysis approach, which would further improve engineering practice with cost savings and production of more accurate and consistent analysis results.

Marzougui et al. (2004) developed a detailed suspension model and incorporated it into the previously developed FE model of a Chevrolet C2500 pickup truck (Zaouk et al. 1997). Pendulum tests were conducted at the Federal Outdoor Impact Laboratory (FOIL) of the FHWA and compared with simulation results of deformations, displacements and accelerations at various locations. Crash simulations were performed using the upgraded vehicle model and the results were compared with crash data from previously conducted full-scale tests.

Mohan et al. (2005) developed a detailed FE model for the three-strand low-tension cable barriers. The model addressed the important issues with cable modeling for crash simulations by defining soil and post, post and hook-bolt, cable and hook-bolt, and cable and vehicle interactions. The CMB model was then combined with the FE model of a Chevrolet C2500 pickup truck and used in the simulation of CMBs placed on a flat terrain. The simulation results were compared to data from a full-scale crash test with the same setup. Cable pullout and soli-post dynamic deflections from the simulation were found to correlate well with the crash test. Angular displacements of the pickup truck in the simulation were similar to those in the crash test. Recorded test data such as maximum dynamic deflection allowed by the cable barriers and the vehicle's acceleration at the center of gravity compared well with the simulation results.

To facilitate the use of FE simulation to evaluate roadside safety structures at higher test levels specified by the NCHRP Report 350, Mohan et al. (2007) improved and validated a previously developed model of a 1996 Ford F800 single unit truck. This 8172-kg (18,000-lb) truck was the one used by NCHRP Report 350 as the standard vehicle for test level 4. Simulations were performed using the improved model and the results were compared with those from a full-scale crash test. The global kinematics and acceleration time histories of the truck from simulation correlated well with the crash test. Mohan et al. also suggested further improving the normal forces on non-impacted tires so as to correlate well with the vehicle's yaw by considering frictions between the tire and barrier and between the tires and ground.

In the work by Marzougui et al. (2007a), they investigated penetration of low-tension CMBs placed on flat and sloped medians using FEA and vehicle dynamics analysis coupled with full-scale crash testing. The FE model of a Chevrolet C2500 pickup truck was used in the

simulation of CMBs placed on a flat terrain and the results showed that the vehicle was retained by the barriers. The FE model of a Ford Crown Victoria was used in the simulation of CMBs placed on a 6:1 sloped median and 1.22 m (4 ft) from the ditch centerline. The Crown Victoria was found to under-ride the CMBs with almost no resistance from the cables. The simulation results using the Crown Victoria model were confirmed by full-scale crash tests (No. 04010 and 04011) performed at the FHWA/FOIL. A conclusion from the simulation results was that the sloped terrain caused the vehicle to be relatively lower than the cable and hence reduced the effectiveness of the CMBs. In both simulations, the impact speed and angle were 62 mph (100 km/hr) and 25°, respectively.

Marzougui et al. (2007a) also performed vehicle dynamics analysis using the two models noted above along with the model of a small sedan, a Mitsubishi Mirage, to further investigate the effect of sloped (6:1) terrain on CMB performance. It was determined that the suspension of the mid-sized vehicle tended to be fully compressed due to the dynamic forces imposed by the terrain, speed, and angle when the vehicle started up the slope on the opposite side of the median. These conditions are likely to place the nose of the vehicle below the lowest cable and hence allow under-riding the barrier. Future work recommended by Marzougui et al. (2007a) was to further analyze alternative designs and barrier placement retrofits to improve the CMB performance on sloped terrain. Their suggested retrofits involved adding a fourth cable, using a closer post spacing, using a stronger cable/post connection, and incorporating ties to connect the three cables.

In the study of Marzougui et al. (2007b), they developed a FE W-beam model and validated it using full-scale crash testing. The model was shown to give an accurate representation of the real system by comparing the roll and yaw angles. Using the validated model, they performed four simulations of a passenger truck impacting the W-beam with different rail heights. The simulation results showed that the effectiveness of the barrier to redirect a vehicle could be compromised when the rail height was lower than recommended. Using vehicle dynamics simulations, Marzougui et al. (2009) investigated the performance of a three-strand CMB placed behind a curb. Five different curbs, three different vehicles (small passenger car, mid-sized passenger car and pickup truck), different impact angles (5°, 15°, 25°), various impact speeds (50 km/hr, 70 km/hr, 100 km/hr) were considered. For each of the five curbs studied, the maximum height of the bottom cable and the minimum height of the top cable were determined as functions of the distance from the curb to the cable barrier. It should be noted that vehicle dynamics simulations could not take into account the contact between the vehicle and cable barrier. In fact, there was no cable barrier model in the simulation models. Therefore, deformations of the vehicle and cable barrier were not considered. Although the study provided insights into the placement of CMB behind curbs, the lack of vehicle-barrier interactions in the simulation raised concerns on the effectiveness of the recommended placements.

Most recently, Opiela et al. (2009) developed the FE model of a 2007 Chevrolet Silverado 1500 2WD. This FE model has 942,491 nodes, 872,960 shell elements, 2,654 beam elements, and 53,286 solids elements, with detailed front and rear suspension systems intended for good behavior in oblique impact situations. This FE model was further validated by Marzougui et al. (2010) using crash test data and simulation results of an oblique impact into

a New Jersey barrier complying with MASH testing conditions. Extended validation was performed by Marzougui et al. (2012) to include interior components attached to the door in the FE model. The standard FMVSS full-frontal, offset-frontal, and side impacts were simulated and the simulation results were compared to test data. The FE model was also used to simulate the centerline pole impact to illustrate its robustness.

Researchers from the roadside safety group at Worcester Polytechnic Institute (WPI) utilized FE models in a number of roadside safety studies. Ray (1996a) analyzed data of full-scale crash tests and developed a criterion using statistical parameters to assess the repeatability of full-scale crash test and to evaluate simulation results compared to crash data. Ray (1996b) reviewed the history of using FEA in roadside safety research, and presented the vehicle, occupant, and roadside hardware models that had been developed to date. Ray and Patzner (1997) developed a nonlinear FE model of a modified eccentric loader breakaway cable terminal (MELT) and used it in simulating a full-scale crash test involving a small passenger car. Simulation results were analyzed and compared to crash data, and the FE model was recommended to be used in the evaluation of new design alternatives. Plaxico et al. (1997) developed a 3D FE model of a modified three-beam guardrail and simulated the impact of a compact automobile. The computational model was then calibrated with data from an actual field test that was previously conducted as part of a full-scale crash test program carried out under the auspices of FHWA. Plaxico et al. (1998) developed the FE model of a breakaway timber post and soil system used in the breakaway cable terminal (BCT) and the modified eccentric loader BCT. Simulation results were compared and found to correlate well to data from physical tests. Patzner et al. (1999) examined the effects of post strength and soil strength on the overall performance of the MELT terminal system using a nonlinear FE model. A matrix of twelve simulations of particular full-scale crash test scenarios was used to establish the combinations of post and soil strengths that produce favorable results. The parametric study showed that certain combinations of soil and post strengths increased the hazardous possibilities of wheel snagging, pocketing, or rail penetration, while other combinations produced more favorable results.

In the work of Plaxico et al. (2000), the impact performance of two strong-post W-beam guardrails, the G4 (2W) and G4 (1W), were compared. After validating the FE model of the G4 (W2) guardrail with data of a full-scale crash test, the FE model of the G4 (1W) guardrail was developed. The two guardrails were compared with respect to deflection, vehicle redirection, and occupant risk factors. The two systems were found to perform similarly in collisions and both satisfied the requirements of the NCHRP Report 350 for the test 3-11 conditions. Using LS-DYNA simulations and laboratory experiments, Plaxico et al. (2003) investigated the failure mechanism of the bolted connection of a W-beam rail to a guardrail post, which could have a significant effect on the performance of a guardrail system. A computationally efficient and accurate FE model of the rail-to-post connection was developed to be used in the analysis of guardrail system performance using LS-DYNA. Orengo et al. (2003) presented a method to model tire deflation in LS-DYNA simulations along with examples to use the model. Deflated tires have significantly different behaviors from those of inflated tires, as observed in real world crashes and in full-scale crash tests. A vehicle's kinematics is strongly coupled to the behaviors of deflated tires; therefore, modeling such behaviors is critical to accurate roadside hardware simulations. Ray et al.

(2004) used LS-DYNA simulations to determine if an extruded aluminum bridge rail will pass the full-scale crash tests for test levels three and four conditions of the NCHRP Report 350. The simulation results, which were supported by a subsequent AASHTO LRFD analysis, indicated a high likelihood of passing the crash tests.

FE simulations have also been used by researchers at the Midwest Roadside Safety Facility (MwRSF). Reid (1996) utilized FEA in the study of material property influence on automobile crash structures and attempted to develop crashworthiness guidelines for design engineers. In one of his later works, Reid (1998) demonstrated through two simple examples the potential modeling issues that could be easily overlooked in FE impact simulations: contact definition and damping. He also suggested ways to check for modeling errors and to make improvements. In the work of Reid and Bielenberg (1999), FE simulations were performed for a bullnose median barrier impacted by a 2000-kg (4405-lb) pickup truck to determine the cause of failure and to evaluate a potential solution to the problem. Reid and Coon (2002) presented details on the development of the hook-bolt model used in the CMBs. In a collaborative work to improve the FE model of a Chevrolet C2500 pickup truck (Reid and Marzougui 2002; Tiso et al. 2002), structural modeling methods were introduced for model improvement through refining meshes, using better material models, adding details to simplified components, and improving connections between components. Suspension modeling, which is critical to the correct vehicle dynamics, was also investigated in this collaborative work, and a new model was successfully developed with significant improvements.

To educate roadside safety engineers and promote the use of simulation, Reid (2004) summarized ten years of the simulation efforts at MwRSF on the development of new roadside safety appurtenances. More recently, Reid and Hiser (2004) studied the friction effects, particularly between solid elements, on component connections and interactions in crash modeling and analysis. In their work on modeling bolted connections that allowed for slippage, Reid and Hiser (2005) investigated two modeling techniques that are based on discrete-spring clamping and stressed clamping models with deformable elements, respectively. The simulation results for both models compared well with test data, with the stressed clamping model with deformable elements having better accuracy accompanied by significantly increased computational cost. Hiser and Reid (2005) also investigated improved FE modeling methods for slip base structures, which could have a considerable potential for reducing the amount of crash resistance and thus occupant injury when struck by errant vehicles. They developed and evaluated two bolt preloading methods, with one using discrete spring elements and the other using pre-stressed solid elements. Similar to their findings in the work of modeling hook-bolts, they found that the method using solid elements was more accurate than that using discrete spring elements when the impact conditions became more severe. As a result, the model using pre-stressed solid elements was incorporated into the FE model of a cable guardrail system. The results showed that the slip base model was acceptable in both end-on impact and length-of-need impact simulations.

In the study by Reid et al. (2009), they investigated the potential of increasing the suggested flare rates for strong post W-beams to reduce guardrail installation lengths, which would result in decreased guardrail construction and maintenance costs, and reduce the impact

frequency. Both computer simulation and full-scale crash tests were used in the evaluation of increased flare rates up to, and including, 5:1. Simulation results indicated that the conventional G4 (1S) guardrail modified to incorporate a routed wood block could not successfully meet NCHRP Report 350 crash test criteria when installed at any steeper flare rates than the 15:1 recommended in the Roadside Design Guide. Their study also showed that the Midwest Guardrail System (MGS) could meet NCHRP Report 350 impact criteria when installed at a 5:1 flare rate, yet with greater impact severities during testing than anticipated. Reid et al. also indicated that whenever roadside or median slopes are relatively flat (10:1 or flatter), increasing the flare rate on guardrail installations becomes practical and has some major advantages including significantly reducing guardrail lengths and associated costs. The study, however, did not give any indications of W-beam performance on steeper slopes.

FE simulations were also found in the work of other researchers in roadside safety research. Whitworth et al. (2004) evaluated the crashworthiness of a modified W-beam guardrail using detailed FE models of the guardrail and a Chevrolet C2500 pickup truck. The simulation results were compared and found to match well to crash test data in terms of roll and yaw angles. Simulations were also performed to evaluate the effect of certain guardrail design parameters, such as rail mounting height and routed/non-routed blockouts, on the crashworthiness and safety performance of the system. In the work of Bligh et al. (2004), FEA was utilized to develop new roadside features to address three roadside safety issues. An alternative to the popular T6 tubular W-beam bridge rail was developed to address problems with vehicle instability observed in full-scale crash testing. A retrofit connection to TxDOT's grid-slot portable concrete barrier was developed to limit dynamic barrier deflections to levels that are more practical for work zone deployment. Finally, crashworthy mow strip configurations were developed for use when vegetation control around guard fence systems is desired to reduce the cost and risk associated with hand mowing. In a project funded by the New Jersey DOT, Gabler et al. (2005) evaluated the post-impact performance of two median barrier systems in New Jersey: a three-strand cable median barrier system and a modified three-beam median barrier system. FE modeling was adopted as a major means for the investigation. The project also included field investigation of crashes into the subject barriers and a survey of the median barrier experience of other state DOTs. This study concluded that the three-strand cable barriers were capable of containing and redirecting passenger vehicles, that cable barriers were effective at reducing the incidence of cross-median collisions in wider medians, and that cable barriers reduced the overall collision severity despite typically increasing the total number of accidents.

Computer simulations are also used by international researchers on roadside safety research. Using LS-DYNA simulations, Atahan (2002) analyzed a strong-post W-beam system that had failed in a previously conducted full-scale crash test. After identifying the cause of failure and incorporating necessary improvements, a new W-beam system was developed and showed improved performance based on simulation results. Atahan (2003) studied the impact performance of G2 steel weak-post W-beams installed at the slope-break point on non-level terrains using LS-DYNA simulations. His results showed that there was a risk of increased vehicle instability when the roadside slope adjacent to the W-beam guardrail became steeper than 6:1. Atahan and Cansiz (2005) investigated the failure of a bridge rail-to-guardrail

transition design in a full-scale crash test in which the vehicle rolled over the guardrail. They used full-scale LS-DYNA simulations to replicate the crash tests and identified the cause of the failure attributed to the low height of the W-beam rails. In the work by Atahan (2007), LS-DYNA simulation was used to study the crashworthiness behavior of a bridge rail-to-guardrail transition structure under 8,000 kg of impact load. This work demonstrated the effectiveness of FE simulations for its replications of the actual dynamic interactions and mechanics of the crash. Atahan also pointed out that the use of a real soil model other than the simplified spring soil model could improve the accuracy of FE simulations but would significantly increase the computational costs.

FE simulation, particularly with LS-DYNA, has been increasingly used in roadside safety research. In addition to the abovementioned references, FHWA published several manuals on using LS-DYNA material models and evaluation of these models (Lewis 2004; Murray et al. 2005; Murray 2007; Reid et al. 2004). These references are also useful in crash modeling work using LS-DYNA.

3. Finite Element Modeling of Vehicles and the CMB

The simulation work of this project included: 1) the vehicles (i.e. 1996 Dodge Neon and 2006 Ford F250) impacting the current NCDOT CMB placed on the outer 6:1 median slope of a four-lane freeway; 2) the vehicles impacting a retrofit CMB placed on the outer 6:1 median slope of a four-lane freeway; 3) the vehicles impacting the current NCDOT CMB placed on the outer 6:1 median slope of a six-lane freeway; and 4) the vehicles impacting the current NCDOT CMB placed on the inner 4:1 median slope of a six-lane freeway. In Cases 1) and 3), the CMB was placed 4, 6, and 8 ft from the median centerline. In Cases 2) and 4), the CMB was placed 8 ft and 6 ft from the median centerline, respectively. The FE models of the CMB and two vehicles were obtained from previously conducted NCDOT projects.

In all simulation cases, the vehicle left the shoulder with prescribed speeds; therefore, vehicle trajectories were included in these simulations. The impact speed was defined in the vehicle's travel direction, and the impact angle was defined as one between the vehicle's travel direction and the longitudinal direction of the barrier. Both front-side and backside impacts were simulated in this project. The vehicle's initial impact point on the W-beam or CMB was in the middle of the effective barrier length and midway between the two adjacent posts.

3.1 FE Models of a Passenger Car and Pick-up Truck

The vehicle models used in this project were a small passenger car (1996 Dodge Neon) and a pick-up truck (2006 Ford F250), whose curb weights were 2,400 lb (1,090 kg) and 5,504 lb (2,499 kg), respectively. Both FE models were originally developed at NCAC and validated using frontal-impact tests that were conducted on flat terrain according to FMVSS.

In the simulation of a vehicle crashing on a sloped median, a robust suspension model was required to ensure the correct dynamic behavior of the vehicle. The suspension models of both vehicles were evaluated and corrected for cross-median simulations, as illustrated in Fig. 3.1. The vehicle models were shown to possess good numerical stability and correct dynamic behavior on sloped medians.

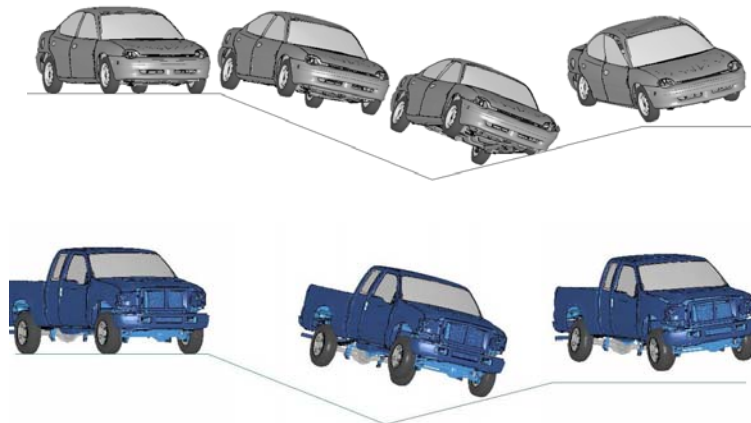


Fig. 3.1: FE simulations of a Dodge Neon and a Ford F250 crossing a sloped median

3.2 FE Model of the CMB on Curved Median

The CMB studied in this project was the generic three-strand low-tension system based on the current NCDOT design, as shown in Fig. 3.2. In the FE model, the effective length of the CMB was approximately 400 ft (122 m). The CMB model was obtained from a previous

NCDOT research project in which the contacts between cables and other components were upgraded to beam-based contacts to improve numerical accuracy and stability. The CMB model was combined with FE models of a four-lane and a six-lane freeway, both with a 46-ft median. Median slopes of the four-lane freeway were 6:1 and 6:1; and they were 4:1 and 6:1 for the six-lane freeway. The radius of horizontal curvature for both medians was 1,910 ft (582 m) to obtain a 3° curve. Figure 3.3 illustrates the placement of a CMB on a four-lane divided freeway used in this project.

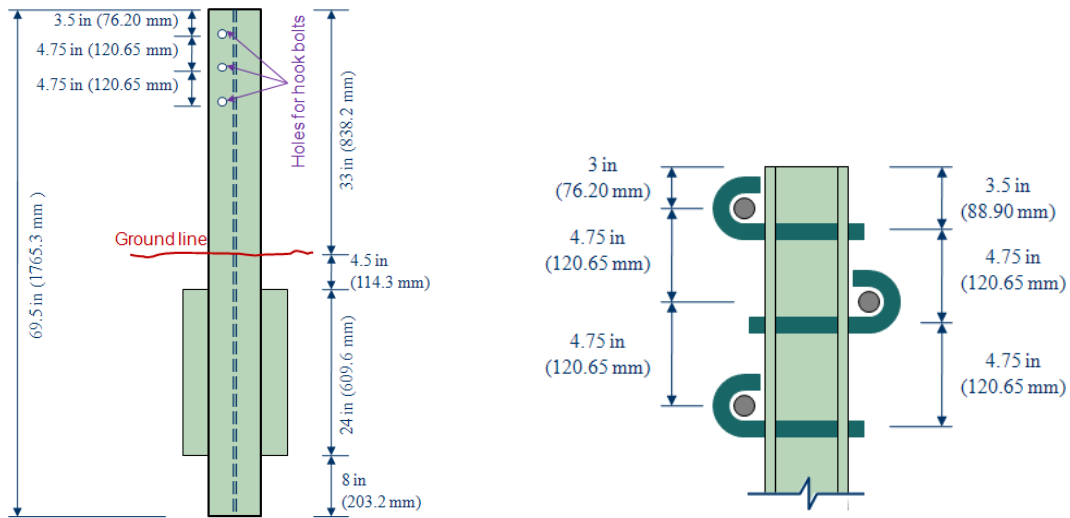


Fig. 3.2: Post geometry and cable positions of the CMB in the current NCDOT design

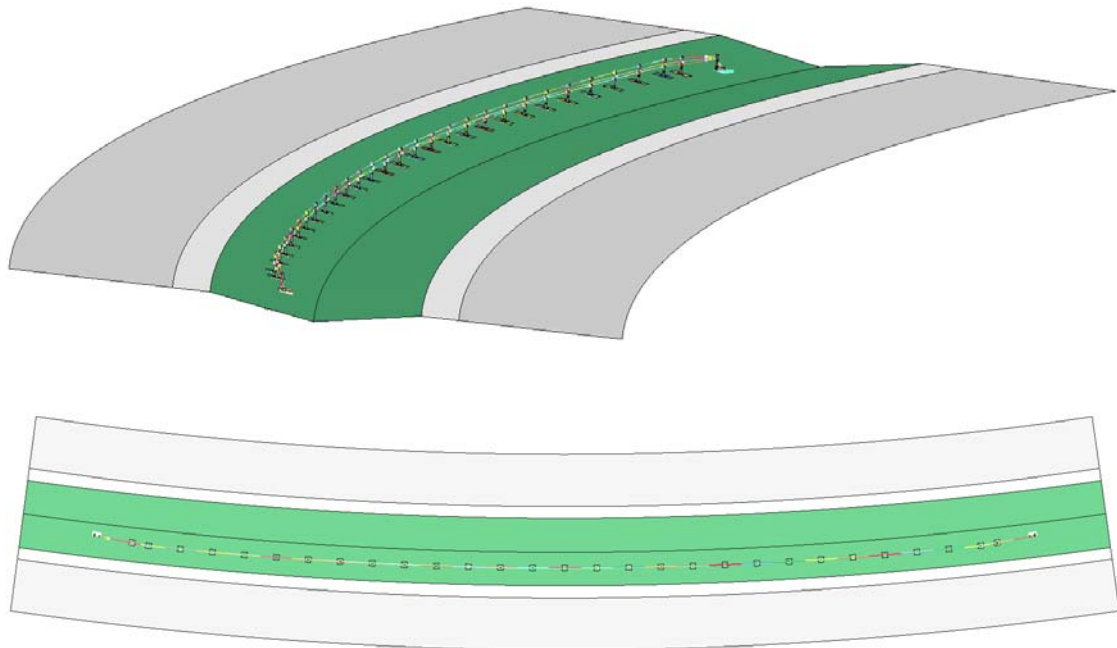


Fig. 3.3: Placement of a CMB on a four-lane divided freeway with horizontal curvature

3.3 Simulation Setup

The simulation work of this project was categorized into four major groups: Cases 1 to 4 based on freeway type, CMB design, and CMB placement on the median. Table 3.1 gives a summary of the four cases with details on the distances of the CMB from the median centerline and departure angles of the impacting vehicle.

Table 3.1: Categories of simulation work

Case No.	Freeway Type	Median Slopes	CMB Design	CMB Placement	Distance of CMB from Median Centerline	Departure Angle(s)
1	Four-lane	6:1 and 6:1	NCDOT current	Outer 6:1 slope	4 ft (1.22 m)	20°, 25°, 30°
					6 ft (1.83 m)	20°, 25°, 30°
					8 ft (2.44 m)	20°, 25°, 30°
2	Four-lane	6:1 and 6:1	Retrofit	Outer 6:1 slope	6 ft (1.83 m)	25°
					8 ft (2.44 m)	25°
3	Six-lane	6:1 and 4:1	NCDOT current	Outer 6:1 slope	4 ft (1.22 m)	20°, 25°, 30°
					6 ft (1.83 m)	20°, 25°, 30°
					8 ft (2.44 m)	20°, 25°, 30°
4	Six-lane	6:1 and 4:1	NCDOT current	Inner 4:1 slope	6 ft (1.83 m)	25°

For each of the scenarios in Table 3.1, the 1996 Dodge Neon and 2006 Ford F250 were used to impact the CMB from both front-side and backside. The vehicles departed from the shoulder with an initial speed of 62.1 mph (100 km/hr) and at an angle (i.e., 20°, 25°, or 30°), as specified in Table 3.1. The reason for the use of departure angles was that the angle at which the vehicle impacted the CMB was very difficult to prescribe due to the existence of horizontal curvature and median slopes. It should be noted that a significant difference exists between the departure angle and the impact angle, as illustrated in Fig. 3.4.

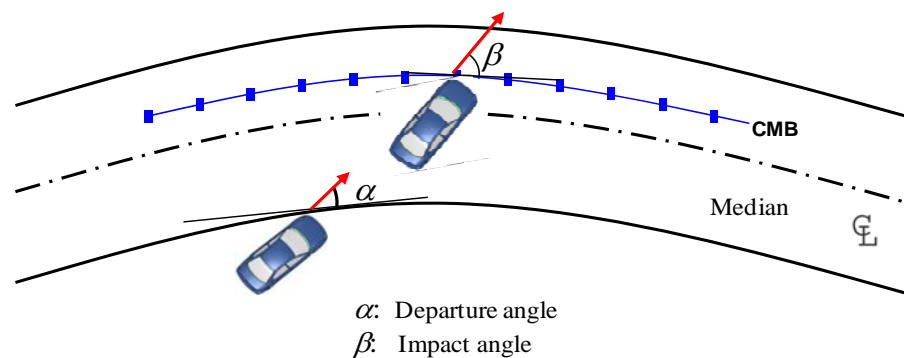


Fig. 3.4: Definitions of departure and impact angles

Based on discussions with NCDOT engineers, the most critical impact scenario was considered as one in which the vehicle knocked down a post. In this situation, the cables would likely be dragged down by the post and become less effective than at their normal

heights. Upon inspecting preliminary simulation results, it was found that the vehicle needed to be positioned such that the front-left tire knocks down the post upon impacting the CMB. This situation is illustrated in Fig. 3.5 where a Ford F250 is shown impacting the CMB at a post.

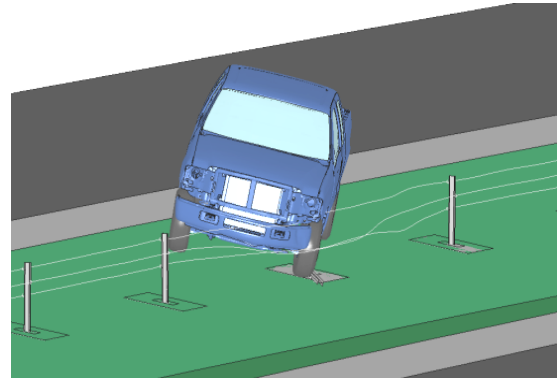


Fig. 3.5: A Ford F250 impacting the CMB by first knocking down the post

Unlike the case of a straight median, positioning the vehicle on a curved median was very challenging. This was because simply translating the vehicle along the curved shoulder line would not work: it might align the vehicle to target the post, but it would also change the designated departure angle to unacceptable values. In addition, before the vehicle's front-left tire hit the post, the front bumper had already been in contact with the cables, which could deform the target post to some degree. Finally, the vehicle had to cross the bottom of the ditch in backside impacts, which would cause tire rotations when going up the slope. For all of the above mentioned reasons, each successful run required two to four additional trial runs to correctly position the vehicle. As a result, all simulation models were adjusted at runtime.

4. Simulation Results and Analysis

In this section, the FE simulations results for the four cases listed in Table 3.1 are presented. Simulations of Cases 1 and 2 are for vehicles crashing into the CMB on a four-lane freeway, with the former using NCDOT’s current CMB design and the latter a retrofit CMB design. Simulations of Cases 3 and 4 are for vehicles crashing into the CMB on a six-lane freeway, with the former having the CMB on the 6:1 slope and the later on the 4:1 slope. For each of the CMB placements, both front-side and backside impacts were performed using both the 1996 Dodge Neon and the 2006 Ford F250.

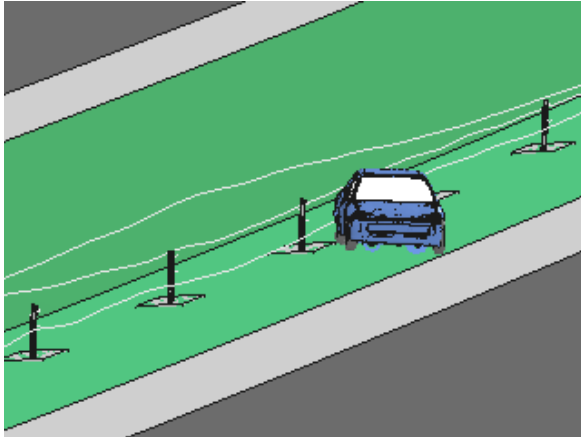
4.1 Case 1: CMB on 6:1 Slope of Four-lane Freeway

In this case, the NCDOT’s current CMB was placed on a four-lane freeway with a 46-ft (14 m) median. The median included two 6-ft (1.83 m) shoulders and median slopes were 6:1 and 6:1 (see Fig. 1.6). The CMB was placed on the outer 6:1 slope at three distances from the median centerline: 4, 6, and 8 feet. A 1996 Dodge Neon and a 2006 Ford F250 were used to impact the CMB from front-side and backside. Both vehicles were launched from the shoulder with an initial velocity of 62.1 mph (100 km/hr) and departure angles of 20°, 25°, and 30°. The simulation results of the Dodge Neon impacting the CMB are summarized in Table 4.1.

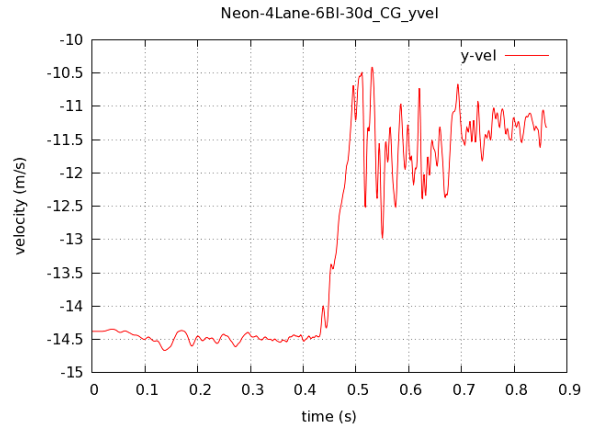
Table 4.1: Simulation results of Dodge Neon impacting the NCDOT CMB on a four-lane freeway

Impact Side	Departure Angle	Distance of CMB from Median Centerline (CMB on Outer 6:1 Slope)		
		4 ft (1.22 m)	6 ft (1.83 m)	8 ft (2.44 m)
Front	20°	Retained within median	Retained within median	Retained within median
	25°	Retained within median	Retained within median	Retained within median
	30°	Retained within median	Retained within median	Retained within median
Back	20°	Retained within median	Retained within median	Retained within median
	25°	Retained within median	Retained within median	Entered travel lane
	30°	Retained within median	Entered travel lane	Retained within median

The simulation results showed that the CMB generally performed well under impacts of the Dodge Neon, both from the front-side and backside. At 4 ft (1.22 m) from the median centerline, the CMB had the best performance and was able to retain the vehicle within the median for all impact scenarios. With a 30° backside impact, the CMB at 6 ft (1.83 m) from the centerline did not retain/redirect the vehicle within the median. The vehicle penetrated through the CMB between the middle and bottom cable with no cable fully engaged. Figure 4.1a shows the vehicle penetrating through the CMB and Fig. 4.1b shows the time history of the vehicle’s traversal velocity, which shows a velocity of approximately 11.5 m/s at the time of 0.86 seconds. This means that the vehicle will eventually enter the opposing travel lane due to lack of engagement of any of the cables. This could be due to the curvature effect for this barrier placement, which may represent the occasional CMB penetrations by small vehicles on the current design.



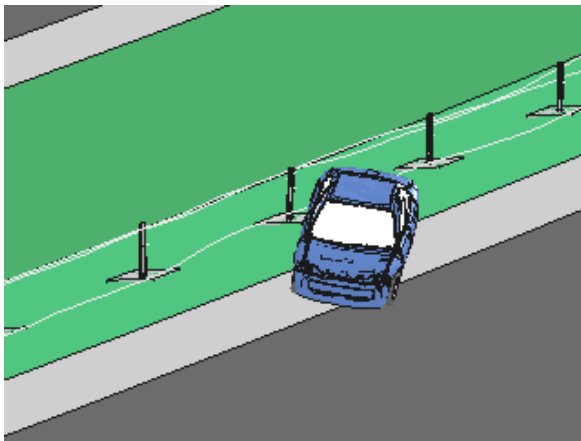
a. Dodge Neon penetrating through CMB



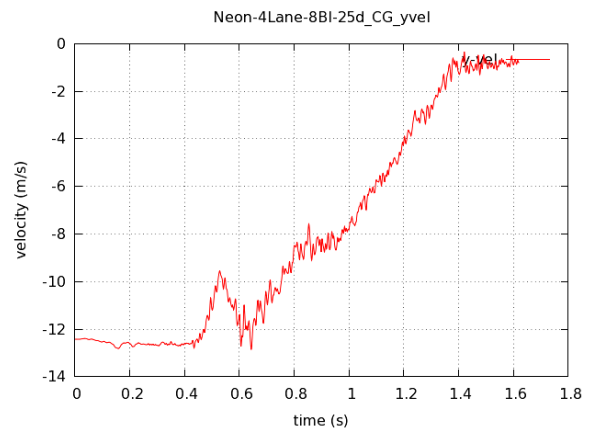
b. Time history of traversal velocity

Fig. 4.1: A Dodge Neon impacting the CMB placed at 6 ft from the median centerline, 30° backside impact

At 8 ft (2.44 m) from the centerline, the CMB successfully retained the vehicle within the median for all the scenarios except for the case of 25° backside impact. Figure 4.2a shows the instant when the vehicle under-rides the middle and top cables and partially engages with the bottom cable. At this instant, the vehicle has just entered the opposing travel lane with its front left bumper. From the time history of the vehicle's traversal velocity shown in Figure 4.2b, it can be seen that the vehicle's velocity is approaching zero. This means that the vehicle is unlikely to have further large displacement in the traverse direction.



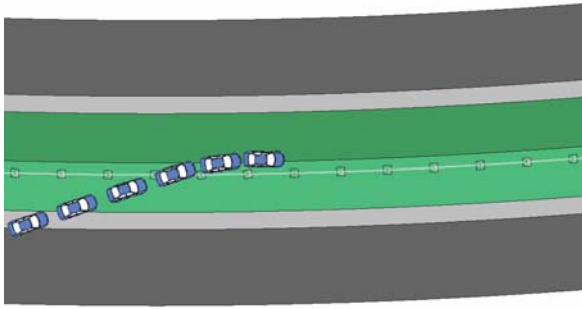
a. Dodge Neon penetrating through CMB



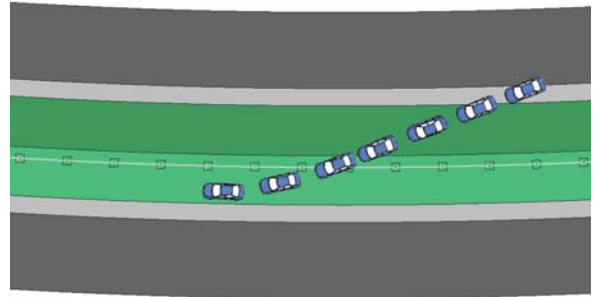
b. Time history of traversal velocity

Fig. 4.2: A Dodge Neon impacting the CMB placed at 8 ft from the median centerline, 25° backside impact

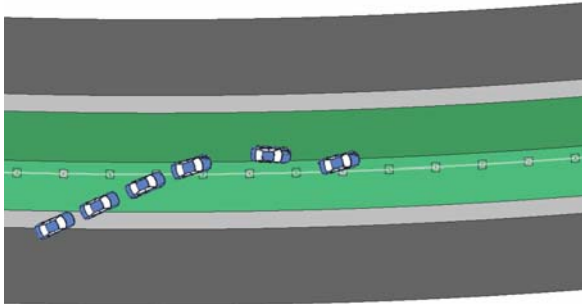
Figures 4.3 to 4.5 show the displacement paths of the Dodge Neon in all the scenarios given in Table 4.1.



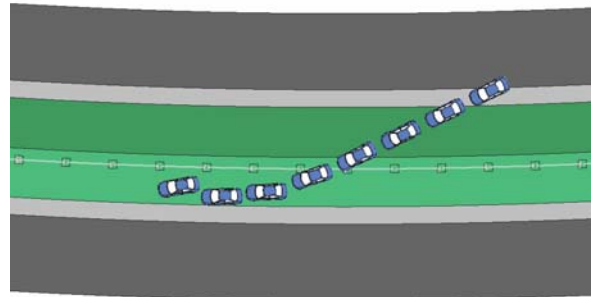
a. Front-side impact at 20°



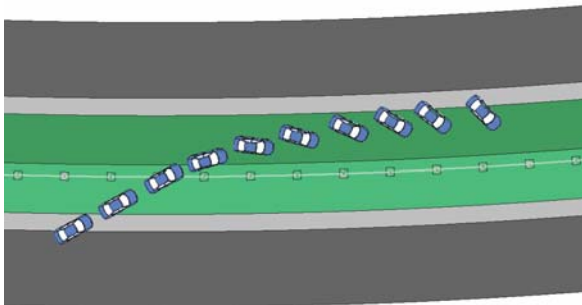
b. Backside impact at 20°



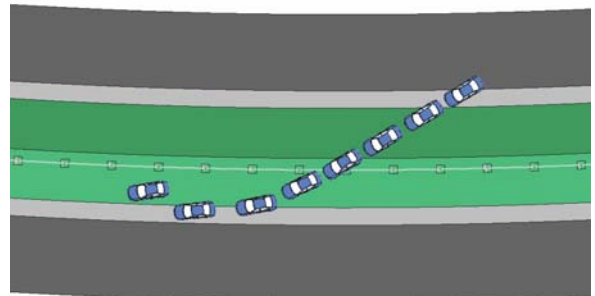
c. Front-side impact at 25°



d. Backside impact at 25°

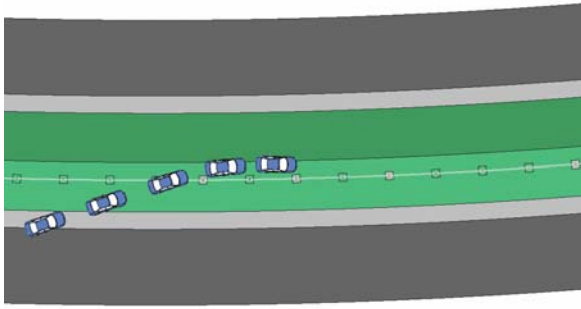


e. Front-side impact at 30°

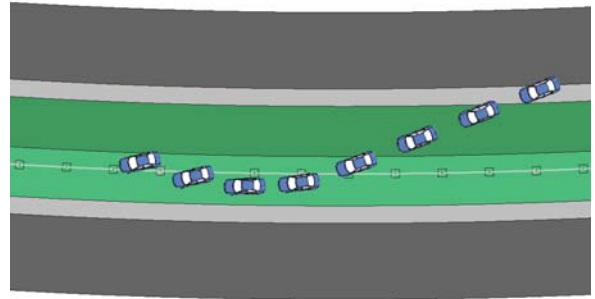


f. Backside impact at 30°

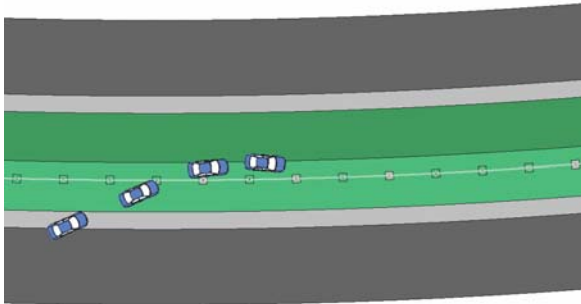
Fig. 4.3: A Dodge Neon impacting the CMB placed at 4 ft from the median centerline on the 6:1 slope of a four-lane freeway



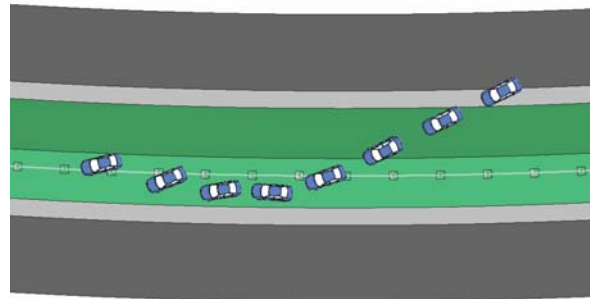
a. Front-side impact at 20°



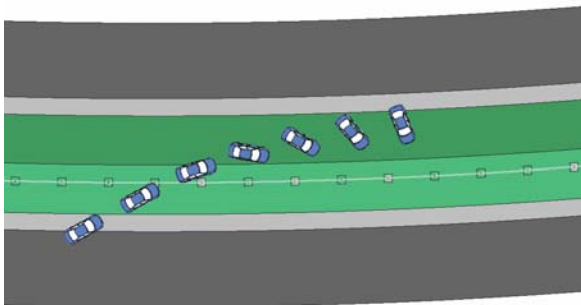
b. Backside impact at 20°



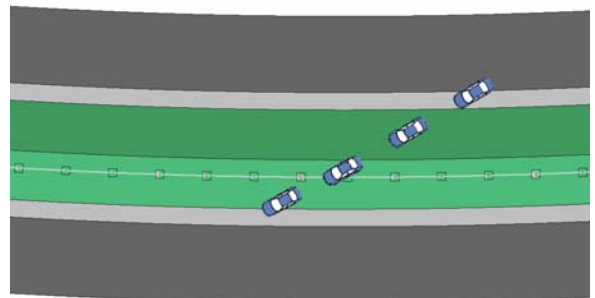
c. Front-side impact at 25°



d. Backside impact at 25°

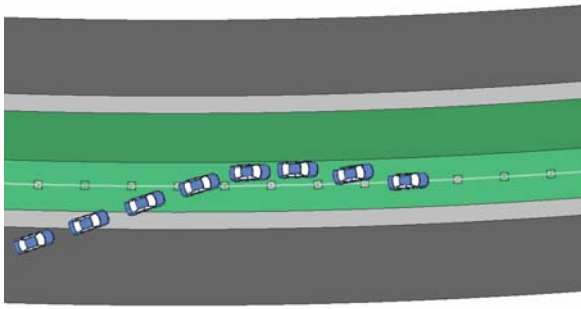


e. Front-side impact at 30°

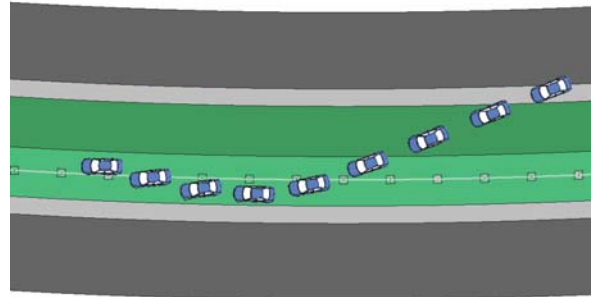


f. Backside impact at 30°

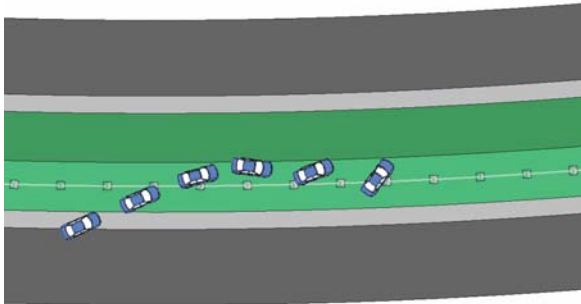
Fig. 4.4: A Dodge Neon impacting the CMB placed at 6 ft from the median centerline on the 6:1 slope of a four-lane freeway



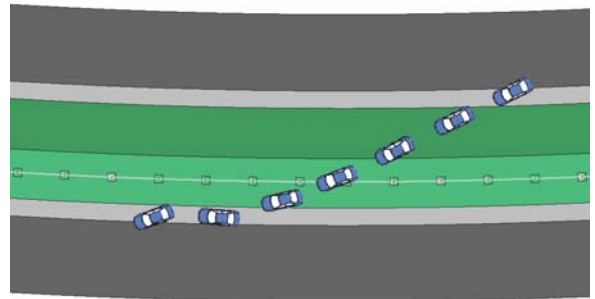
a. Front-side impact at 20°



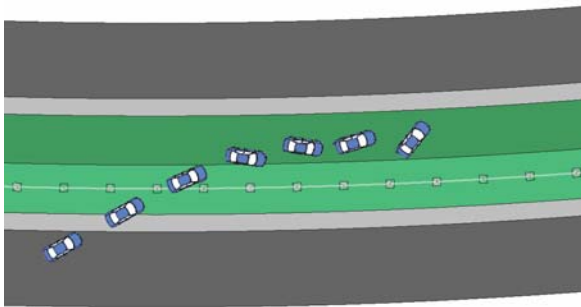
b. Backside impact at 20°



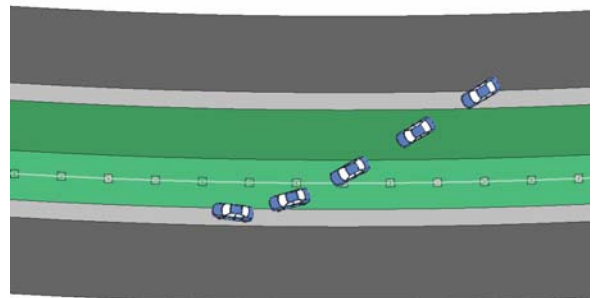
c. Front-side impact at 25°



d. Backside impact at 25°



e. Front-side impact at 30°



f. Backside impact at 30°

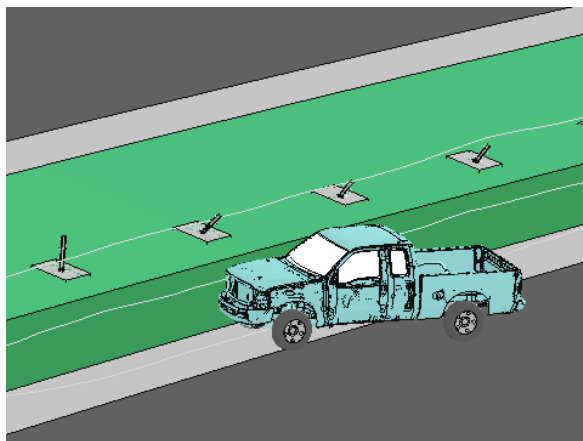
Fig. 4.5: A Dodge Neon impacting the CMB placed at 8 ft from median centerline on the 6:1 slope of a four-lane freeway

Table 4.2 shows the simulation results of the Ford F250 impacting the CMB placed on a four-lane freeway. The impact conditions and the CMB placement were the same as those in Table 4.1 for the Dodge Neon.

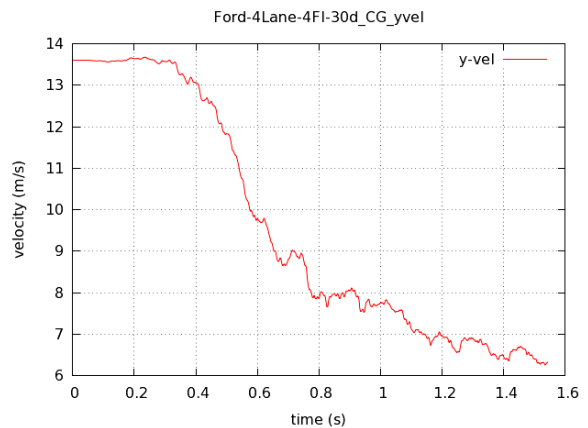
Table 4.2: Simulation results of a Ford F250 impacting the NCDOT CMB on a four-lane freeway

Impact Side	Departure Angle	Distance of CMB from Median Centerline (CMB on Outer 6:1 Slope)		
		4 ft (1.22 m)	6 ft (1.83 m)	8 ft (2.44 m)
Front	20°	Retained within median	Retained within median	Retained within median
	25°	Retained within median	Retained within median	Retained within median
	30°	Entered travel lane	Retained within median	Entered travel lane
Back	20°	Retained within median	Retained within median	Retained within median
	25°	Retained within median	Retained within median	Entered travel lane
	30°	Entered travel lane	Rolled over in travel lane	Entered travel lane

Under the front-side impacts of the Ford F250, the CMB was most effective when placed at 6 ft (1.83 m) from the centerline: it successfully retained the vehicle within the median for impacts at all angles. At 4 ft (1.22 m) from the centerline, the CMB retained the vehicle within the median for the cases of 20° and 25°, but failed for the 30° impact. At the 30° departure angle, the vehicle partially engaged with the three cables and eventually overrode them. The vehicle started to spin on the shoulder and entered the opposing travel lane. Figure 4.6a shows the instant at which the vehicle overrides the cables and spins into the opposing travel lane. Figure 4.6b shows the time history of vehicle’s traversal velocity, which is shown to be more than 6 m/sec at the end of the simulation. This means that the vehicle will go further into the opposing travel lane.



a. Ford F250 penetrating through CMB

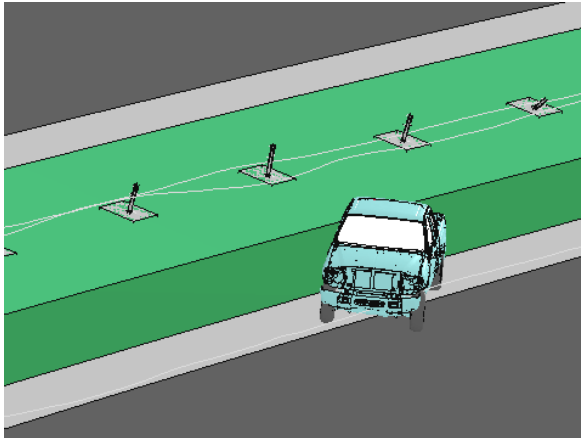


b. Time history of traversal velocity

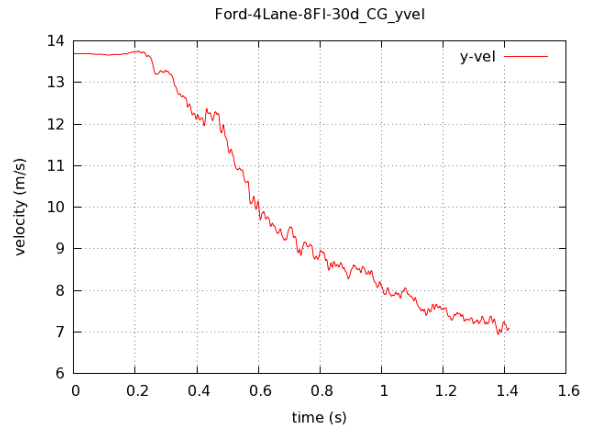
Fig. 4.6: A Ford F250 impacting the CMB placed at 4 ft from the median centerline, 30° front-side impact

At 8 ft (2.44 m) from the centerline, the CMB was successful for the cases of 20° and 25°, front-side impacts but failed for the 30° case. In this failed case, only the top cable was

partially engaged with the lower part of the vehicle, resulting in a penetration into the opposing travel lane with no vehicle redirection. Figure 4.7a shows the instant at which the vehicle has just entered the opposing travel lane. Figure 4.7b shows the time history of vehicle's traversal velocity, which is shown to be approximately 7 m/sec at the end of the simulation. This means that the vehicle will go further into the opposing travel lane.



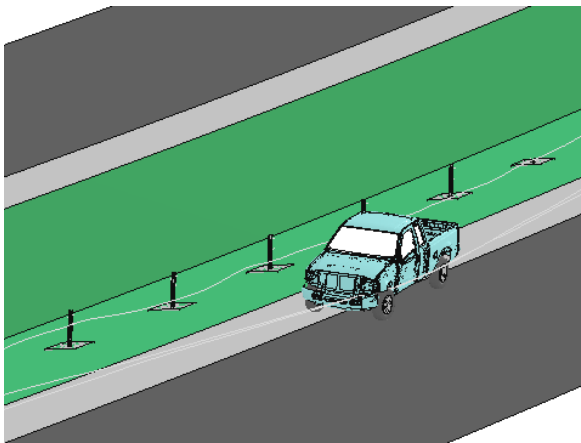
a. Ford F250 penetrating through CMB



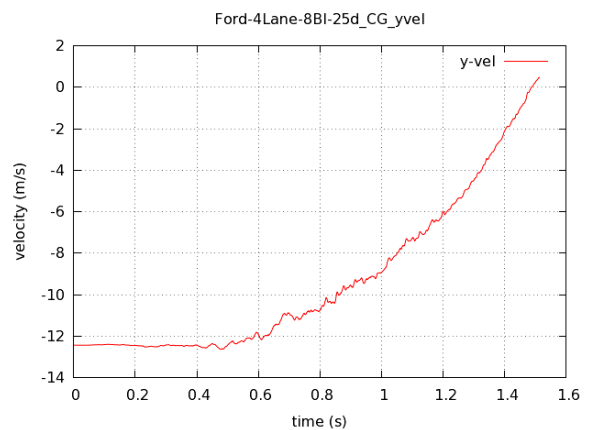
b. Time history of traversal velocity

Fig. 4.7: A Ford F250 impacting the CMB placed at 8 ft from the median centerline, 30° front-side impact

For backside impacts by the Ford F250, the simulation results showed that the CMB did not perform well when placed at 8 ft (2.44 m) from the median centerline. Although the CMB redirected and retained the vehicle within the median for the case of 20°, it failed for the cases of 25° and 30°; that is, the vehicle entered the opposing travel lane. In the two failed cases, the vehicle (partially) engaged with the cables, but the short traversal distance for cable deflection was insufficient to redirect the vehicle before entering the opposing travel lane. Figures 4.8 and 4.9 show the instants of vehicle penetrations for the cases of 25° and 30° impacts, respectively, along with the time history of the vehicle's traversal velocity.

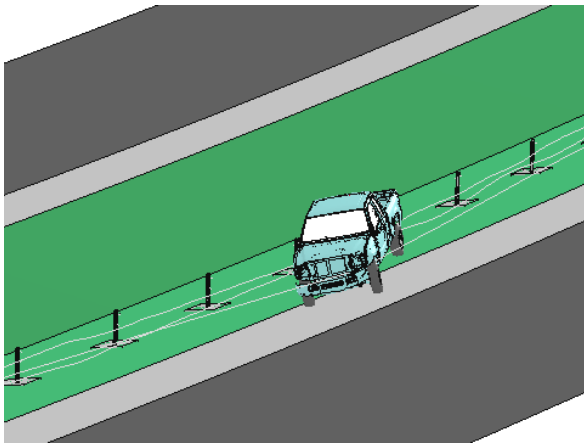


a. Ford F250 penetrating through CMB

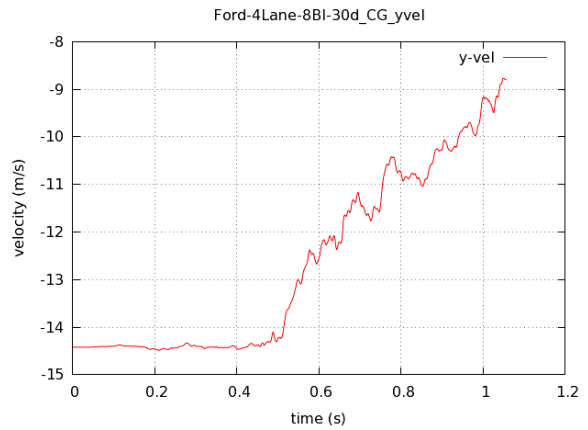


b. Time history of traversal velocity

Fig. 4.8: A Ford F250 impacting the CMB placed at 8 ft from the median centerline, 25° backside impact



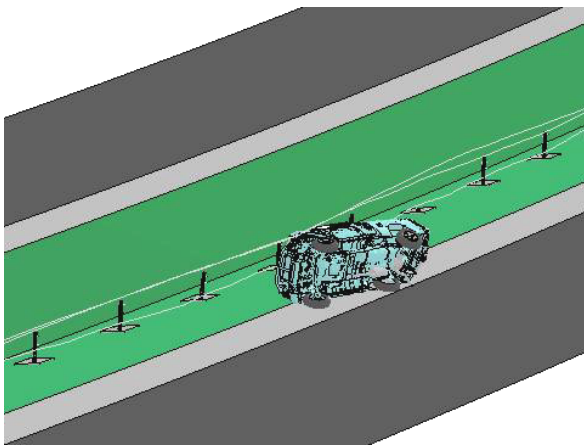
a. Ford F250 penetrating through CMB



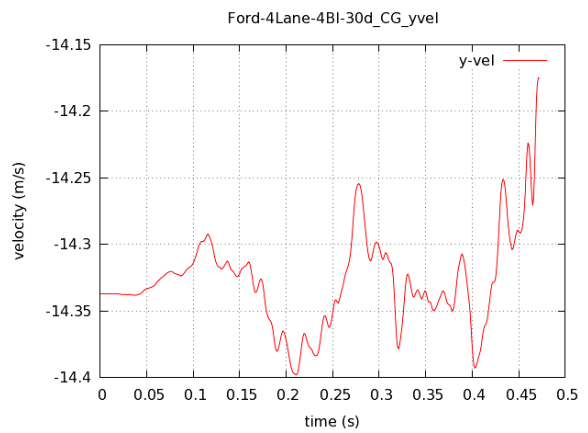
b. Time history of traversal velocity

Fig. 4.9: A Ford F250 impacting the CMB placed at 8 ft from the median centerline, 30° backside impact

When placed at 4 ft (1.22 m) and 6-ft (1.83 m) from the centerline, the CMB performed similarly in backside impacts: it retained the Ford F250 within the median for the cases of 20° and 25° backside impacts but failed for the 30° case. In both failed cases, the vehicle initially engaged with the cables but lost cable engagement before being redirected. Figures 4.10 and 4.11 show the instants of vehicle penetrations in these two failed cases, along with the time history of the vehicle's traversal velocity.

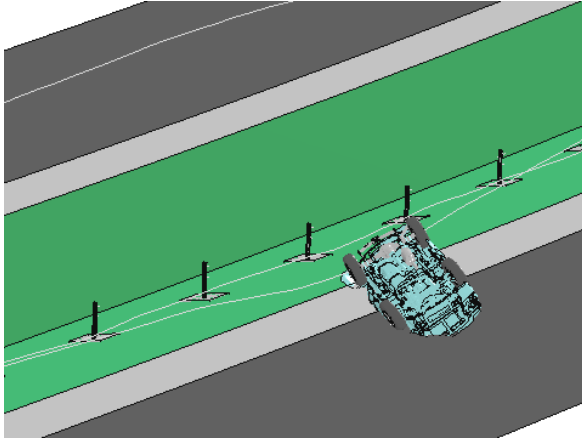


a. Ford F250 penetrating through CMB

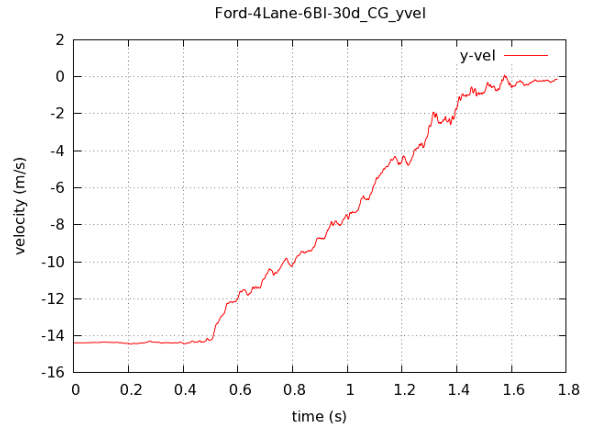


b. Time history of traversal velocity

Fig. 4.10: A Ford F250 impacting the CMB placed at 4 ft from the median centerline, 30° backside impact



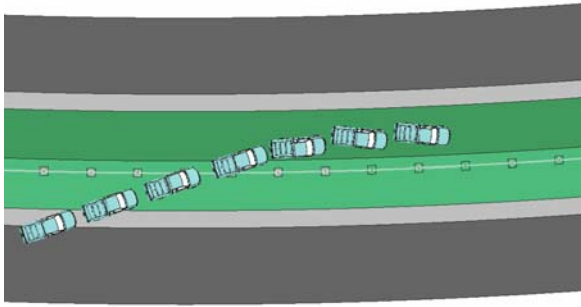
a. Ford F250 penetrating through CMB



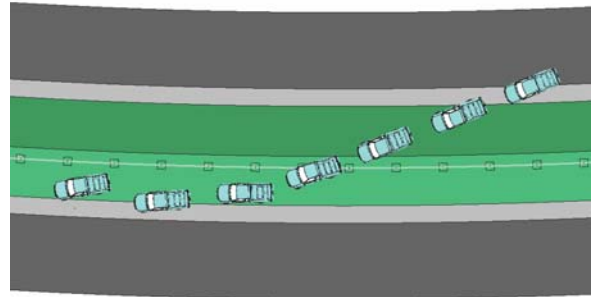
b. Time history of traversal velocity

Fig. 4.11: A Ford F250 impacting the CMB placed at 6 ft from the median centerline, 30° backside impact

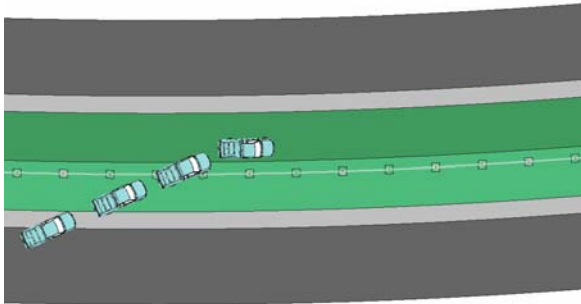
Figures 4.12 to 4.14 show the displacement paths of the Ford F250 in all the impact scenarios given in Table 4.2. For the current NCDOT CMB design on a four-lane freeway, the simulation results show that placing the CMB at 8 ft (2.44 m) from the centerline on the outer 6:1 slope may not leave enough space for the cables to deflect under impacts of a pick-up truck. At 4 ft (1.22 m) and 6 ft (1.83 m), the CMB was shown to be more effective than at 8 ft (2.44 m).



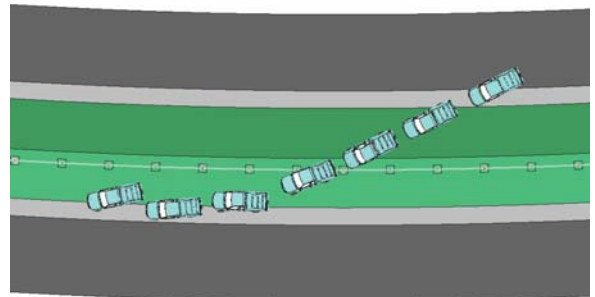
a. Front-side impact at 20°



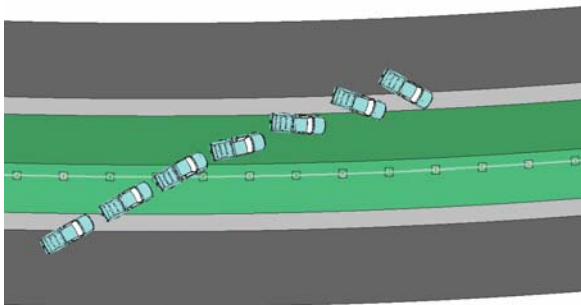
b. Backside impact at 20°



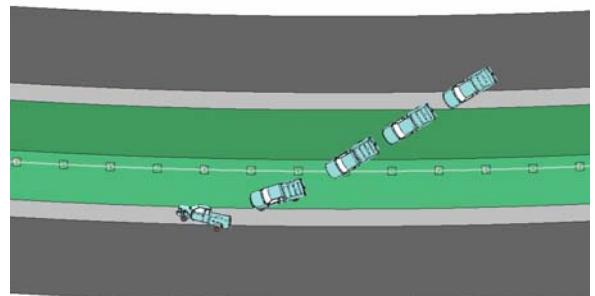
c. Front-side impact at 25°



d. Backside impact at 25°

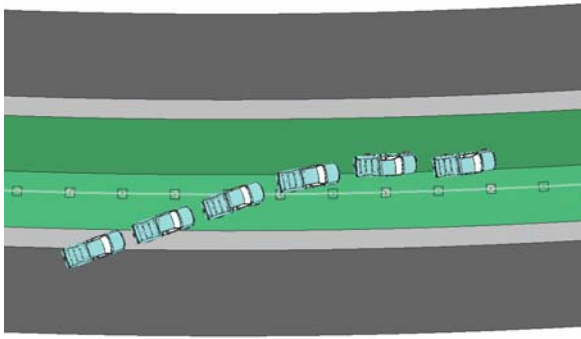


e. Front-side impact at 30°

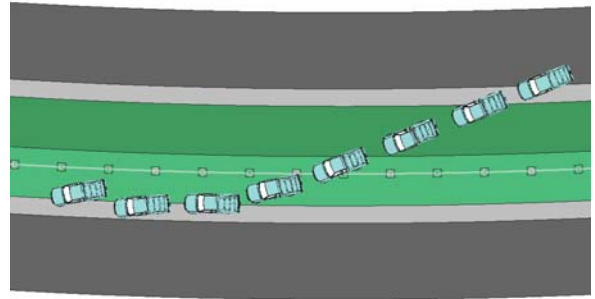


f. Backside impact at 30°

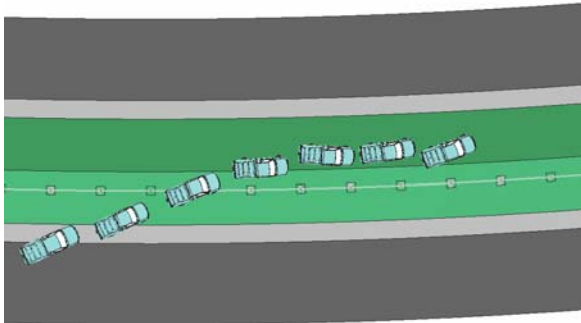
Fig. 4.12: A Ford F250 impacting the CMB placed at 4 ft from the median centerline on the 6:1 slope of a four-lane freeway



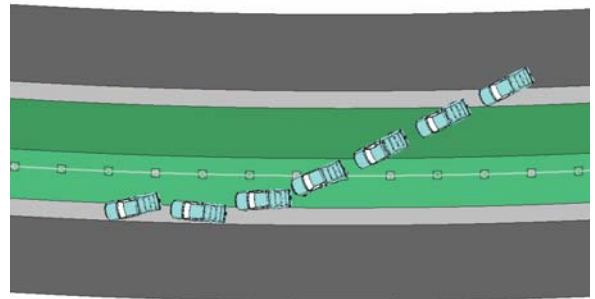
a. Front-side impact at 20°



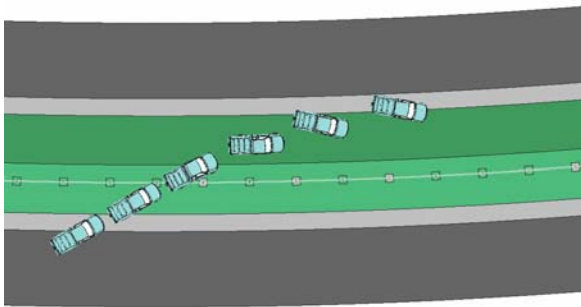
b. Backside impact at 20°



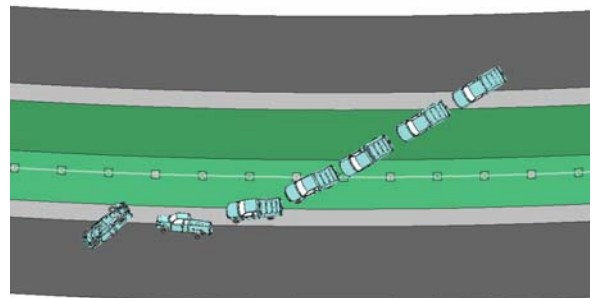
c. Front-side impact at 25°



d. Backside impact at 25°

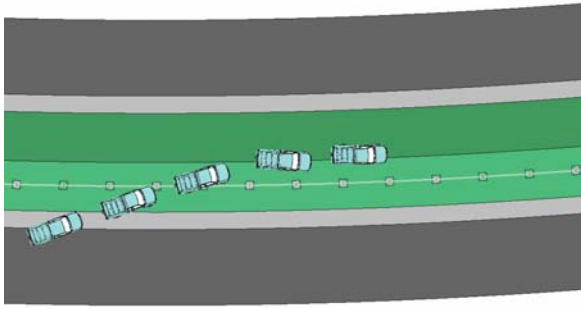


e. Front-side impact at 30°

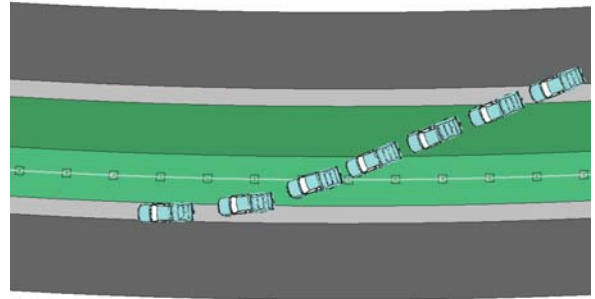


f. Backside impact at 30°

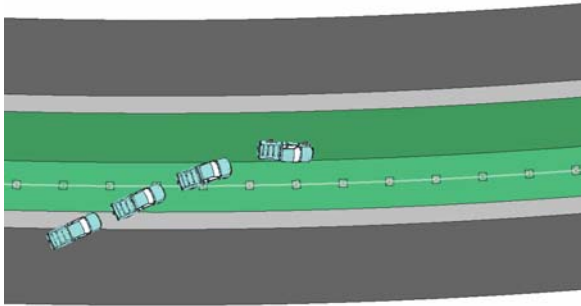
Fig. 4.13: A Ford F250 impacting the CMB placed at 6 ft from the median centerline on the 6:1 slope of a four-lane freeway



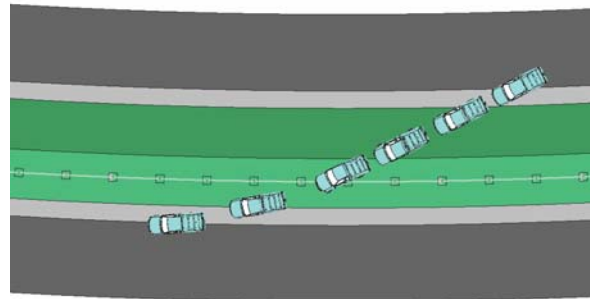
a. Front-side impact at 20°



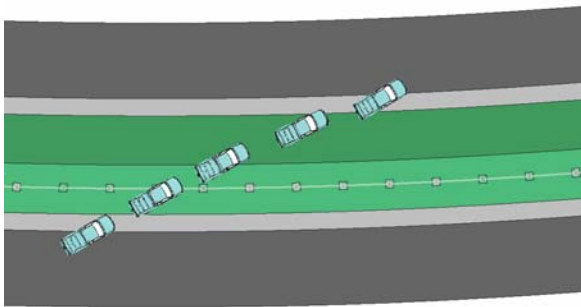
b. Backside impact at 20°



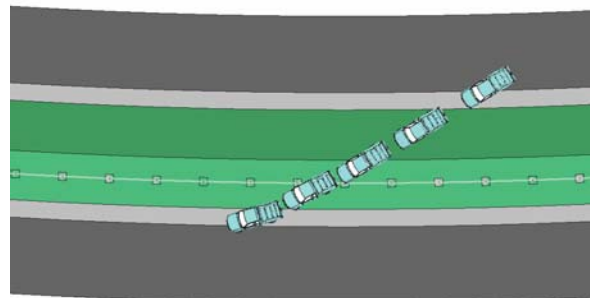
c. Front-side impact at 25°



d. Backside impact at 25°



e. Front-side impact at 30°



f. Backside impact at 30°

Fig. 4.14: A Ford F250 impacting the CMB placed at 8 ft from the median centerline on the 6:1 slope of a four-lane freeway

4.2 Case 2: CMB on 6:1 Slope of Four-lane Freeway – Retrofit Design

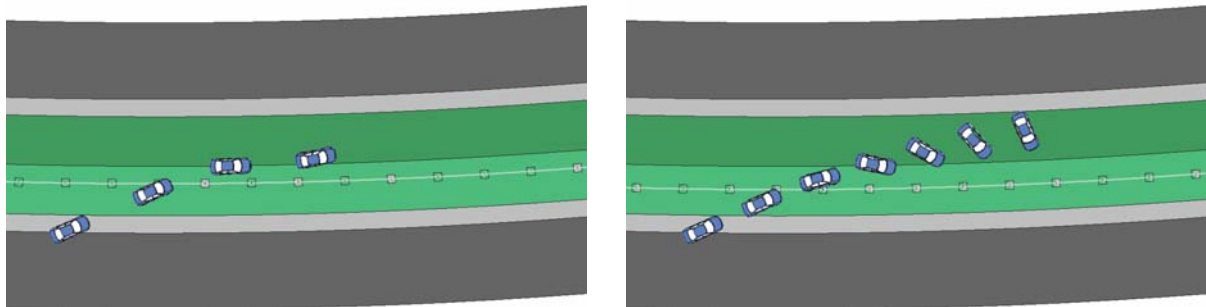
In this case, a retrofit CMB design was evaluated for its performance on four-lane freeways under vehicular impacts of the Dodge Neon and Ford F250. The retrofit design was obtained by lowering the middle and bottom cables in the current NCDOT design from 25.25 in (641 mm) and 20.5 in (521 mm) to 20.5 in (521 mm) and 17 in (432 mm), respectively. Also in the retrofit design, all three cables were placed on the opposite sides of the post as compared to the current NCDOT design.

The retrofit CMB was placed at two locations on the outer 6:1 slope: 6 ft (1.83 m) and 8 ft (2.44 m). The CMB was evaluated under both front-side and backside impacts at 62 mph (100 km/hr) and 25°. Table 4.3 summarizes the simulation results for both the Dodge Neon and Ford F250.

Table 4.3: Simulation results of vehicle impacting the retrofit CMB on a four-lane freeway

Impact Vehicle	Impact Side	Departure Angle	Distance of CMB from Median Centerline (CMB on Outer 6:1 Slope)	
			6 ft (1.83 m)	8 ft (2.44 m)
Dodge Neon	Front	25°	Retained within median	Retained within median
	Back	25°	Retained within median	Retained within median
Ford F250	Front	25°	Entered into travel lane	Entered into travel lane
	Back	25°	Retained within median	Entered into travel lane

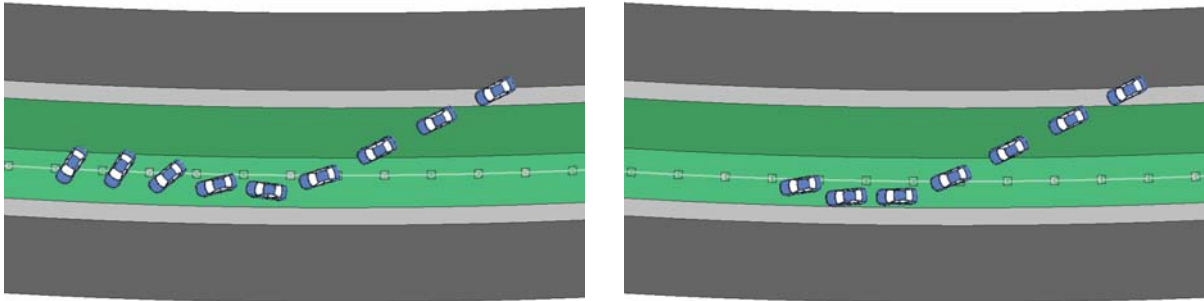
The simulation results showed that the retrofit design performed well at both locations under impacts of the Dodge Neon: the vehicle was retained within the median. It was also observed that cable engagement for the 6-ft (1.83 m) placement was slightly better than that for the 8-ft (2.44 m) placement for front-side impacts. For backside impacts, however, the cable engagement was slightly better at 8 ft (2.44 m) than at 6 ft (1.83 m). Figures 4.15 and 4.16 show the displacement paths of the Dodge Neon in the impact scenarios given in Table 4.3.



a. CMB placed at 6 ft

b. CMB placed at 8 ft

Fig. 4.15: Front-side impact at 25° by a Dodge Neon with the CMB (retrofit) on a four-lane freeway

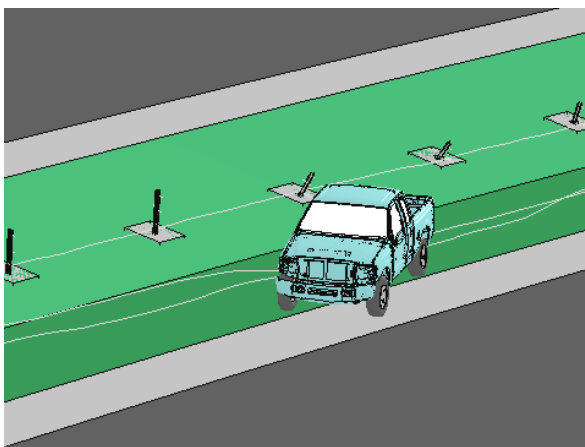


a. CMB placed at 6 ft

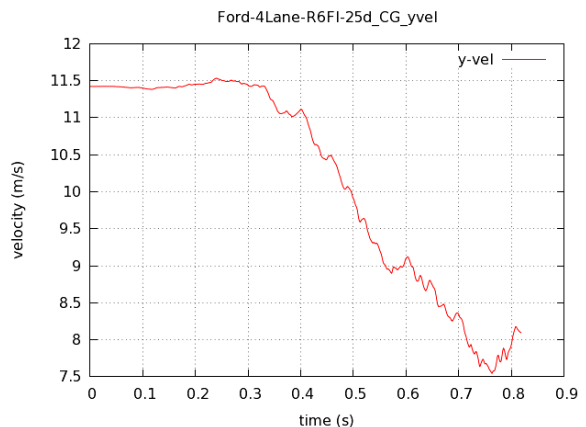
b. CMB placed at 8 ft

Fig. 4.16: Backside impact at 25° by a Dodge Neon with the CMB (retrofit) on a four-lane freeway

Under impacts of the Ford F250, the results for the CMB at 6 ft (1.83 m) were mixed: the vehicle was redirected for the backside impact, but overrode the CMB for the front-side impact due to the reduced effective cable heights. In the failed case, the vehicle only partially engaged with the top cable, which did not have enough post retention for the front-side hit. The partial engagement was not sufficient to fully redirect the vehicle, which eventually overrode all three cables and entered the opposing travel lane. At 8 ft (2.44 m), the CMB failed for both the front-side and backside impacts: the CMB did not have full cable engagement for the front-side impact and did not have enough traversal distance for cable deflection for the backside impact. Figures 4.17 to 4.19 show the instants of vehicle penetrations in the three failed cases, along with the time history of the vehicle's traversal velocity. Figures 4.20 and 4.21 show the displacement paths of the Ford F250 in the impact scenarios given in Table 4.3.

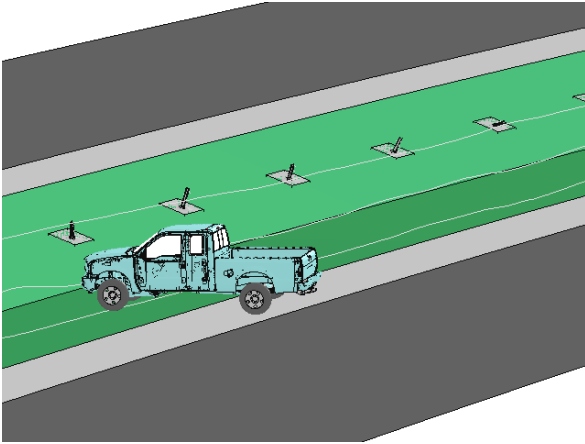


a. Ford F250 penetrating through CMB

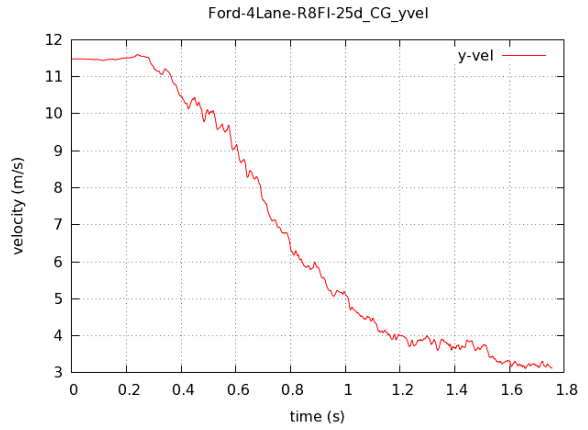


b. Time history of traversal velocity

Fig. 4.17: A Ford F250 impacting the CMB (retrofit) at 6 ft from the median centerline, 25° front-side impact

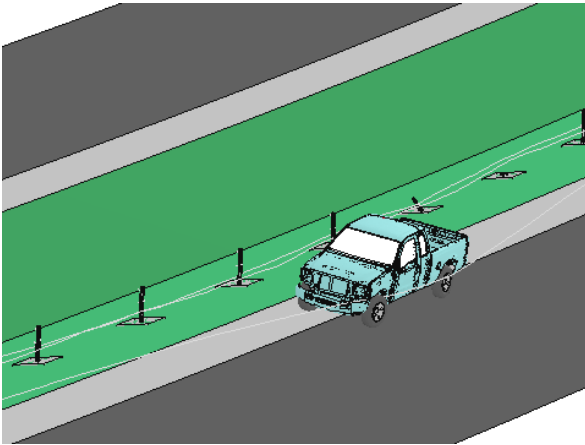


a. Ford F250 penetrating through CMB

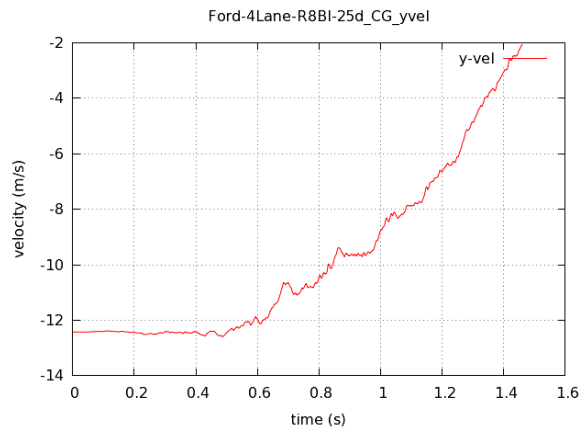


b. Time history of traversal velocity

Fig. 4.18: A Ford F250 impacting the CMB (retrofit) at 8 ft from the median centerline, 25° front-side impact

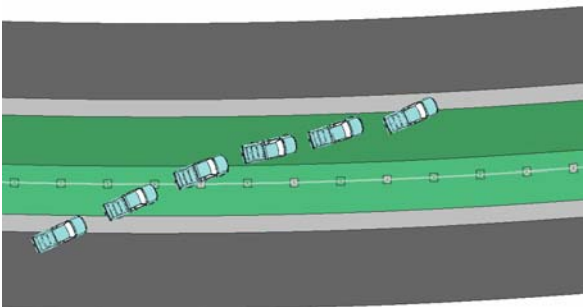


a. Ford F250 penetrating through CMB

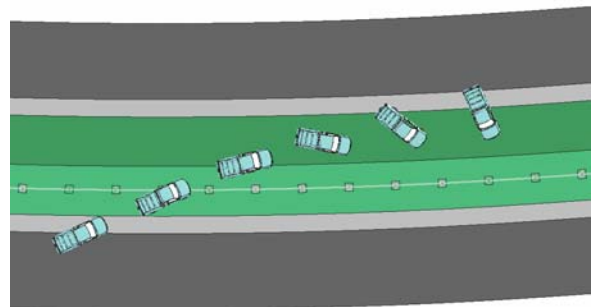


b. Time history of traversal velocity

Fig. 4.19: A Ford F250 impacting the CMB (retrofit) at 8 ft from the median centerline, 25° backside impact

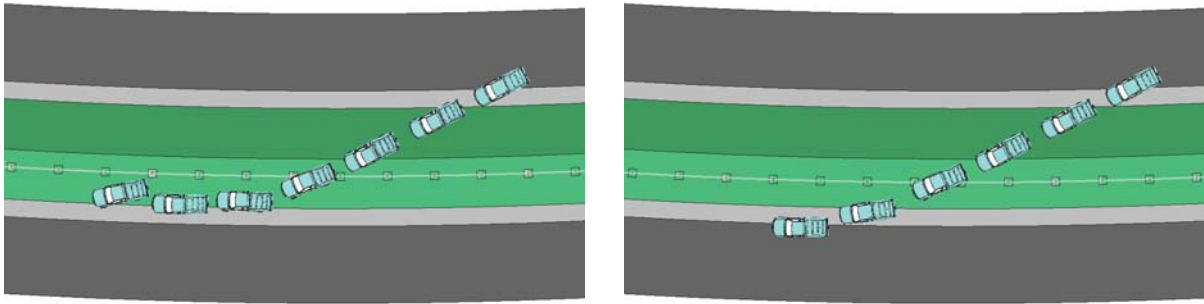


a. CMB placed at 6 ft



b. CMB placed at 8 ft

Fig. 4.20: Front-side impact at 25° by a Ford F250 with the CMB (retrofit) on a four-lane freeway



a. CMB placed at 6 ft

b. CMB placed at 8 ft

Fig. 4.21: Backside impact at 25° by a Ford F250 with the CMB (retrofit) on a four-lane freeway

The simulation results showed that the retrofit CMB was more effective at 6 ft (1.83 m) from the centerline than at 8 ft (2.44 m). Under impacts of the Ford F250, the retrofit CMB had slightly improved performance over the current design for a 25° backside impact, but degraded performance for a 25° front-side impact.

4.3 Case 3: CMB on 6:1 Slope of Six-lane Freeway

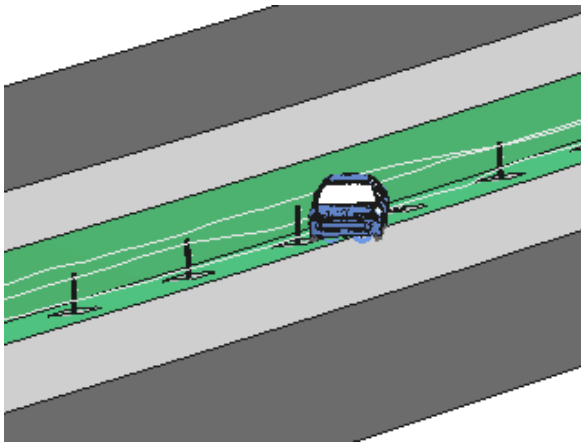
In this case, the NCDOT current CMB was placed on a six-lane freeway with a 46-ft (14 m) median. The median included two 14-ft (4.27 m) shoulders and the median slopes were 6:1 and 4:1 (see Fig. 1.7). The CMB was placed on the outer 6:1 slope at three distances from the median centerline: 4, 6, and 8 feet. The Dodge Neon and Ford F250 were used to impact the CMB from the front-side and backside; both were launched from the shoulder with an initial velocity of 62.1 mph (100 km/hr) and departure angles of 20°, 25°, and 30°. The simulation results of the Dodge Neon impacting the CMB are summarized in Table 4.4.

Table 4.4: Simulation results of Dodge Neon impacting the NCDOT CMB on a six-lane freeway

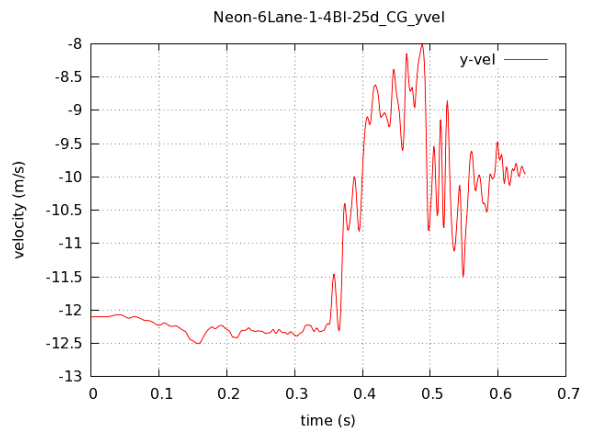
Impact Side	Departure Angle	Distance of CMB from Median Centerline (CMB on Outer 6:1 Slope)		
		4 ft (1.22 m)	6 ft (1.83 m)	8 ft (2.44 m)
Front	20°	Retained within median	Retained within median	Retained within median
	25°	Retained within median	Retained within median	Retained within median
	30°	Retained within median	Retained within median	Retained within median
Back	20°	Retained within median	Retained within median	Retained within median
	25°	Entered travel lane	Retained within median	Retained within median
	30°	Rollover on median	Retained within median	Entered travel lane

The simulation results showed that the CMB at 6 ft (1.83 m) performed the best under impacts of the Dodge Neon; the vehicle was retained within the median for all departure angles in both front-side and backside impacts. At 4 ft (1.22 m) from the median centerline, the CMB performed well in all three front-side impacts but failed in the case of the 25° backside impact. In this failed case, the vehicle under rode the top and middle cables and

overrode the bottom cable. This was mainly due to the suspension compression at the bottom of the ditch, similar to the vehicle penetration observed in a crash test where the CMB was installed 4 ft from the median centerline and impacted by a Ford Crown Victoria (WSDOT 2006). Figure 4.22 shows the instant when the vehicle penetrated through the CMB along with the time history of the vehicle's traversal velocity. It can be seen that the vehicle's traversal velocity was 10 m/sec at 0.64 seconds when the vehicle had lost engagement with all cables. This means that the vehicle will eventually enter the opposing travel lane. For the case of the 30° backside impact with the CMB placed at 4 ft (1.22 m), the vehicle rolled over within the median. The traversal velocity was found to be approximately zero at the last instance; so the vehicle would remain within the median.



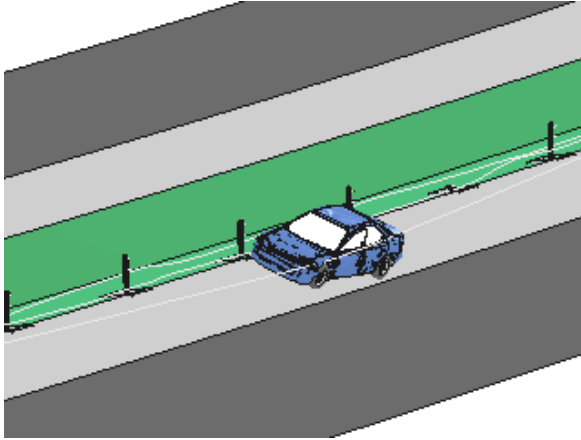
a. Dodge Neon penetrating through CMB



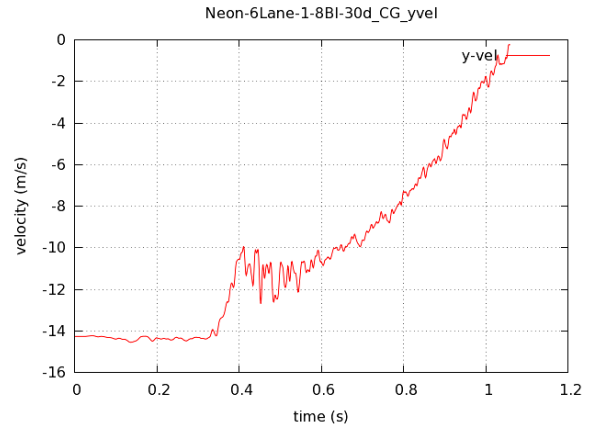
b. Time history of traversal velocity

Fig. 4.22: A Dodge Neon impacting the CMB placed at 4 ft from the median centerline, 25° backside impact

At 8 ft (2.44 m) from the centerline, the CMB successfully retained the vehicle within the median in all scenarios except for the 30° backside impact. In this failed case, the vehicle engaged with the cables and was redirected when partially entering the opposing travel lane. This was mainly due to the relatively short traversal distance (15 ft or 4.57 m) and the large impact angle. Figure 4.23 shows the instant when the vehicle penetrated through the CMB along with the time history of the vehicle's traversal velocity. It can be seen that the vehicle's traversal velocity was approximately zero at the instant shown in Fig. 23a. This means that the vehicle will not encroach further into the opposing travel lane.



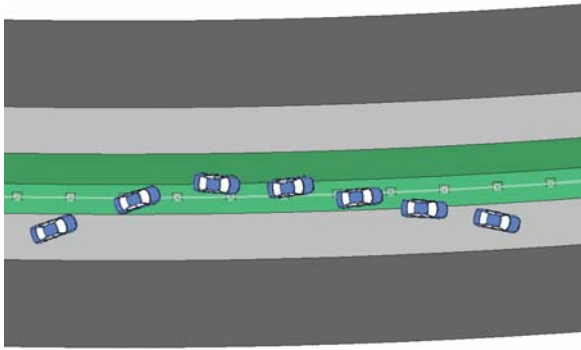
a. Dodge Neon penetrating through CMB



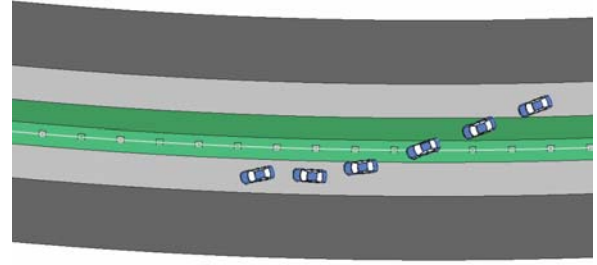
b. Time history of traversal velocity

Fig. 4.23: A Dodge Neon impacting the CMB placed at 8 ft from the median centerline, 30° backside impact

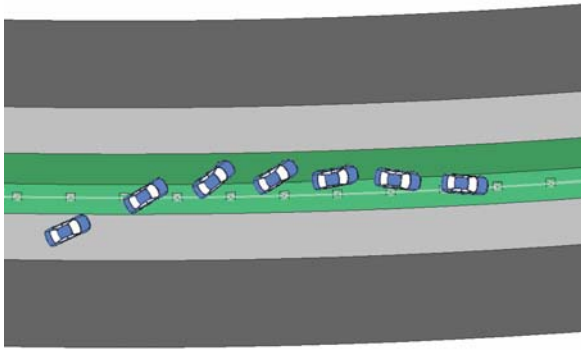
Figures 4.24 to 4.26 show the displacement paths of the Dodge Neon in the impact scenarios given in Table 4.4.



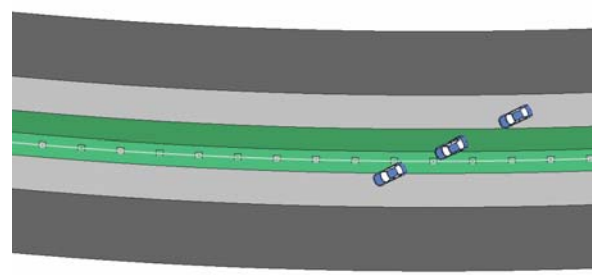
a. Front-side impact at 20°



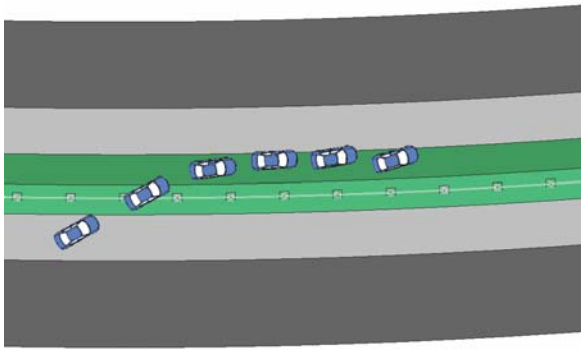
b. Backside impact at 20°



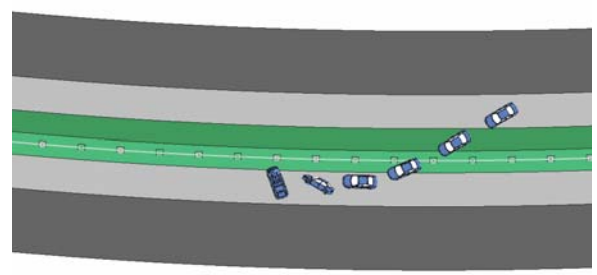
c. Front-side impact at 25°



d. Backside impact at 25°

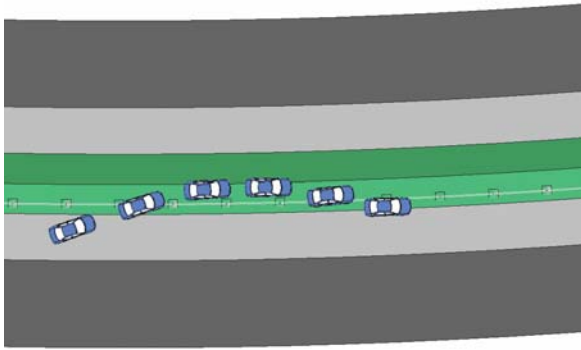


e. Front-side impact at 30°

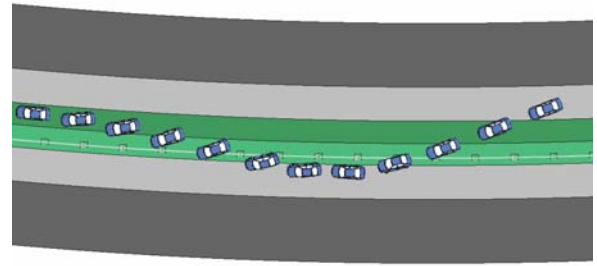


f. Backside impact at 30°

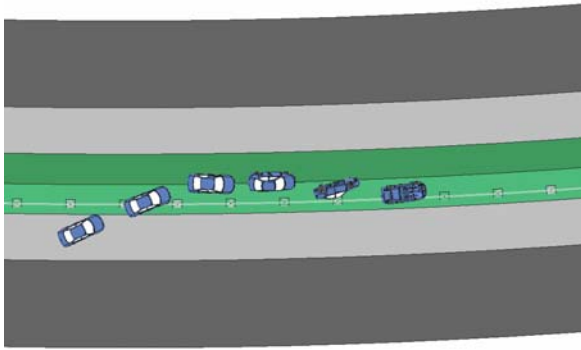
Fig. 4.24: Dodge Neon impacting the CMB placed at 4 ft from the median centerline on the 6:1 slope of a six-lane freeway



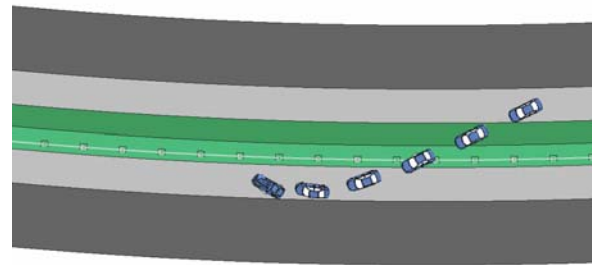
a. Front-side impact at 20°



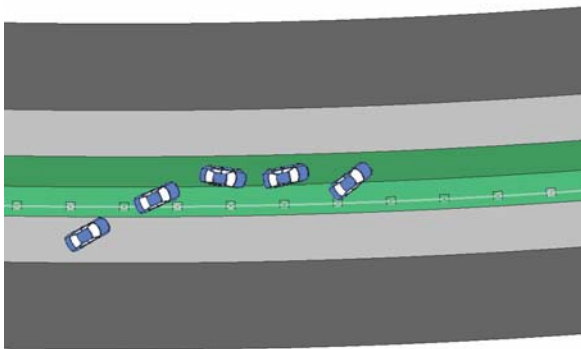
b. Backside impact at 20°



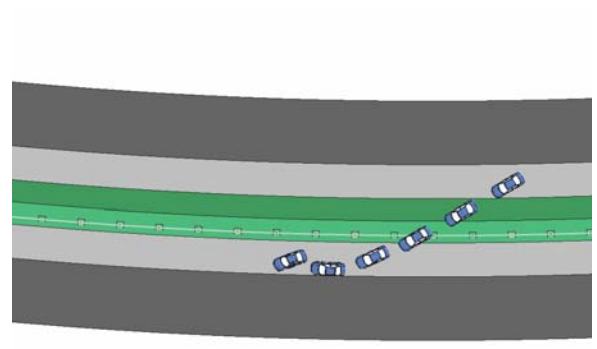
c. Front-side impact at 25°



d. Backside impact at 25°

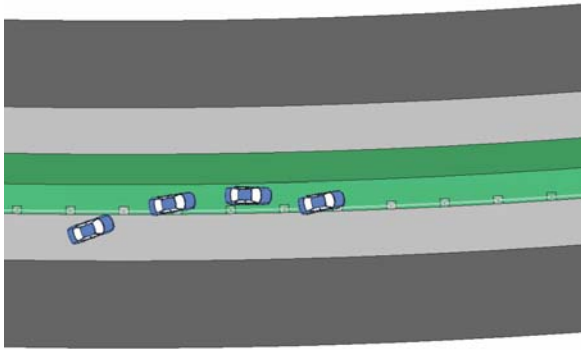


e. Front-side impact at 30°

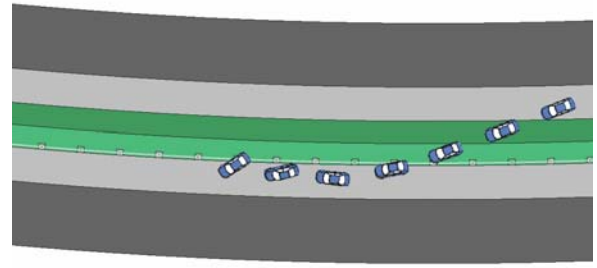


f. Backside impact at 30°

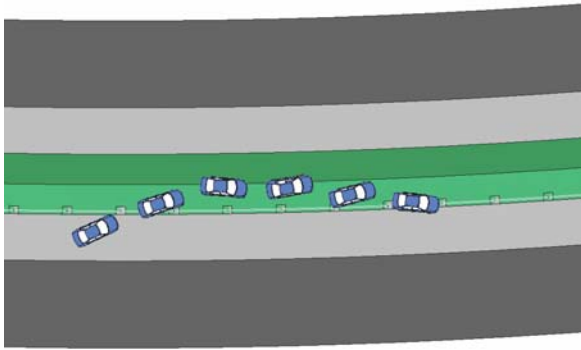
Fig. 4.25: Dodge Neon impacting the CMB placed at 6 ft from the median centerline on the 6:1 slope of a six-lane freeway



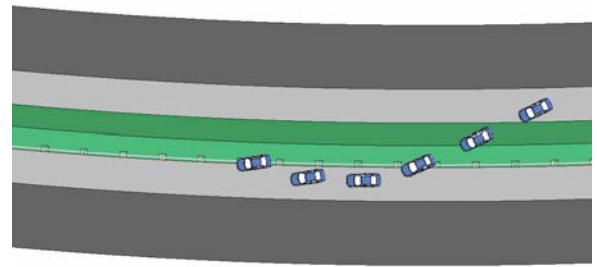
a. Front-side impact at 20°



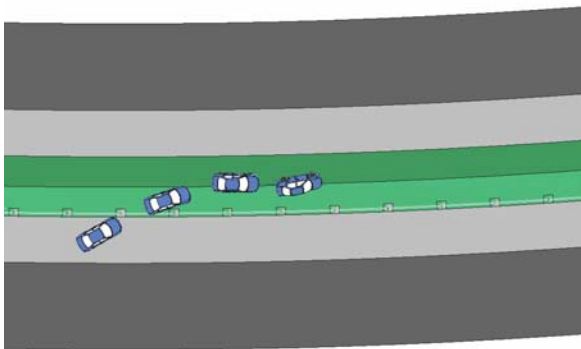
b. Backside impact at 20°



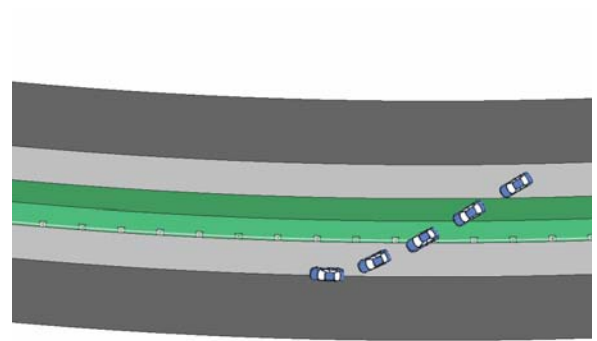
c. Front-side impact at 25°



d. Backside impact at 25°



e. Front-side impact at 30°



f. Backside impact at 30°

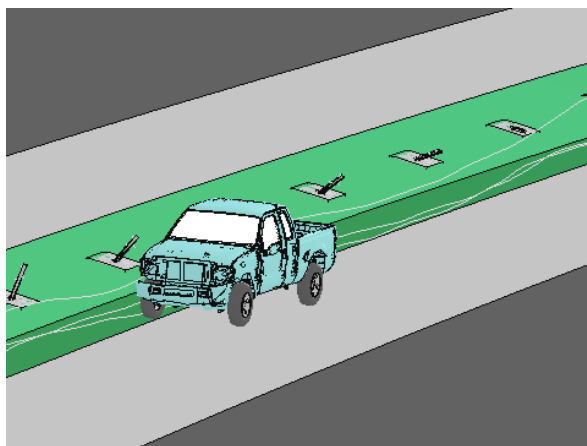
Fig. 4.26: Dodge Neon impacting the CMB placed at 8 ft from the median centerline on the 6:1 slope of a six-lane freeway

Table 4.5 summarizes the simulation results of the Ford F250 impacting the CMB placed at 4, 6, and 8 ft on a six-lane freeway.

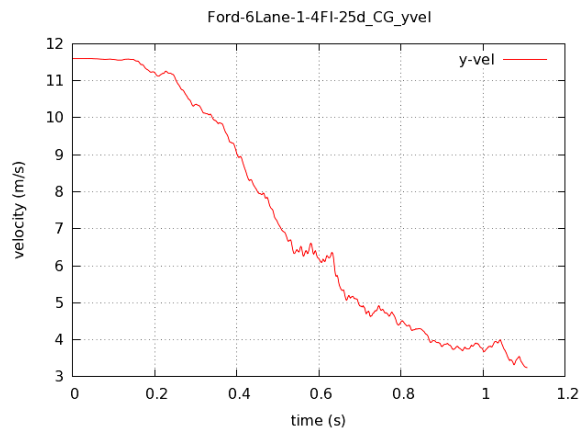
Table 4.5: Simulation results of Ford F250 impacting the NCDOT CMB on a six-lane freeway

Impact Side	Departure Angle	Distance of CMB from Median Centerline (CMB on Outer 6:1 Slope)		
		4 ft (1.22 m)	6 ft (1.83 m)	8 ft (2.44 m)
Front	20°	Retained within median	Retained within median	Retained within median
	25°	Entered travel lane	Retained within median	Retained within median
	30°	Entered travel lane	Entered travel lane	Retained within median
Back	20°	Retained within median	Entered travel lane	Rollover into travel lane
	25°	Retained within median	Entered travel lane	Rollover into travel lane
	30°	Entered travel lane	Entered travel lane	Rollover into travel lane

For front-side impacts by the Ford F250, the simulation results showed that the CMB at 8 ft (2.44 m) successfully retained the vehicle for all three angles. At 6 ft (1.83 m) from the centerline, the CMB was successful for the 20° and 25° impacts but failed for the 30° case in which the vehicle overrode the CMB after partial engagement with the cables on the vehicle’s lower body. At 4 ft (1.22 m), the CMB was successful only for the 20° impact; the vehicle overrode the CMB in the 25° and 30° impacts, similar to the case of the CMB at 6 ft (1.83 m) under the 30° impact. The results in Table 4.5 suggest that for front-side impacts by the larger vehicle (i.e., Ford F250), the further the CMB placed from the centerline, the better the vehicle-CMB engagement and thus the better the barrier’s performance. Figures 4.27 to 4.29 show the instants when the vehicle penetrates through the CMB for the above three failed cases in front-side impacts, along with the time history of the vehicle’s traversal velocity.

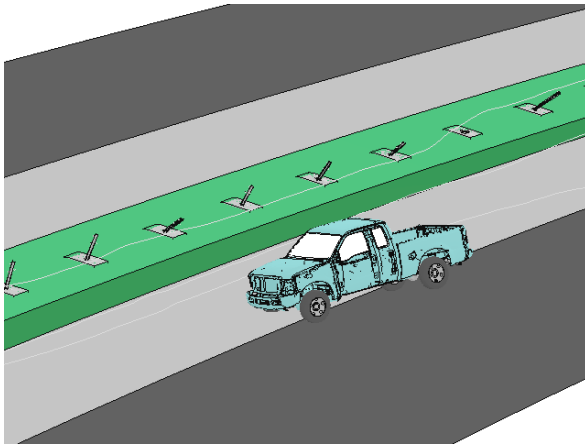


a. Ford F250 penetrating through CMB

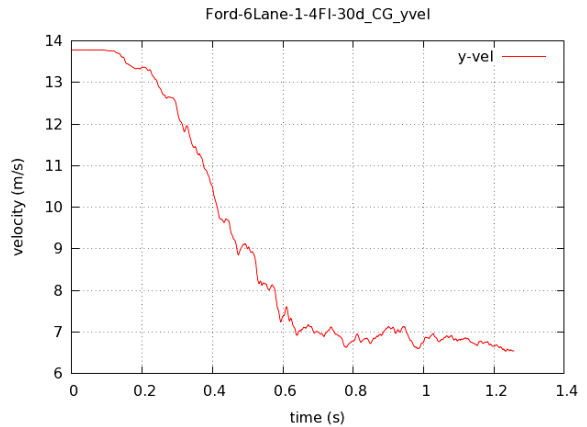


b. Time history of traversal velocity

Fig. 4.27: A Ford F250 impacting the CMB placed at 4 ft from the median centerline, 25° front-side impact

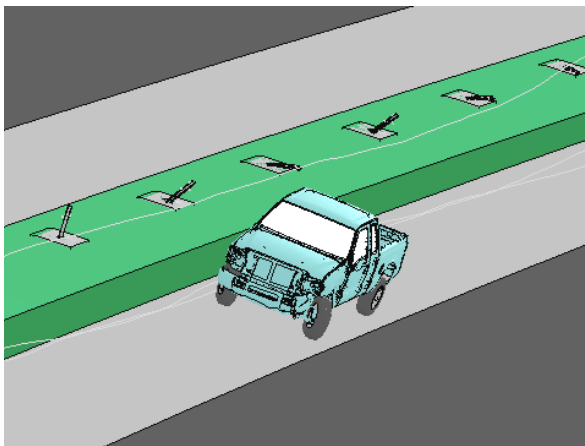


a. Ford F250 penetrating through CMB

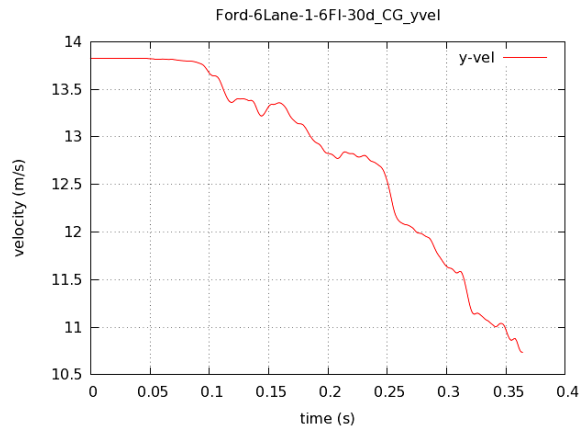


b. Time history of traversal velocity

Fig. 4.28: A Ford F250 impacting the CMB placed at 4 ft from the median centerline, 30° front-side impact



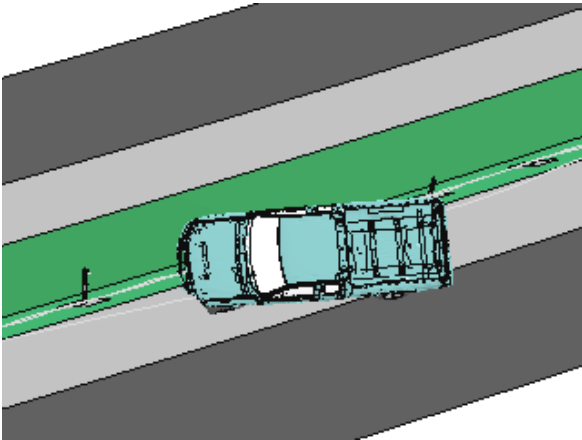
a. Ford F250 penetrating through CMB



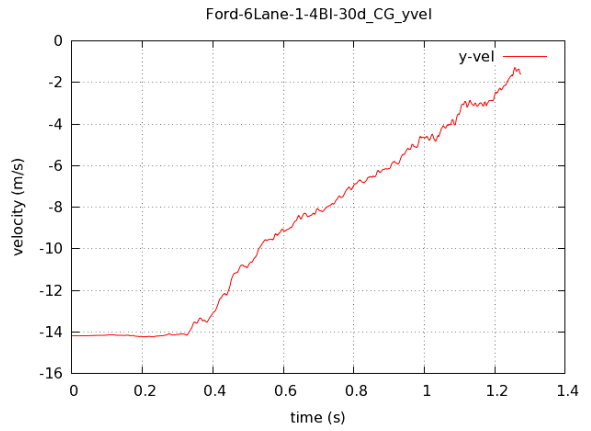
b. Time history of traversal velocity

Fig. 4.29: A Ford F250 impacting the CMB placed at 6 ft from the median centerline, 30° front-side impact

For backside impacts by the Ford F250, only two cases were successful: 20° and 25° impacts for the CMB placed at 4 ft (1.22 m) from the centerline. In the 30° impact at this location, the middle cable was engaged with the vehicle's lower body and caused the vehicle to roll over into the travel lane after it was redirected on the shoulder. At 6 ft (1.83 m), the CMB was able to engage with the vehicle, but the relatively short traversal distance was insufficient to redirect the vehicle before it entered the opposing travel lane. At 8 ft (2.44 m), the CMB had a similar issue as it did for the placement at 6 ft (1.83 m): short traversal distance. In addition, the vehicle experienced rollover for all the three departure angles. Figures 4.30 to 4.36 show the instants when the vehicle penetrates through the CMB for the seven failed cases in backside impacts, along with the time history of the vehicle's traversal velocity.

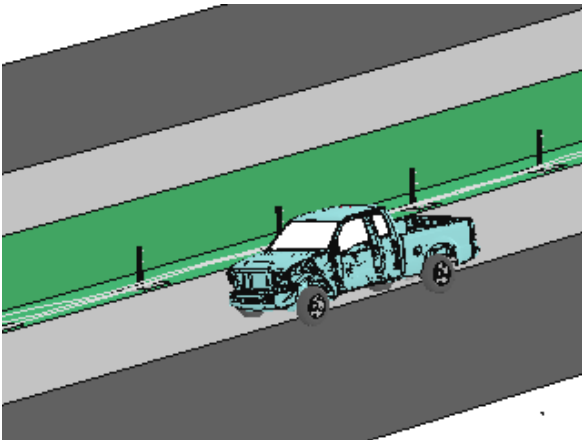


a. Ford F250 penetrating through CMB

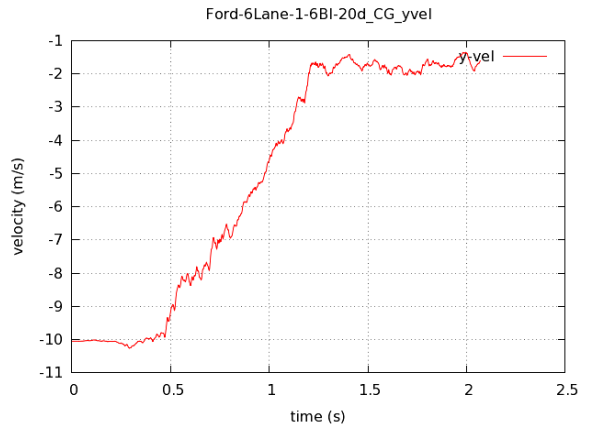


b. Time history of traversal velocity

Fig. 4.30: A Ford F250 impacting the CMB placed at 4 ft from the median centerline, 30° backside impact

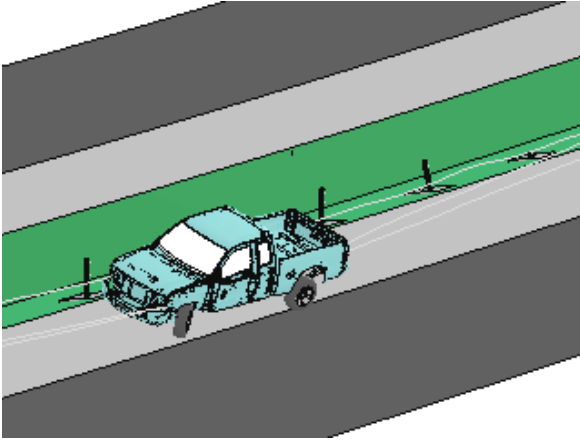


a. Ford F250 penetrating through CMB

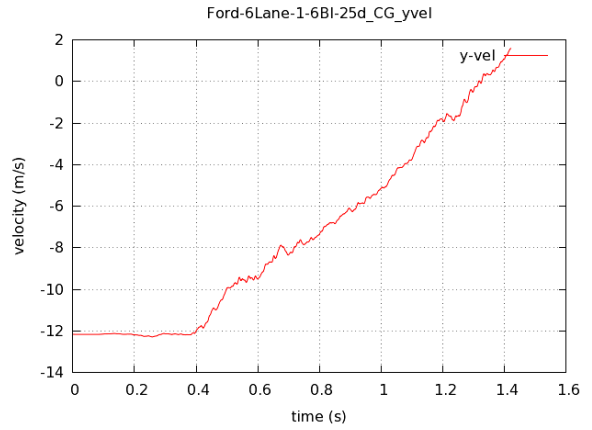


b. Time history of traversal velocity

Fig. 4.31: A Ford F250 impacting the CMB placed at 6 ft from the median centerline, 20° backside impact

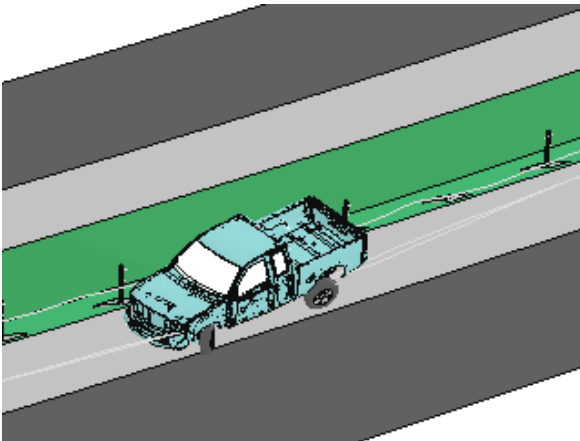


a. Ford F250 penetrating through CMB

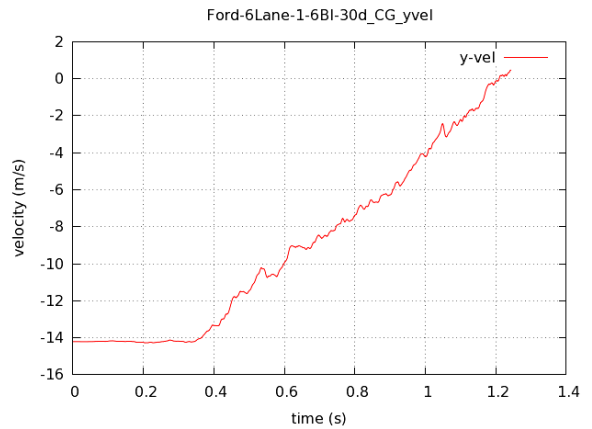


b. Time history of traversal velocity

Fig. 4.32: A Ford F250 impacting the CMB placed at 6 ft from the median centerline, 25° backside impact

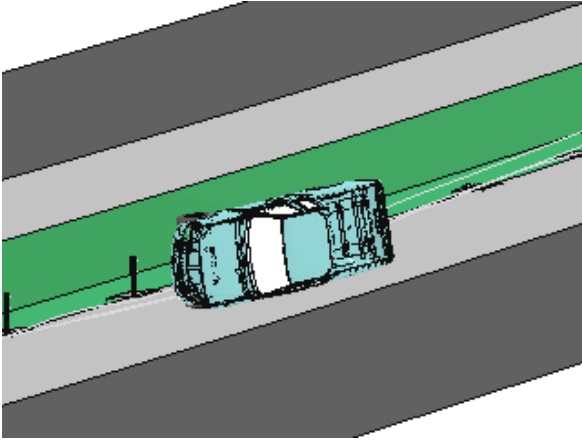


a. Ford F250 penetrating through CMB

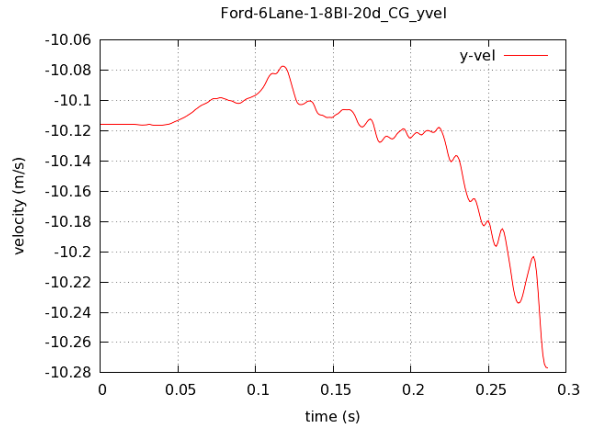


b. Time history of traversal velocity

Fig. 4.33: A Ford F250 impacting the CMB placed at 6 ft from the median centerline, 30° backside impact

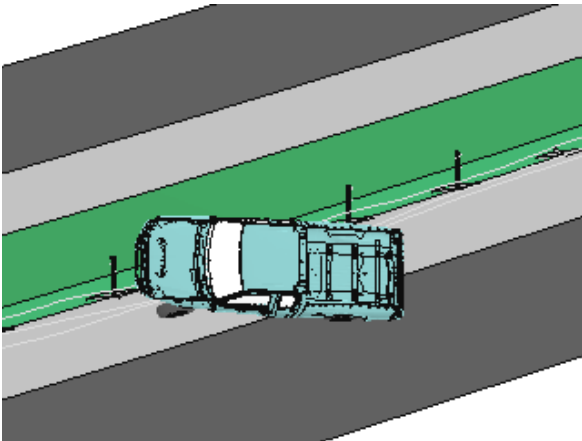


a. Ford F250 penetrating through CMB

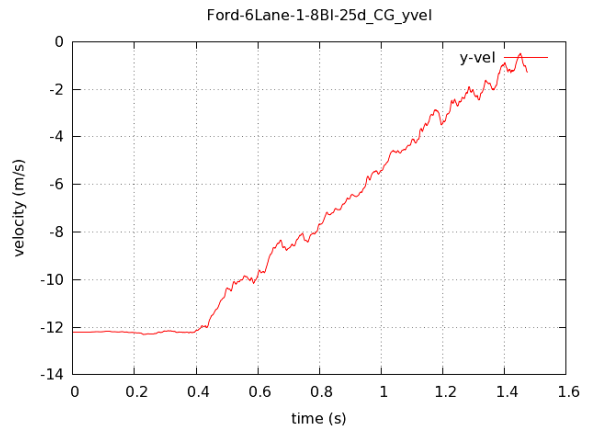


b. Time history of traversal velocity

Fig. 4.34: A Ford F250 impacting the CMB placed at 8 ft from the median centerline, 20° backside impact

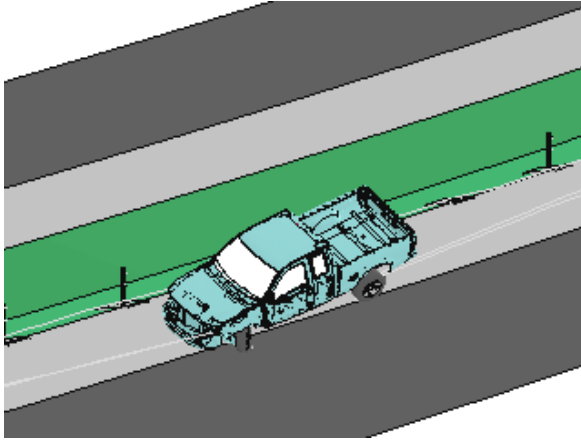


a. Ford F250 penetrating through CMB

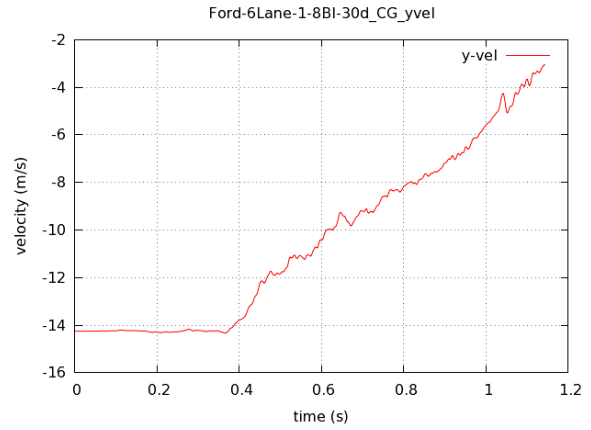


b. Time history of traversal velocity

Fig. 4.35: A Ford F250 impacting the CMB placed at 8 ft from the median centerline, 25° backside impact



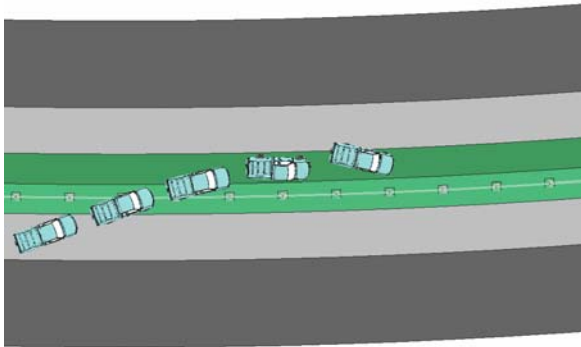
a. Ford F250 penetrating through CMB



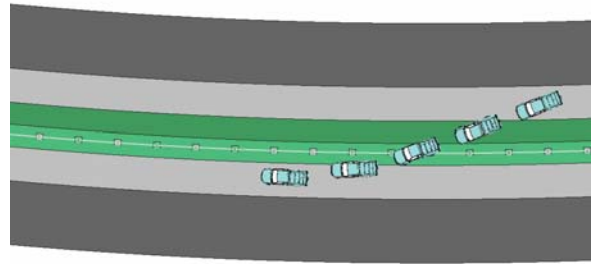
b. Time history of traversal velocity

Fig. 4.36: A Ford F250 impacting the CMB placed at 8 ft from the median centerline, 30° backside impact

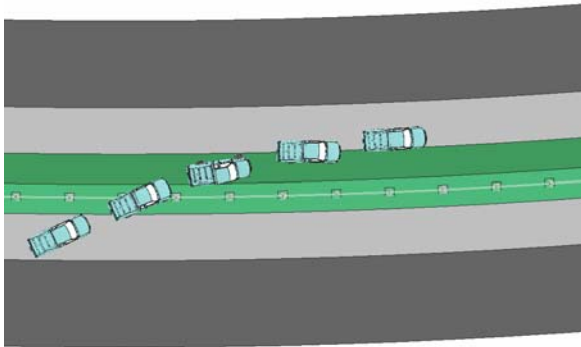
Figures 4.37 to 4.39 show the displacement paths of the Ford F250 for the impact scenarios given in Table 4.5.



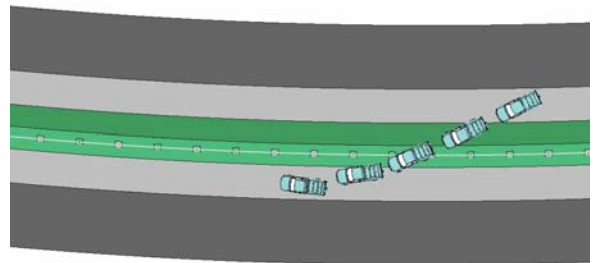
a. Front-side impact at 20°



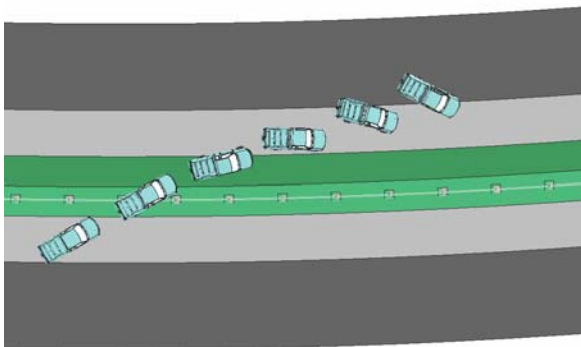
b. Backside impact at 20°



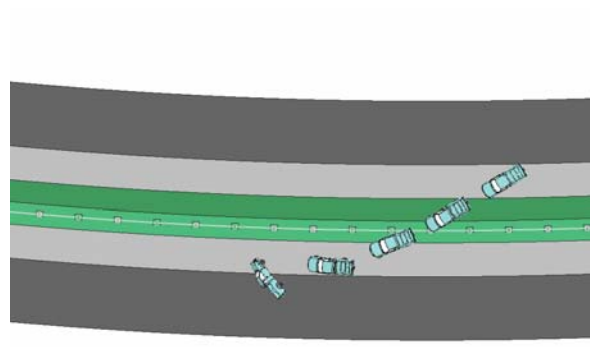
c. Front-side impact at 25°



d. Backside impact at 25°

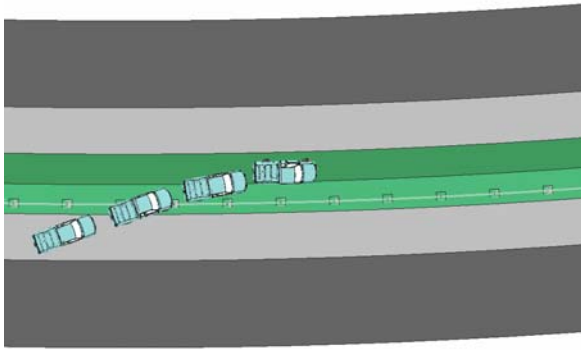


e. Front-side impact at 30°

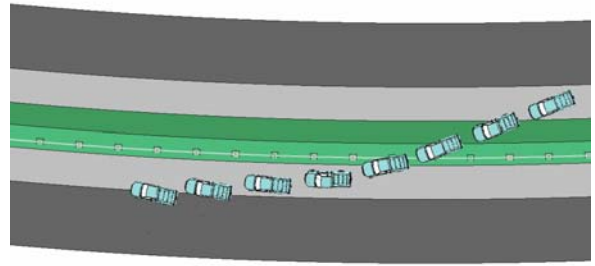


f. Backside impact at 30°

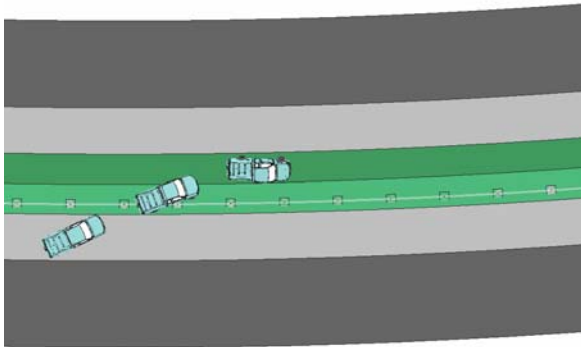
Fig. 4.37: A Ford F250 impacting the CMB placed at 4 ft from the median centerline on the 6:1 slope of a six-lane freeway



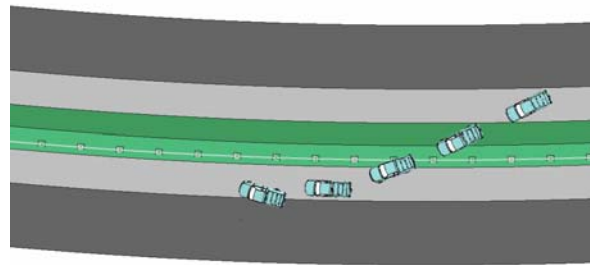
a. Front-side impact at 20°



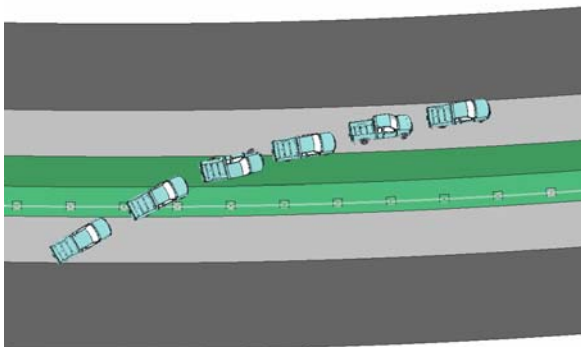
b. Backside impact at 20°



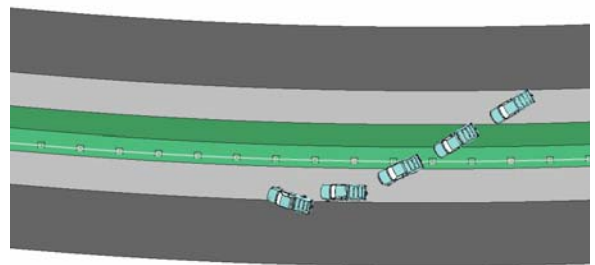
c. Front-side impact at 25°



d. Backside impact at 25°

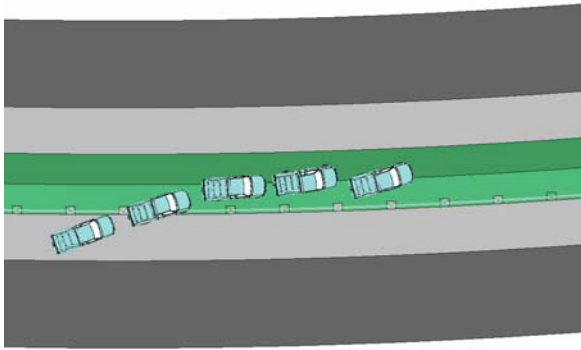


e. Front-side impact at 30°

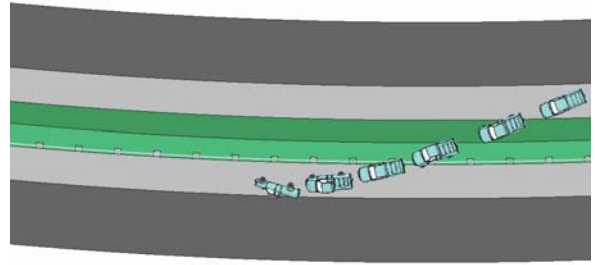


f. Backside impact at 30°

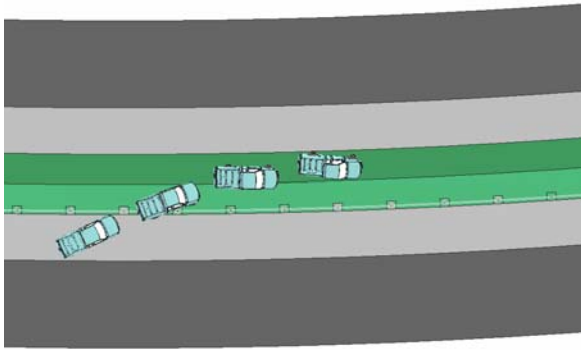
Fig. 4.38: Ford F250 impacting the CMB placed at 6 ft from the median centerline on the 6:1 slope of a six-lane freeway



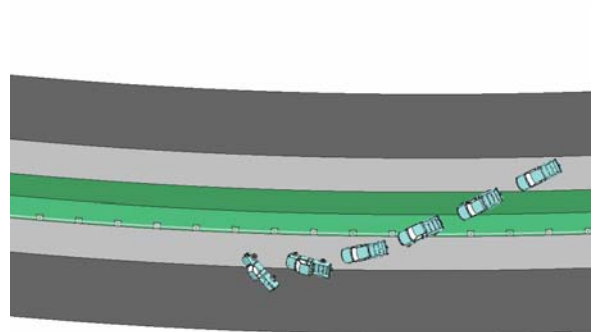
a. Front-side impact at 20°



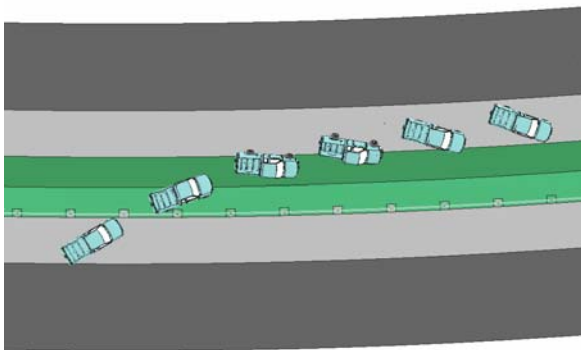
b. Backside impact at 20°



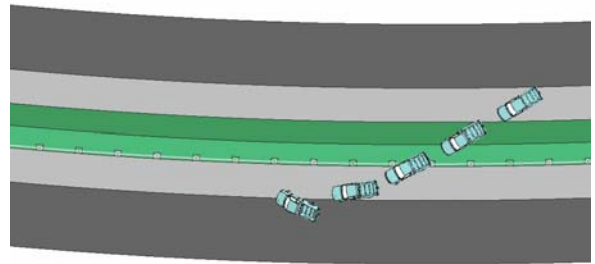
c. Front-side impact at 25°



d. Backside impact at 25°



e. Front-side impact at 30°



f. Backside impact at 30°

Fig. 4.39: Ford F250 impacting the CMB placed at 8 ft from the median centerline on the 6:1 slope of a six-lane freeway

It should be noted that for the CMB placed at 6 ft (1.83 m) the vehicle only partially entered the opposing travel lane in all three backside impacts. In these three backside impacts, the traversal velocity at the last instant indicated that the vehicle had started moving back towards the median centerline. Given that the impact conditions of the simulations represented the worst-case scenarios, the CMB should not be considered ineffective at this location. Nevertheless, compared to the simulation results of the four-lane freeway, it is evident that the 4:1 slope on the six-lane freeway degrades the CMB performance in a backside impact, though the CMB is placed on the 6:1 slope for both four-lane and six-lane freeways.

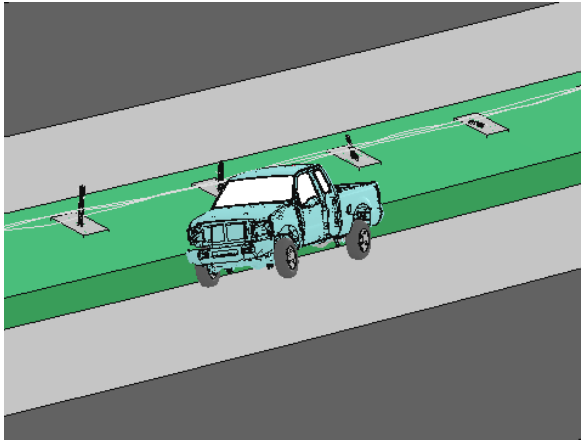
4.4 Case 4: CMB on 4:1 Slope of Six-lane Freeway

In this case, the CMB was placed at 6 ft (1.83 m) from the median centerline on the inner 4:1 slope of the six-lane freeway. The CMB was evaluated under front-side and backside impacts for the Dodge Neon and Ford F250 at 62.1 mph (100 km/hr) with a departure angle of 25°. Table 4.6 summarizes the simulation results for both vehicles.

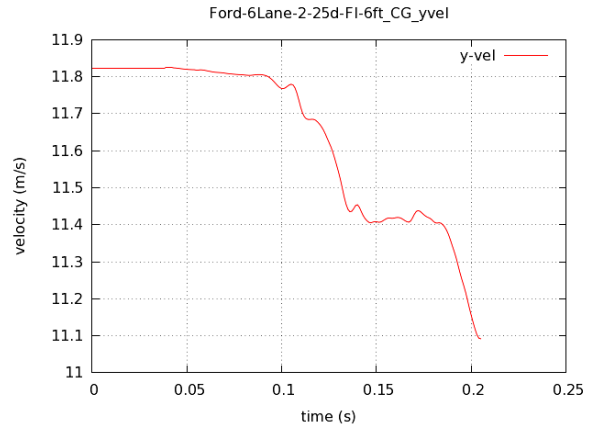
Table 4.6: Simulation results of vehicle impacting the NCDOT CMB on a six-lane freeway

Impact Vehicle	Impact Side	Departure Angle	Distance of CMB from Median Centerline (CMB on inner 4:1 Slope)
			6 ft (1.83 m)
Dodge Neon	Front	25°	Retained within median
	Back	25°	Retained within median
Ford F250	Front	25°	Entered travel lane
	Back	25°	Entered travel lane

For both front-side and backside impacts by the Dodge Neon, the CMB was able to retain the vehicle within the median. The CMB performance was similar to that installed on the 6:1 slope. For the Ford F250, the CMB at this location failed to retain the vehicle in both front-side and backside impacts. In the front-side impact, the vehicle overrode the CMB and entered the opposing travel lane with almost no redirection. In backside impact, the vehicle engaged with the top and middle cables, but entered the opposing travel lane before it was redirected due to the short traversal distance for cable deflection (i.e., 15 ft or 4.57 m). Compared to the results of Table 4.6 with those of Tables 4.4 and 4.5, the CMB appeared to have better performance on the 6:1 slope than on the 4:1 slope of a six-lane freeway. Figures 4.40 and 4.41 show the instants when the vehicle penetrates through the CMB for impacts by the Ford F250, along with the time history of the vehicle’s traversal velocity.

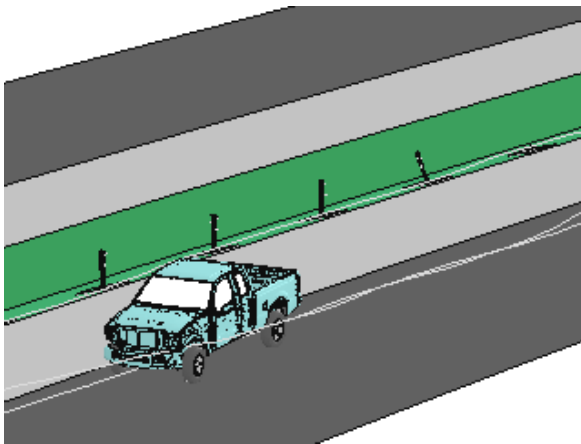


a. Ford F250 penetrating through CMB

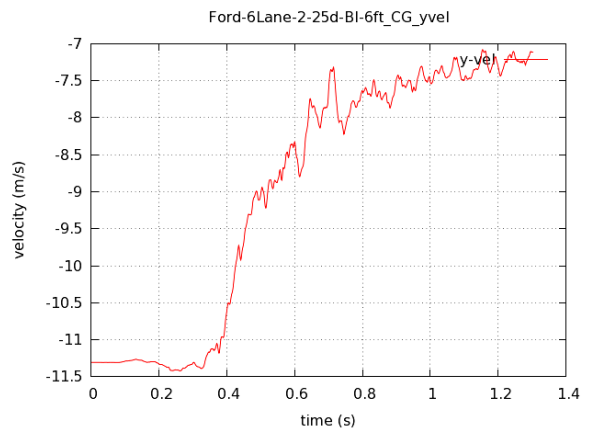


b. Time history of traversal velocity

Fig. 4.40: A Ford F250 impacting the CMB placed at 6 ft from the median centerline, 25° front-side impact



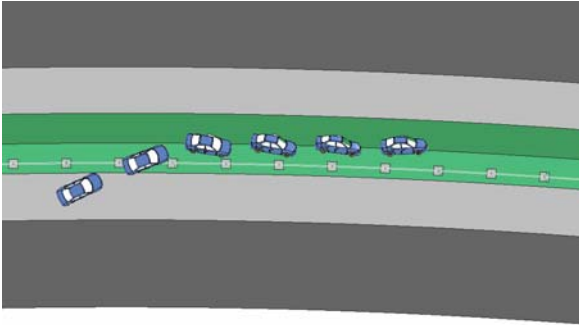
a. Ford F250 penetrating through CMB



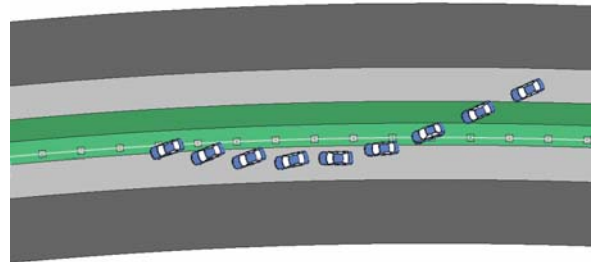
b. Time history of traversal velocity

Fig. 4.41: A Ford F250 impacting the CMB placed at 6 ft from the median centerline, 25° backside impact

Figures 4.42 and 4.43 show the displacement paths of the Dodge Neon and Ford F250 in the impact scenarios given in Table 4.6.

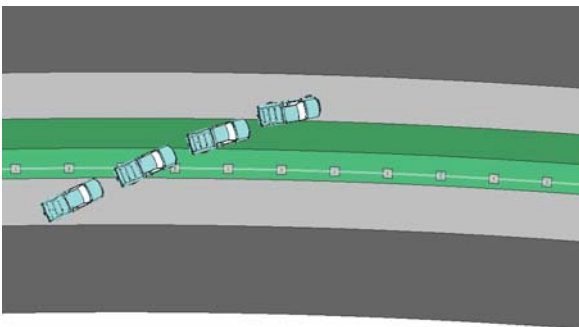


a. Front-side impact at 25°

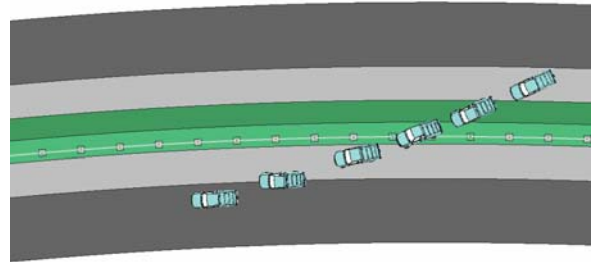


b. Backside impact at 25°

Fig. 4.42: A Dodge Neon impacting the CMB placed at 6 ft from the median centerline on the 4:1 slope of a six-lane freeway



a. Front-side impact at 25°



b. Backside impact at 25°

Fig. 4.43: A Ford F250 impacting the CMB placed at 6 ft from the median centerline on the 4:1 slope of a six-lane freeway

5. Findings and Conclusions

In this project, finite element simulations were performed to study the performance of the generic low-tension cable median barrier (CMB) for both a four-lane and six-lane freeway with a 46-foot median and a 3° horizontal curve. The CMB was evaluated under impacts of a small passenger car (1996 Dodge Neon) and a pick-up truck (2006 Ford F250) for both front-side and backside impacts. The initial velocity of the impacting vehicle was set at 62.1 mph (100 km/hr) and three different angles, 20°, 25°, and 30°, were used to launch the impacting vehicle from the shoulder on the freeway.

Four different CMB placement schemes were studied in this project: 1) the CMB with the current NCDOT design at 4, 6, and 8 ft (1.22, 1.83, and 2.44 m) from the median centerline on the outer 6:1 slope of the four-lane freeway; 2) a retrofit CMB design at 6 and 8 ft (1.83 and 2.44 m) from the median centerline on the outer 6:1 slope of the four-lane freeway; 3) the CMB with the current NCDOT design at 4, 6, and 8 ft (1.22, 1.83, and 2.44 m) from the median centerline on the outer 6:1 slope of the six-lane freeway; and 4) the CMB with the current NCDOT design at 6 ft (1.83 m) from the median centerline on the inner 4:1 slope of the six-lane freeway. The simulation results provided significant insight into the crash mechanisms of vehicles impacting CMBs on medians with a horizontal curve. Some of the major research findings are summarized as follows.

- The horizontal curvature was found to affect CMB performance. When impacted from the concave side of the CMB, the cables were found to generally deflect more than being impacted from the convex side. One contributing factor was the asymmetric shape of the CMB in relation to the impacts from both sides. Another factor might be the difference in actual impact angles: backside impact angles were found to be generally larger than the departure angles and front-side impact angles were generally smaller than the departure angles. At the same departure angle, the difference in impact angles could be as much as 2.5°, depending on the CMB location, departure angle, and vehicle size.
- On the four-lane freeway, the current NCDOT CMB was found to be generally effective under impacts of the Dodge Neon. The two unsuccessful cases were: the CMB placed at 6 ft (1.83 m) from the centerline in the 30° backside impact and the CMB placed at 8 ft (2.44 m) in the 25° backside impact. Under the impacts of the Ford F250, the CMB was shown to be more effective in front-side impacts than in backside impacts. The two cases in which the CMB failed were the 30° front-side impacts when the CMB was placed at 4 ft (1.22 m) and 8 ft (2.44 m). In backside impacts, placing the CMB at 4 ft (1.22 m) and 6 ft (1.83 m) appeared to be more effective than at 8 ft (2.44 m). In addition, the CMB was more effective in small-angle impacts than in large-angle impacts.
- The retrofit CMB when placed at 6 ft (1.83 m) and 8 ft (2.44 m) on the four-lane freeway performed the same as the current NCDOT CMB under the impact of the Dodge Neon at 25°. Under the impacts of the Ford F250, the performance of the retrofit CMB was the same in 25° backside impacts but worse in 25° front-side impacts than the current design. This degraded performance could be contributed to

the lower middle cable and the relative high vehicle profile in a front-side impact. Overall, the retrofit CMB was found to be more effective at 6 ft (1.83 m) than at 8 ft (2.44 m) under 25° impacts.

- On the six-lane freeway, the current NCDOT CMB was also found to be generally effective under impacts of the Dodge Neon. The two unsuccessful cases were: the CMB placed at 4 ft (1.22 m) from the median centerline in the 25° backside impact and the CMB placed at 8 ft (2.44 m) in the 30° backside impact. Under the impacts of the Ford F250, the CMB was shown to be more effective in front-side impacts than in backside impacts when placed at 6 ft (1.83 m) and 8 ft (2.44 m) from the median centerline. When placed at 4 ft (1.22 m) from the median centerline, the CMB was shown to be more effective in backside impacts than in front-side impacts. With the Ford F250, the CMB appeared to favor a larger distance from the median centerline in front-side impacts, and a shorter distance in backside impacts. Compared to the CMB on the four-lane freeway, the CMB on the six-lane freeway was shown to have slightly reduced performance in both front-side and backside impacts by the Ford F250.
- When placed on the inner 4:1 slope of the six-lane freeway, the CMB at 6 ft (1.83 m) was found to be effective under 25° front-side and backside impacts by the Dodge Neon, but ineffective under impacts by the Ford F250. On the 4:1 slope, the CMB did not engage well with the Ford F250 compared to the placement on the 6:1 slope of the six-lane freeway.

The simulation results suggested that the effectiveness of the CMB can be reduced on sloped medians with a horizontal curve, compared to their performance on flat terrain with no curvature (as currently tested to meet the NCHRP Report 350 or MASH requirements). A common issue on sloped medians is the increased potential of vehicle rollovers, particularly for large-sized vehicles. It was observed that the large-sized vehicle (i.e., Ford F250) had a greater tendency to rollover in a backside impact than in a front-side impact. Given the severe impact and site conditions used in this project, it is evident that the finite testing requirements for this project exceed the TL-3 requirements for both the NCHRP Report 350 and MASH.

The simulation results of this project should be used to interpret the performance trends of CMBs on four-lane and six-lane freeways with horizontal curvature. They should not be used to draw definitive conclusions about their performance for a specific crash event, because many factors that could affect their performance were not considered in the simulations of this project. These factors included, but were not limited to, impact locations along the longitudinal axes of the barriers, soil conditions, and driver behaviors. Nevertheless, finite element analysis was demonstrated to be a useful tool in crash analysis and could be used in future investigations for other research projects.

6. Recommendations

The finite element simulation results of this project showed that the current NCDOT CMB performed similarly on the 6:1 slope of the four-lane and six-lane freeways under impacts of a small-sized vehicle. The CMB was more effective under the impacts of a pickup truck when placed on the 6:1 slope of a four-lane freeway than on a six-lane freeway. With the consideration of all factors investigated (i.e., freeway types, median slopes, impacting vehicles, impact/departure angles, and NCHRP 350 / MASH test requirements), installing the CMB at 4 ft (1.22 m) from the median centerline on a 6:1 slope appears to perform within acceptable parameters. Based on simulation results of this project, placing the CMB on the 4:1 slope at 6 ft (1.83 m) from the median centerline of a six-lane freeway is not recommended.

It was observed from the simulation results that horizontal curvature increased cable deflections when the CMB was impacted from the concave side. A possible solution to reducing cable deflections could be increasing the retention forces of the posts by intertwining cables around posts, which could be investigated in future research.

7. Implementation and Technology Transfer Plan

In this project, cable median barriers (CMBs) were evaluated when placed on a four-lane and six-lane freeway with a 46-foot median, horizontal curvature, and 4:1 and 6:1 median slopes. All simulation results will be used by NCDOT engineers to assist them with placement of CMBs on horizontal curves where proposed or existing site specific conditions warrant its use. These recommendations will be used to identify potential areas for safety improvements and will assist with making a determination if there is a need to update cable guiderail placement standards and guidelines.

Detailed simulation results will be provided to NCDOT engineers for a comprehensive understanding in evaluating proposed roadside features and/or improving the safety performance of the current system. The modeling and simulation work, along with research findings, will be presented at technical conferences and submitted for publication in technical journals to help researchers and DOT engineers and researchers nationwide with similar needs. The research results of this project will be distributed to the public through this report, which will be made available by NCDOT.

References

1. AASHTO (2006). *Roadside Design Guide*, 3rd edition, American Association of State Highway and Transportation Officials, Washington, D.C.
2. Abdel-Aty, M., Pemmanaboina, R., and Hsia, L. (2006). "Assessing crash occurrence on urban freeways by applying a system of interrelated equations," *Transportation Research Record*, 1953, 1-9.
3. Alberson, D.C., Bligh, R.P., Buth, C.E., and Bullard, D.L., Jr. (2003). "Cable and wire rope barrier design considerations: review," *Transportation Research Record*, 1851, 95-104.
4. Alberson, D.C., Sheikh, N.M., and Chatham, L.S. (2007). "Guidelines for the selection of cable barrier systems," *NCHRP 20-7 (210) Final Report*, Transportation Research Board, National Research Council, Washington, D.C.
5. Albin, R. B., Bullard, D. L., and Menges, W. L. (2001). "Washington State cable median barrier," *Transportation Research Record*, 1743, 71-79.
6. Atahan, A.O. (2002). "Finite element simulation of a strong-post W-beam guardrail system," *Simulation*, 78(10), 587-599.
7. Atahan, A.O. (2003). "Impact behavior of G2 steel weak-post W-beam guardrail on nonlevel terrain," *International Journal of Heavy Vehicle Systems*, 10(3), 209-223.
8. Atahan, A.O. (2007). "Crashworthiness analysis of a bridge rail-to-guardrail transition," *Accident Analysis and Prevention*, in press.
9. Atahan, A.O., and Cansiz, O.F. (2005). "Crashworthiness analysis of a bridge rail-to-guardrail transition," *Finite Elements in Analysis and Design*, 41, 371-396.
10. Bi, J., Fang, H., and Weggel, D.C. (2010). "Finite element modeling of cable median barriers under vehicular impacts," *The 11th International Conference on Structures under Shock and Impact*, Tallinn, Estonia, July 28-30.
11. Bligh, R.P., Abu-Odeh, A.Y., Hamilton, M.E., and Seckinger, N.R. (2004). "Evaluation of roadside safety devices using finite element analysis," *Report 0-1816-1*, Texas Transportation Institute, College Station, TX.
12. Bligh, R.P., and Mak, K.K. (1999). "Crashworthiness of roadside features across vehicle platforms," *Transportation Research Record*, 1690, 68-77.
13. Bligh, R.P., Miaou, S.P., Lord, D., and Cooner, S. (2006). "Median barrier guidelines for Texas," *Report 0-4254-1*, Texas Transportation Institute, College Station, TX.
14. BMI-SG (2004). "Improved Guidelines for Median Safety," *NCHRP 17-14(2) Draft Report of Analysis Findings*, Transportation Research Board, National Research Council, Vienne, VA.
15. Bullard, D.L., and Menges, W.L. (1996). "Crash testing and evaluation of the WSDOT three strand cable rail system," Texas Transportation Institute, College Station, TX.
16. Bullard, D.L., and Menges, W.L. (2000). "NCHRP Report 350 Test 3-11 of the Washington three-strand cable barrier with New York cable terminal," Texas Transportation Institute, College Station, TX.
17. Caliendo, C., Guida, M., and Parisi, A. (2007). "A crash-prediction model for multilane roads," *Accident Analysis and Prevention*, 39, 657-670.

18. Choi, J., Kim, S., Heo, T.Y., and Lee, J. (2010). "Safety effects of highway terrain types in vehicle crash model of major rural roads," *KSCCE Journal of Civil Engineering*, 15(2), 405-412.
19. Donnell, E.T., Harwood, D.W., Bauer, K.M., Mason, J.M., and Pietrucha, M.T. (2002). "Cross-median collisions on Pennsylvania interstates and expressways," *Transportation Research Record*, 1784, 91-99.
20. ESI (2003). *PAM-CRASH Solver Reference Manual, v2003.1*, ESI Group.
21. Gabauer, D.J. and Gabler, H.C. (2009). "Differential rollover risk in vehicle-to-traffic barrier collisions," *Annals of Advances in Automotive Medicine*, Vol. 53.
22. Gabler, H.C., Gabauer, D.J., and Bowen, D. (2005). "Evaluation of cross median crashes," *Final Report FHWA-NJ-2005-004*, Rowan University, Glassboro, NJ.
23. Hiser, N.R., and Reid, J.D. (2005). "Modeling slip base mechanisms," *International Journal of Crashworthiness*, 10(5), 463-472.
24. Hiss, J.G. F., Jr., and Bryden, J.E. (1992). "Traffic barrier performance," *Report 155*, New York State Department of Transportation, Albany, NY.
25. Hu, W. and Donnell, E.T. (2010). "Median barrier crash severity: Some new insights," *Accident Analysis and Prevention*, 42, 1697-1704.
26. Hunter, W.W., Stewart, J.R., Eccles, K.A., Huang, H.F., Council, F.M., and Harkey, D.L. (2001). "Three-strand cable median barrier in North Carolina: in-service evaluation," *Transportation Research Record*, 1743, 97-103.
27. Kan, C.D., Marzougui, D., Bahouth, G.T., and Bedewi, N.E. (2001). "Crashworthiness evaluation using integrated vehicle and occupant finite element models," *International Journal of Crashworthiness*, 6, 387-398.
28. Lewis, B. A. (2004). "Manual for LS-DYNA soil material model 147," *FHWA-HRT-04-095*, U.S. Department of Transportation, Federal Highway Administration, McLean, VA.
29. LSTC (2007). *LS-DYNA Keyword User's Manual, version 971*, Livermore Software Technology Corporation (LSTC), Livermore, CA.
30. Lu, G., Chitturi, M.V., Ooms, A.W. and Noyce, D.A. (2010). "Ordinal discrete choice analyses of wisconsin cross-median crash severities," *Transportation Research Record*, 2148, 47-58.
31. Lynch, J.M., Crowe, N.C., and Rosendahl, J.F. (1993). "Interstate across median accident study: a comprehensive study of traffic accidents involving errant vehicles which cross the median divider strips on North Carolina interstate highways," In: 1993 AASHTO Annual Meeting Proceedings, Publisher American Association of State Highway and Transportation Officials, 125-133.
32. MacDonald, D.B. and Batiste, J.R. (2007). "Cable Median Barrier - Reassessment and Recommendations," *WSDOT Report*, Washington State Department of Transportation, Olympia, WA.
33. Mackerle, J. (2003). "Finite element crash simulations and impact-induced injuries: an addendum. a bibliography (1998–2002)," *The Shock and Vibration Digest*, 35(4), 273-280.
34. Marzougui, D., Bahouth, G., Eskandarian, A., Meczkowski, L., and Taylor, H. (2000). "Evaluation of portable concrete barriers using finite element simulation," *Transportation Research Record*, 1720, 1-6.

35. Marzougui, D., Kan, C.D., and Opiela, K. (2010). "Comparison of the crash test and simulation of an angle impact of a 2007 Chevrolet Silverado pick-up truck into a New Jersey-shaped concrete barrier for MASH conditions," The National Crash Analysis Center, The George Washington University.
36. Marzougui, D., Kan, C.D., McGinnis, R.G., and Opiela, K. (2009). "Analyzing the effects of end-anchor spacing & initial tension on cable barrier deflection using computer simulation," *NCAC 2009-W-007*.
37. Marzougui, D., Mahadevaiah, U., Kan, C.D., Opiela, K. (2009). "Analyzing the effects of cable barriers behind curbs using computer simulation," *NCAC 2009-W-008*.
38. Marzougui, D., Mahadevaiah, U., Tahan, F., Kan, C.D., McGinnis, R., Powers, R. (2012). "Guidance for the selection, use, and maintenance of cable barrier systems," NCHRP Report 711, Transportation Research Board, National Research Council, Washington, D.C.
39. Marzougui, D., Mohan, P., Kan, C.D., and Opiela, K. (2007). "Performance evaluation of low-tension three-strand cable median barriers," *Transportation Research Record*, 2025, pp. 34-44.
40. Marzougui, D., Mohan, P., Kan, C.D., and Opiela, K. (2007a). "Performance evaluation of low-tension three-strand cable median barriers," *Transportation Research Record*, to be published.
41. Marzougui, D., Mohan, P., Kan, C.D., and Opiela, K. (2007b). "Evaluation of rail height effects on the safety performance of W-beam barriers," *2007 TRB Annual Meeting*, Washington, D.C.
42. Marzougui, D., Samaha, R.R., Cui, C., and Kan, C.D. (2012). "Extended validation of the finite element model for the 2007 Chevrolet Silverado pick-up truck," *NCAC 2012-W-003*.
43. Marzougui, D., Zink, M., Zaouk, A.K., Kan, C.D., and Bedewi, N.E. (2004). "Development and validation of a vehicle suspension finite element model for use in crash simulations," *International Journal of Crashworthiness*, 9(6), 565-576.
44. MASH-1 (2009). *Manual for Assessing Safety Hardware*, 1st ed., American Association of State and Highway Transportation Officials, Washington, D.C.
45. Medina, J.C. and Benekohal, R.F. (2006) "High Tension Cable Median Barrier: A Scanning Tour Report".
46. Medina, J.C. and Benekohal, R.F. (2006). "A scanning tour to identify effective and efficient approaches of reducing the number and severity of freeway median crossover crashes," *Report No, FHWA-IL/UI-TOL-18*, Department of Civil and Environmental Engineering, University of Illinois at Urbana-Champaign.
47. Miaou, S.P., Bligh, R.P., and Lord, D. (2005). "Developing guidelines for median barrier installation: benefit-cost analysis with Texas data," *Transportation Research Record*, 1904, 3-19.
48. Miaou, S.P., Hu, P.S., Wright, T., Rathi, A.K., and Davis, S.C. (1992). "Relationship between truck accidents and highway geometric design: a poisson regression approach," *Transportation Research Record*, 1376, 10-18.
49. Mohamedshah, Y.M., Paniati, J.F., and Hobeika, A.G. (1993). "Truck accident models for interstates and two-lane rural roads," *Transportation Research Record*, 1407, 35-41.

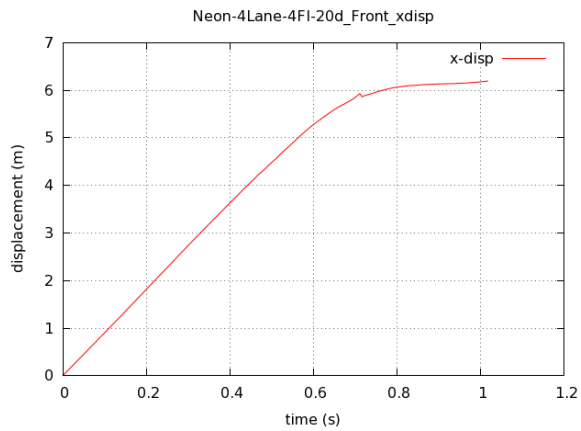
50. Mohan, P., Marzougui, D., and Kan, C.D. (2007). "Validation of a single unit truck model for roadside hardware impact," *International Journal of Vehicle Systems Modelling and Testing*, 2(1), 1-15.
51. Mohan, P., Marzougui, D., Meczkowski, L., and Bedewi, N. (2005). "Finite element modeling and validation of a 3-strand cable guardrail system," *International Journal of Crashworthiness*, 10, 267-273.
52. Murphy, B. (2006). "Cable Median Barrier/Rumble Strips in North Carolina," *In: 57th Annual Traffic and Safety Conference*, Missouri Department of Transportation, Columbia, MO.
53. Murray, Y. D. (2007). "Users manual for LS-DYNA concrete material model 159," *FHWA-HRT-05-062*, U.S. Department of Transportation, Federal Highway Administration, McLean, VA.
54. Murray, Y.D., Reid, J.D., Faller, R.K., Bielenberg, B.W., and Paulsen, T.J. (2005). "Evaluation of LS-DYNA Wood Material Model 143," *FHWA-HRT-04-096*, U.S. Department of Transportation, Federal Highway Administration, McLean, VA.
55. Mussa, R. and Chimba, D. (2006). "Analysis of crashes occurring on Florida six-lane roadways," *Advances in Transportation Studies*, 8, 43-56.
56. NCAC (web1). "NCAC Finite Element Models," <http://www.ncac.gwu.edu/vml/models.html>.
57. NCAC. (web2). "NCAC Publications," <http://www.ncac.gwu.edu/filmlibrary/publications.html>.
58. NCDOT (2002). *Roadway design manual*, North Carolina Department of Transportation, Raleigh, NC.
59. NCDOT (2005). "Median Barriers in North Carolina – Long Term Evaluation," *NCDOT Safety Evaluation Group*, Traffic Safety Systems Management Section, AASHTO TIG Initiative for "Cable Median Barrier" (TIG-CMB), Raleigh, NC.
60. NCDOT (2006). *Roadway Standard Drawings*, North Carolina Department of Transportation, Raleigh, NC.
61. Opiela, K., Kan, C.D., and Marzougui, D. (2009). "Development & initial validation of a 2007 Chevrolet Silverado finite element model," National Crash Analysis Center, George Washington University.
62. Orengo, F., Ray, M.H., and Plaxico, C.A. (2003). "Modeling tire blow-out in roadside hardware simulations using LS-DYNA," *In: 2003 ASME International Mechanical Engineering Congress & Exposition*, Washington, D.C., IMECE2003-55057.
63. Pande, A. and Abdel-Aty, M. (2009). "A novel approach for analyzing severe crash patterns on multilane highways," *Accident Analysis and Prevention*, 41, 985-994.
64. Patzner, G.S., Plaxico, C.A., and Ray, M.H. (1999). "Effects of post and soil strength on performance of modified eccentric loader breakaway cable terminal," *Transportation Research Record*, 1690, 78-83.
65. Plaxico, C.A., Hackett, R. M., and Uddin, W. (1997). "Simulation of a vehicle impacting a modified thrie-beam guardrail," *Transportation Research Record*, 1599, 1-10.
66. Plaxico, C.A., Mozzarelli, F., and Ray, M.H. (2003). "Tests and simulation of a w-beam rail-to-post connection," *International Journal of Crashworthiness*, 8(6), 543-551.

67. Plaxico, C.A., Patzner, G. S., and Ray, M.H. (1998). "Finite element modeling of guardrail timber posts and the post-soil interaction," *Transportation Research Record*, 1647, 139-146.
68. Plaxico, C.A., Ray, M.H., and Hiranmayee, K. (2000). "Impact Performance of the G4(1W) and G4(2W) guardrail systems: comparison under NCHRP Report 350 Test 3-11 conditions," *Transportation Research Record*, 1720, 7-18.
69. Ray, M.H. (1996a). "Repeatability of full-scale crash tests and criteria for validating simulation results," *Transportation Research Record*, 1528, 155-160.
70. Ray, M.H. (1996b). "Use of finite element analysis in roadside hardware design," *Transportation Research Circular*, 453, 61-71.
71. Ray, M.H., and McGinnis, R. G. (1997). "NCHRP Synthesis of Highway Practice 244: Guardrail and Median Barrier Crashworthiness," *Transportation Research Board*, National Research Council, Washington, D.C.
72. Ray, M.H., and Patzner, G. S. (1997). "Finite element model of modified eccentric loader terminal (MELT)," *Transportation Research Record*, 1599, 11-21.
73. Ray, M.H., and Weir, J. A. (2001). "Unreported collisions with post-and-beam guardrails in Connecticut, Iowa, and North Carolina," *Transportation Research Record*, 1743, 111-119.
74. Ray, M.H., Oldani, E., and Plaxico, C.A. (2004). "Design and analysis of an aluminum F-shape bridge railing," *International Journal of Crashworthiness*, 9(4), 349-363.
75. Ray, M.H., Weir, J., and Hopp, J. (2003). "In-service performance of traffic barriers," *NCHRP Report 490*, Transportation Research Board, National Research Council, Washington, D.C.
76. Reid, J. D., and Coon, B.A. (2002). "Finite element modeling of cable hook bolts," In: *7th International LS-DYNA User Conference*, Dearborn, MI.
77. Reid, J.D. (1996). "Towards the understanding of material property influence on automotive crash structures," *Thin-Walled Structures*, 24, 285-313.
78. Reid, J.D. (1998). "Admissible modeling errors or modeling simplifications," *Finite Elements in Analysis and Design*, 29, 49-63.
79. Reid, J.D. (1998). "Critical Impact Point for Longitudinal Barriers," Highway Division.
80. Reid, J.D. (2004). "LS-DYNA simulation influence on roadside hardware," *Transportation Research Record*, 1890, 34-41.
81. Reid, J.D., and Bielenberg, B.W. (1999). "Using LS-DYNA simulation to solve a design problem: bullnose guardrail example," *Transportation Research Record*, 1690, 95-102.
82. Reid, J.D., and Hiser, N.R. (2004). "Friction modelling between solid elements," *International Journal of Crashworthiness*, 9(1), 65-72.
83. Reid, J.D., and Hiser, N.R. (2005). "Detailed modeling of bolted joints with slippage," *Finite Elements in Analysis and Design*, 41, 547-562.
84. Reid, J.D., and Marzougui, D. (2002). "Improved truck model for roadside safety simulations: Part I - structural modeling," *Transportation Research Record*, 1797, 53-62.
85. Reid, J.D., Coon, B.A., Lewis, B.A., Sutherland, S.H., and Murray, Y.D. (2004). "Evaluation of LS-DYNA Soil Material Model 147," *FHWA-HRT-04-094*, U.S. Department of Transportation, Federal Highway Administration, McLean, VA.

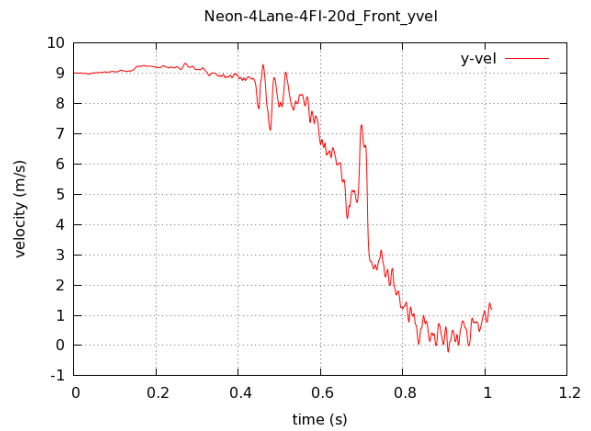
86. Reid, J.D., Kuipers, B.D., Sicking, D.L., and Faller, R.K. (2009). "Impact performance of W-beam guardrail installed at various flare rates," *International Journal of Impact Engineering*, 36, 476-485.
87. Ross Jr, H. E., and Sicking, D.L. (1984). "Guidelines for placement of longitudinal barriers on slopes," *Transportation Research Record*, 970, 3-9.
88. Ross, H.E., Jr., Sicking, D.L., Zimmer, R.A., and Michie, J.D. (1993). "Recommended procedures for the safety performance evaluation of highway features," *NCHRP Report 350*, Transportation Research Board, National Research Council, Washington, D.C.
89. Sheikh, N.M., Alberson, D.C., and Chatham, L.S. (2008). "State of the practice of cable barrier systems," *Transportation Research Record*, 2060, 84-91.
90. Sposito, B., and Johnston, S. (1999). "Three-cable median barrier," *Final Report OR-RD-99-03*, Oregon Department of Transportation, Salem, OR.
91. Stasburg, G., and Crawley, L.C. (2005). "Keeping Traffic on the Right Side of the Road," In: *Public Road*.
92. Stine, J.S., Hamblin, B.C., Brennan, S.N., Donnell, E.T. (2010). "Analyzing the influence of median cross-section design on highway safety using vehicle dynamics simulations," *Accident Analysis and Prevention*, 42, 1769-1777.
93. Tiso, P., Plaxico, C., and Ray, M. (2002). "Improved truck model for roadside safety simulations: Part II - suspension modeling," *Transportation Research Record*, 1797, 63-71.
94. Troy, S. A. (2007). "Median barriers in North Carolina," In: *TRB-AFB20 Committee Summer Meeting*, Rapid City, SD.
95. Venkataraman, N.S. Ulfarsson, G.F., Shankar, V., Oh, J., and Park, M. (2011). "Model of relationship between interstate crash occurrence and geometrics: exploratory insights from random parameter negative binomial approach," *Transportation Research Record*, 2236, 41-48.
96. Whitworth, H. A., Bendidi, R., Marzougui, D., and Reiss, R. (2004). "Finite element modeling of the crash performance of roadside barriers," *International Journal of Crashworthiness*, 9(1), 35-43.
97. WSDOT. (2006). "I-5 Marysville cable median barrier," *WSDOT Report*, Washington State Department of Transportation, Olympia, WA.
98. WSDOT. (2007). "Cable median barrier report." WSDOT Report, Washington State Department of Transportation, Olympia, WA
99. WSDOT. (2008). "Cable median barrier report." WSDOT Report, Washington State Department of Transportation, Olympia, WA
100. WSDOT. (2009). "Cable median barrier report." WSDOT Report, Washington State Department of Transportation, Olympia, WA
101. Zaouk, A.K., Bedewi, N. E., Kan, C.D., and Marzougui, D. (1997). "development and evaluation of a C-1500 pickup truck model for roadside hardware impact simulation," *FHWA-RD-96-212*, Federal Highway Administration, Washington, D.C.
102. Zaouk, A.K., Marzougui, D., and Bedewi, N.E. (2000a). "Development of a detailed vehicle finite element model, Part I: methodology," *International Journal of Crashworthiness*, 5(1), 25-36.

103. Zaouk, A.K., Marzougui, D., and Kan, C.D. (2000b). "Development of a detailed vehicle finite element model, Part II: material characterization and component testing," *International Journal of Crashworthiness*, 5(1), 37-50.
104. Zegeer, C.V., Stewart, J.R., Council, F.M., Reinfurt, D.W., and Hamilton, E. (1992). "Safety effects of geometric improvements on horizontal curves," *Transportation Research Record*, 1356, 11-19.
105. Zhu, L. and J. Rohde (2010). "Development of guidelines for anchor design for high-tension cable guardrails," *Transportation Research Record*, 2195, 115-120.
106. Zweden, J.V. and Bryden, J.E. (1977). "In-service Performance of Highway Barriers," *Report NYSDOT-ERD-77-RR51*, New York State Department of Transportation, Albany, NY.

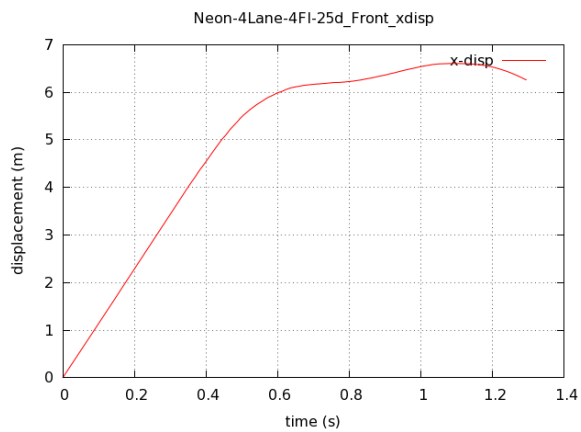
Appendix A. Time History of Traversal Displacements and Velocities



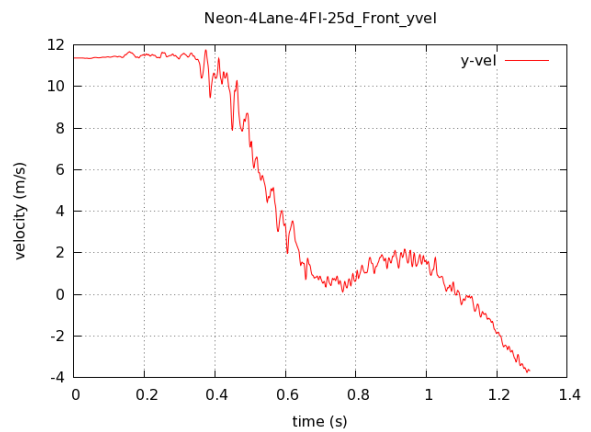
Traversal displacement at a 20° departure angle



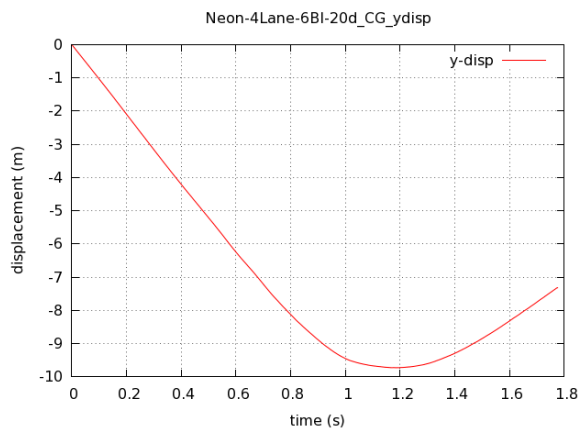
Traversal velocity at a 20° departure angle



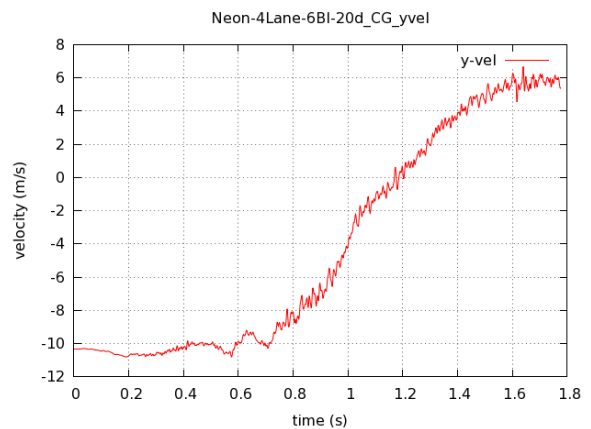
Traversal displacement at a 25° departure angle



Traversal velocity at a 25° departure angle

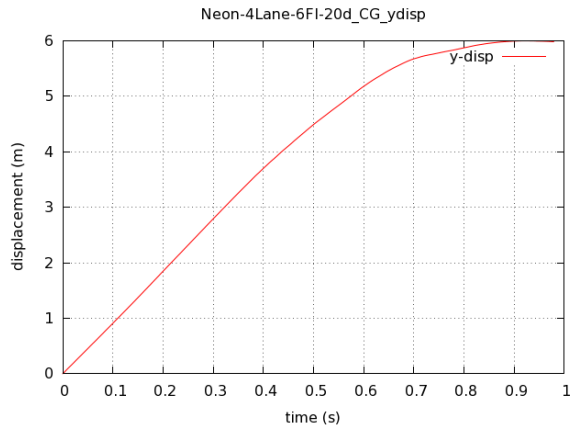


Traversal displacement at a 30° departure angle

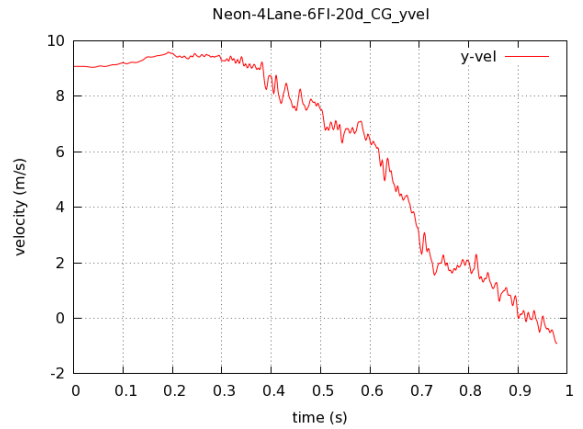


Traversal velocity at a 30° departure angle

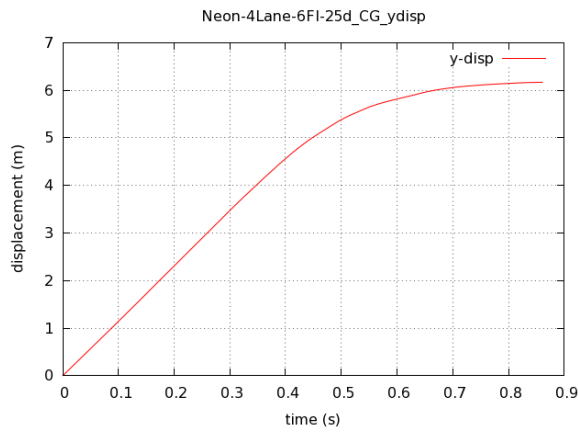
Fig. A.1: Front-side impacts by a Dodge Neon on the CMB placed at 4 ft from the median centerline on the outer 6:1 slope of a four-lane freeway



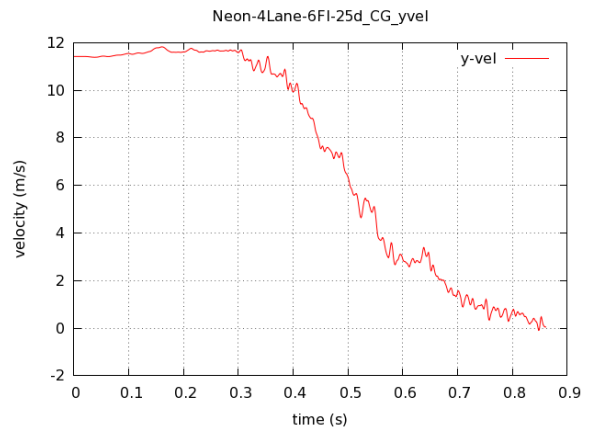
Traversal displacement at a 20° departure angle



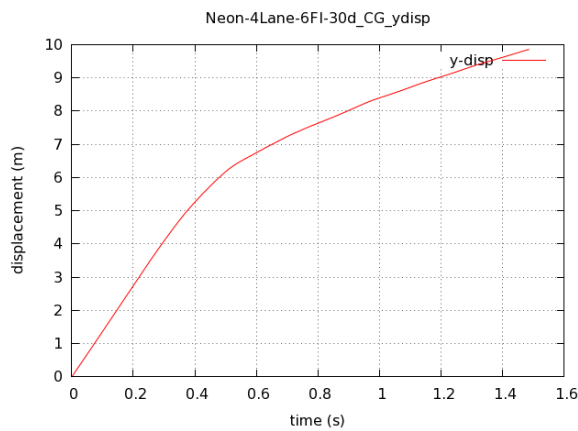
Traversal velocity at a 20° departure angle



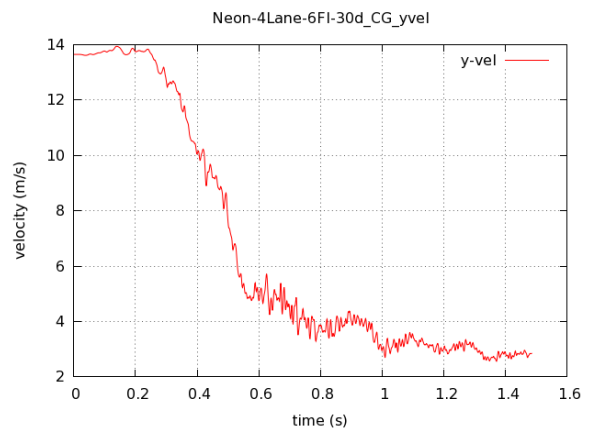
Traversal displacement at a 25° departure angle



Traversal velocity at a 25° departure angle

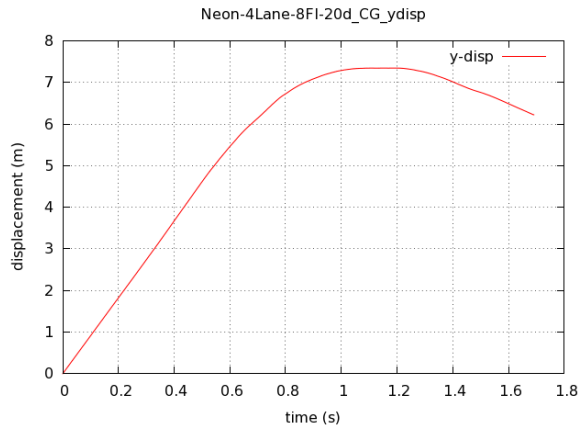


Traversal displacement at a 30° departure angle

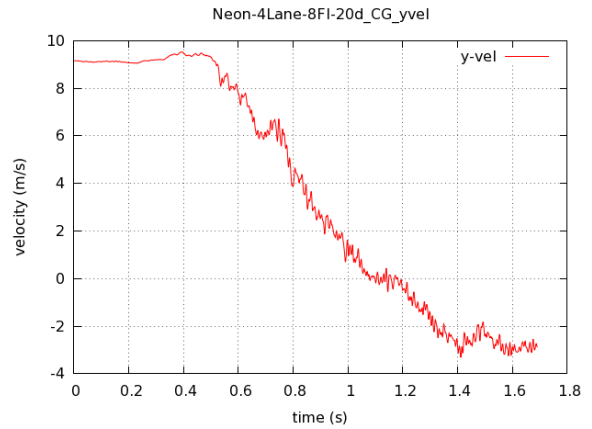


Traversal velocity at a 30° departure angle

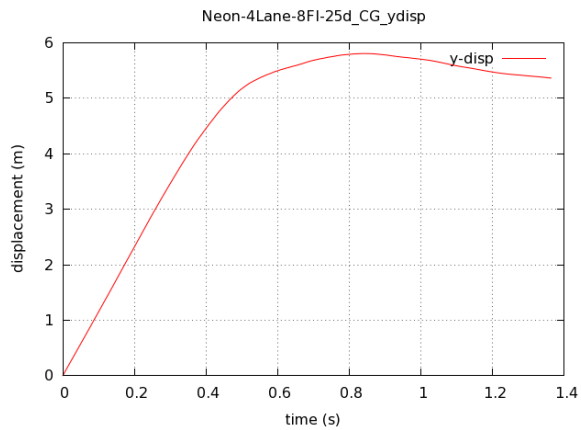
Fig. A.2: Front-side impacts by a Dodge Neon on the CMB placed at 6 ft from the median centerline on the outer 6:1 slope of a four-lane freeway



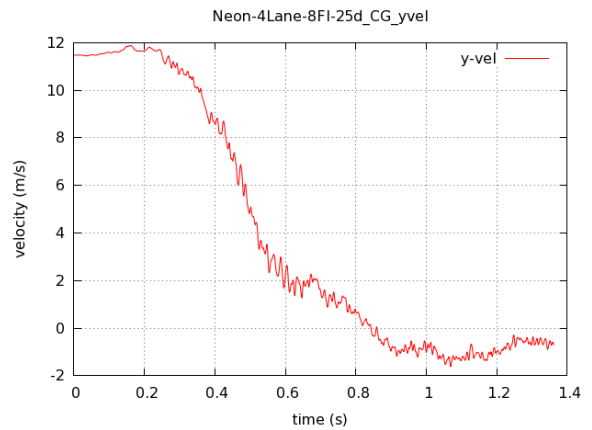
Traversal displacement at a 20° departure angle



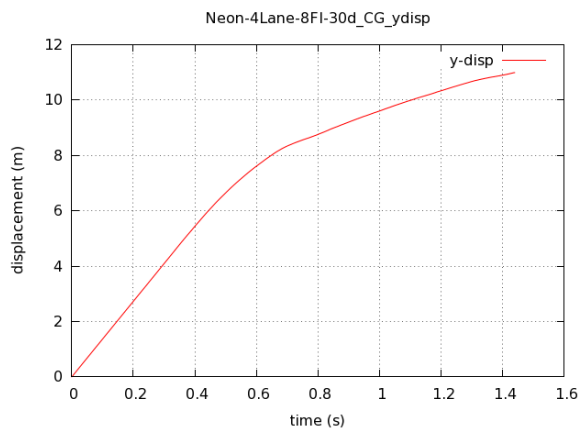
Traversal velocity at a 20° departure angle



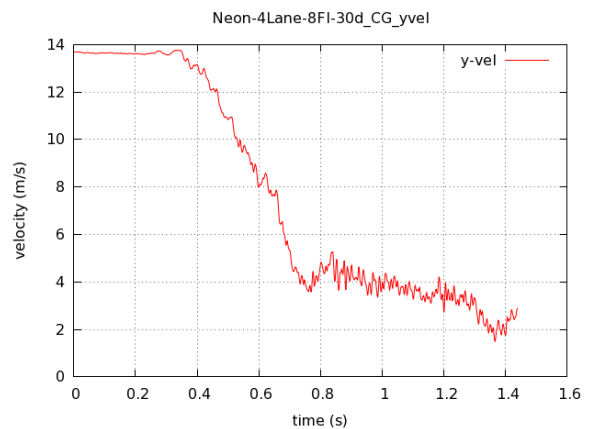
Traversal displacement at a 25° departure angle



Traversal velocity at a 25° departure angle

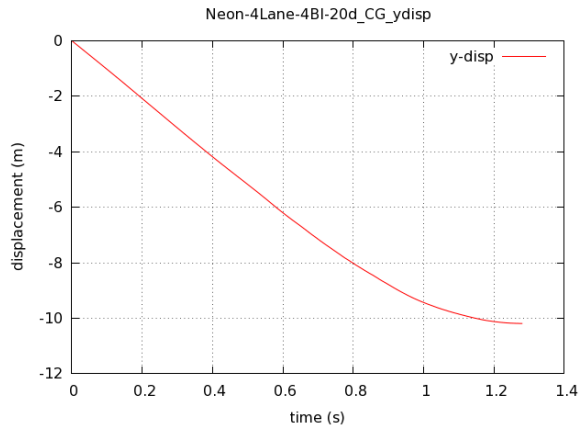


Traversal displacement at a 30° departure angle

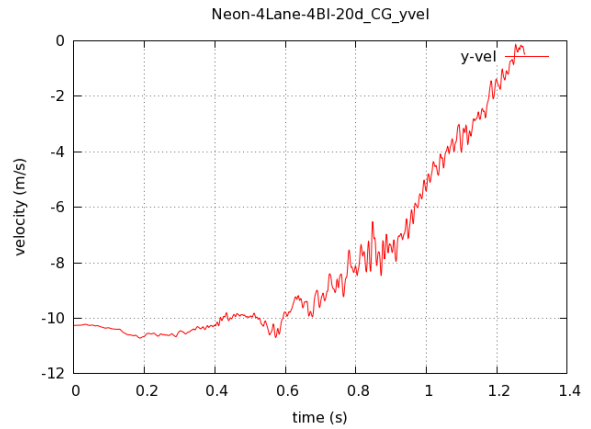


Traversal velocity at a 30° departure angle

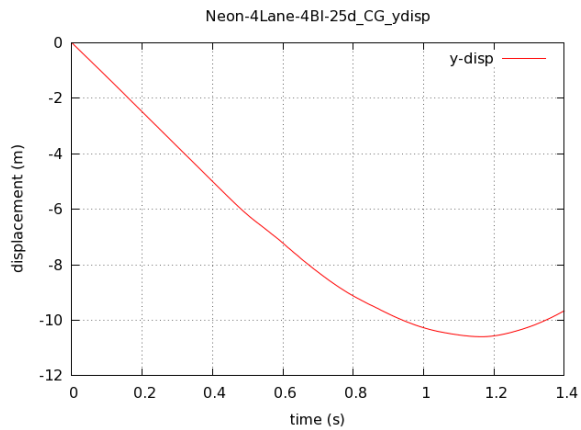
Fig. A.3: Front-side impacts by a Dodge Neon on the CMB placed at 8 ft from the median centerline on the outer 6:1 slope of a four-lane freeway



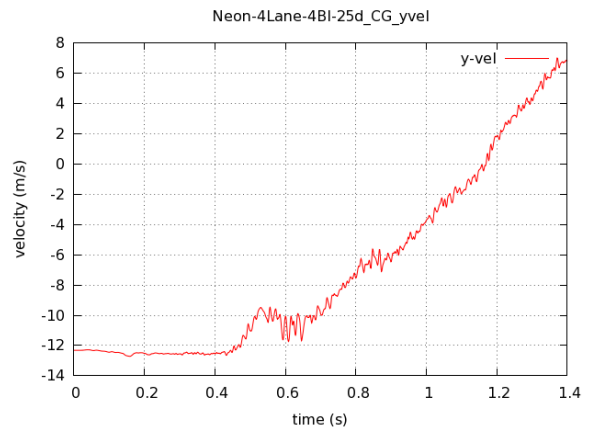
Traversal displacement at a 20° departure angle



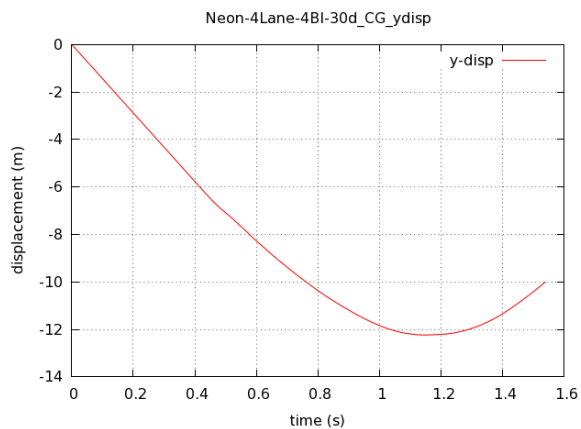
Traversal velocity at a 20° departure angle



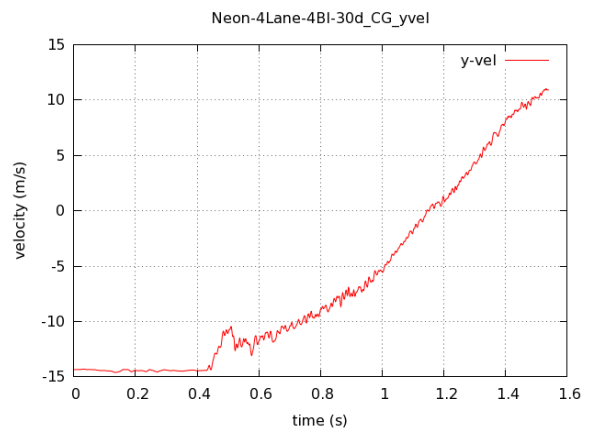
Traversal displacement at a 25° departure angle



Traversal velocity at a 25° departure angle

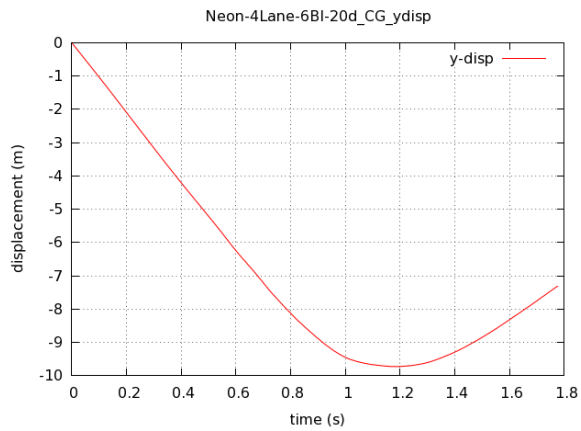


Traversal displacement at a 30° departure angle

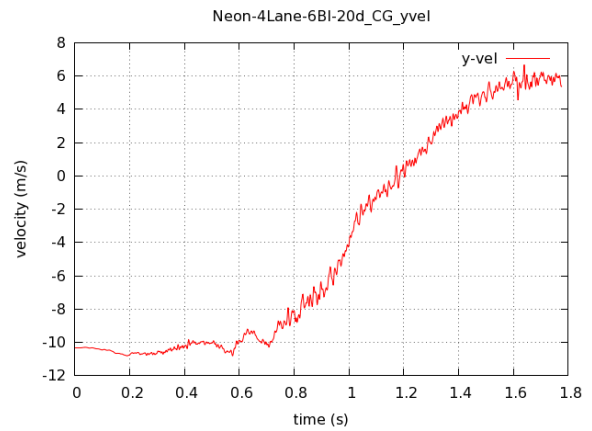


Traversal velocity at a 30° departure angle

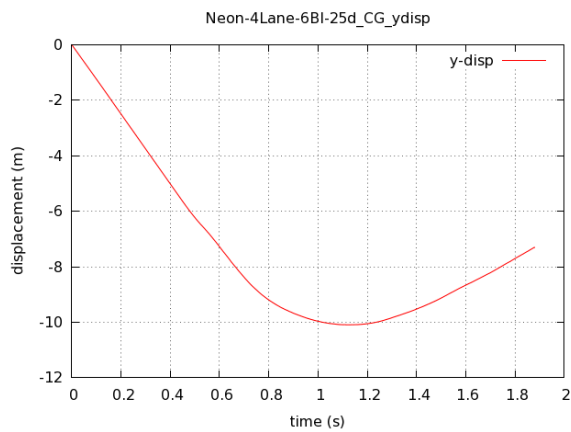
Fig. A.4: Backside impacts by a Dodge Neon on the CMB placed at 4 ft from the median centerline on the outer 6:1 slope of a four-lane freeway



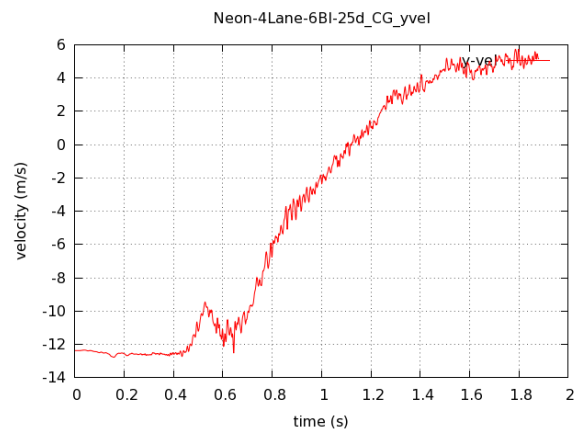
Traversal displacement at a 20° departure angle



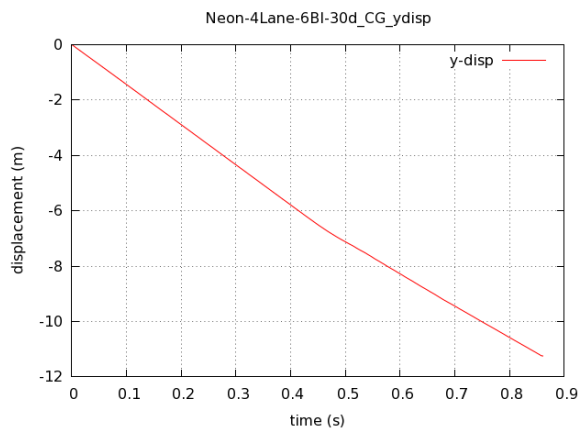
Traversal velocity at a 20° departure angle



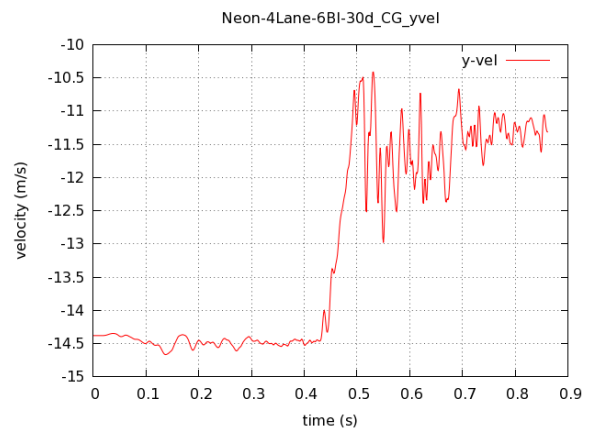
Traversal displacement at a 25° departure angle



Traversal velocity at a 25° departure angle

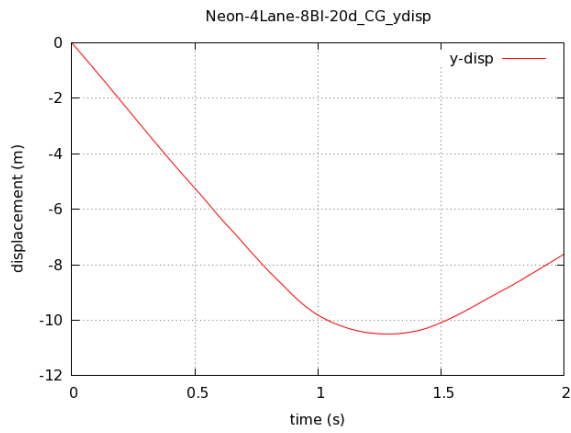


Traversal displacement at a 30° departure angle

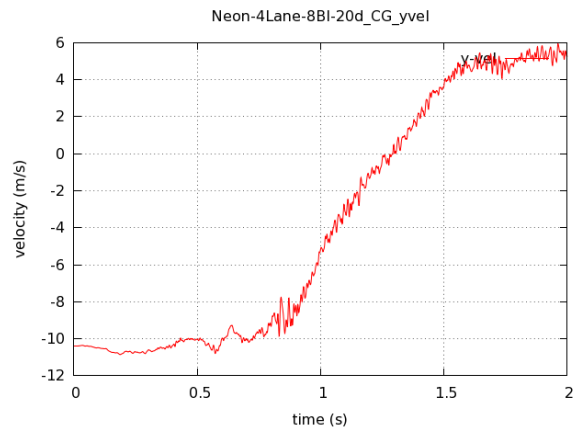


Traversal velocity at a 30° departure angle

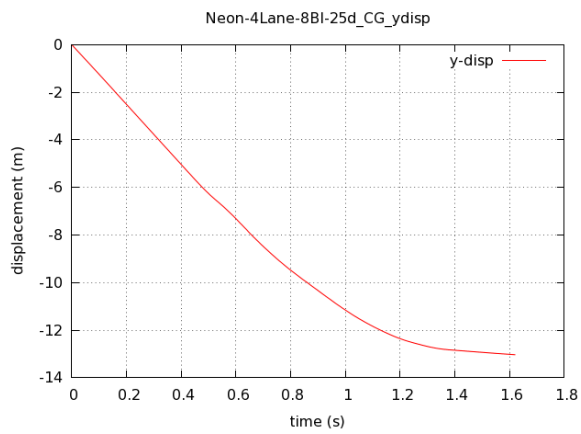
Fig. A.5: Backside impacts by a Dodge Neon on the CMB placed at 6 ft from the median centerline on the outer 6:1 slope of a four-lane freeway



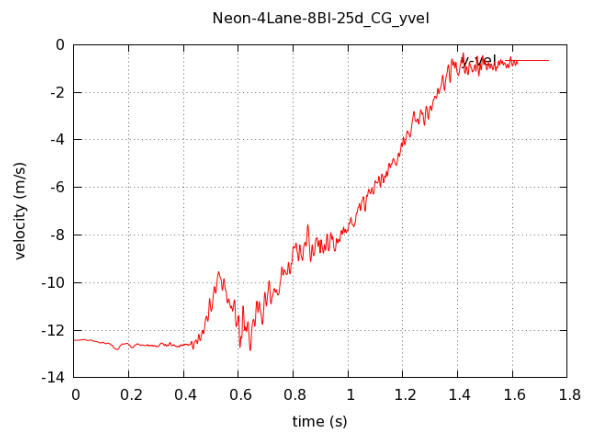
Traversal displacement at a 20° departure angle



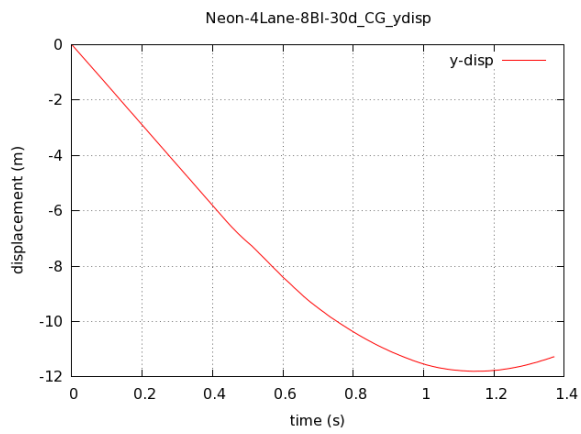
Traversal velocity at a 20° departure angle



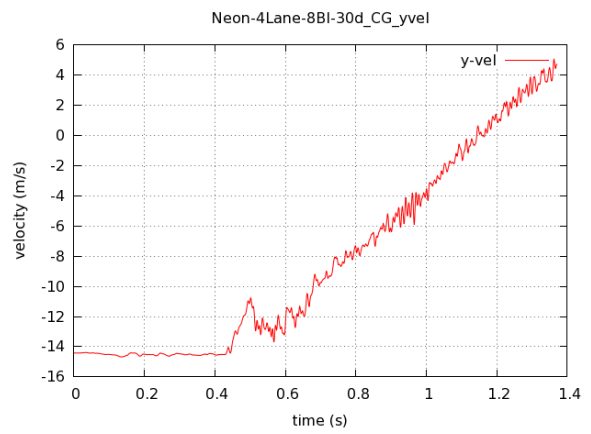
Traversal displacement at a 25° departure angle



Traversal velocity at a 25° departure angle

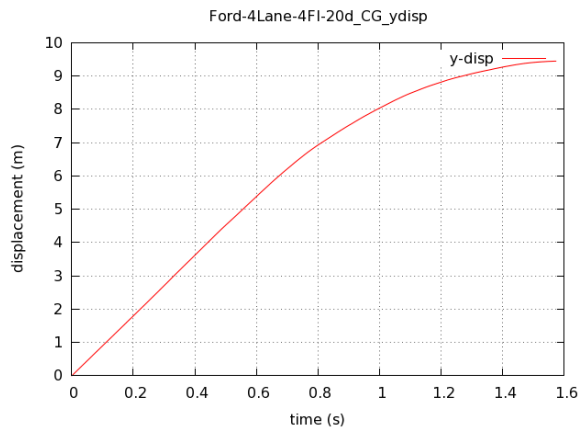


Traversal displacement at a 30° departure angle

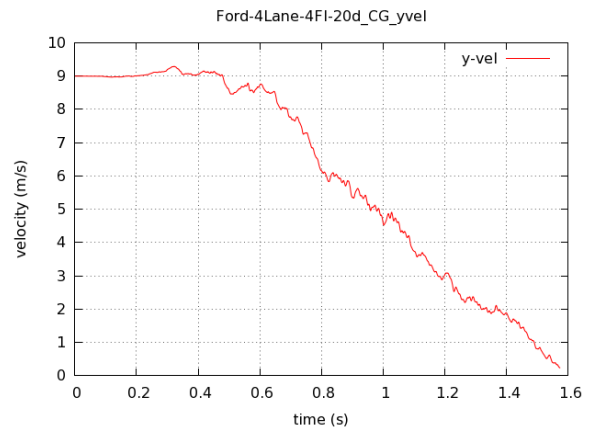


Traversal velocity at a 30° departure angle

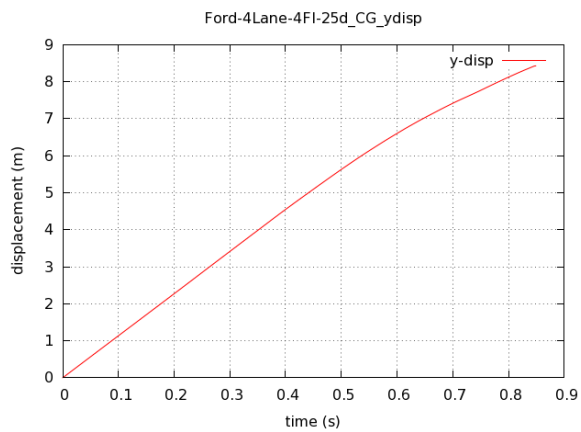
Fig. A.6: Backside impacts by a Dodge Neon on the CMB placed at 8 ft from the median centerline on the outer 6:1 slope of a four-lane freeway



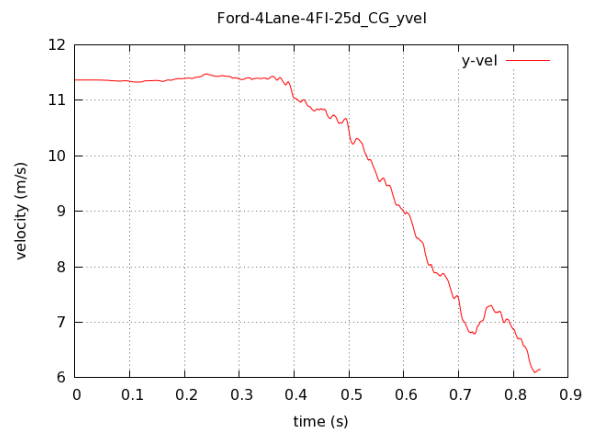
Traversal displacement at a 20° departure angle



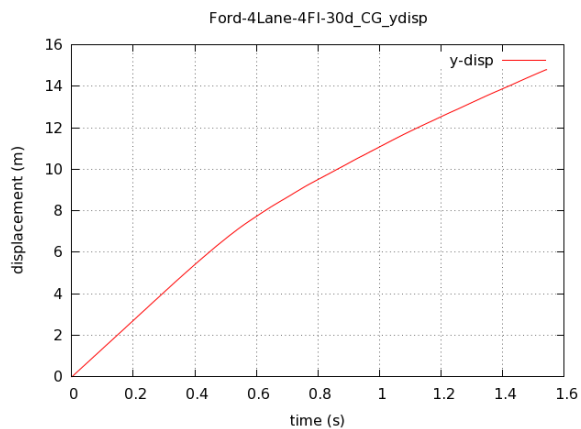
Traversal velocity at a 20° departure angle



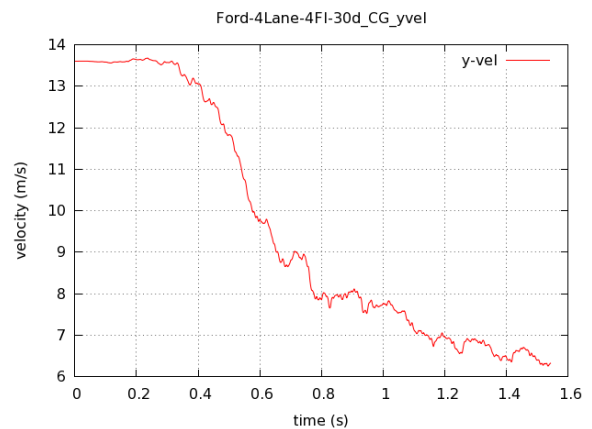
Traversal displacement at a 25° departure angle



Traversal velocity at a 25° departure angle

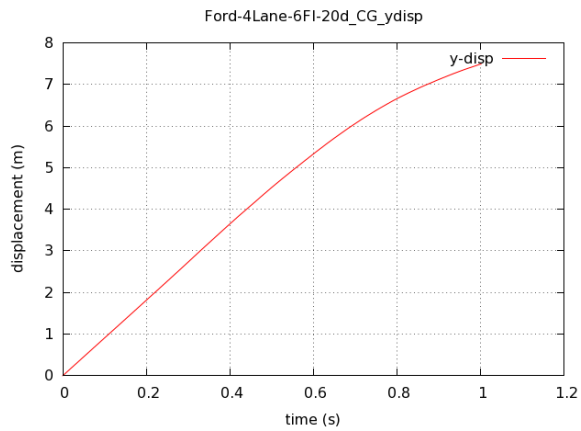


Traversal displacement at a 30° departure angle

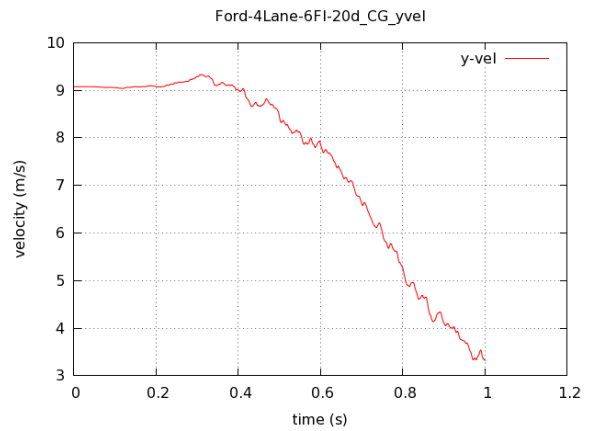


Traversal velocity at a 30° departure angle

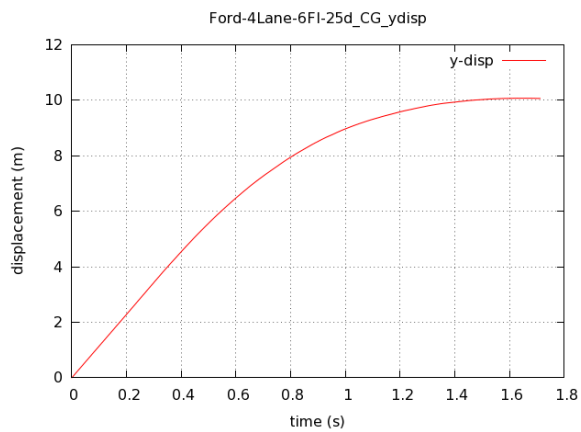
Fig. A.7: Front-side impacts by a Ford F250 on the CMB placed at 4 ft from the median centerline on the outer 6:1 slope of a four-lane freeway



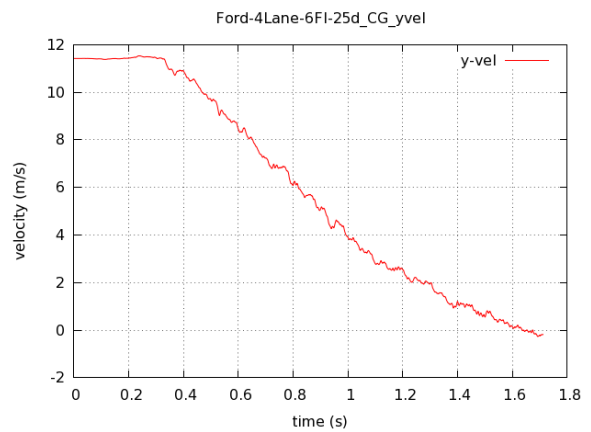
Traversal displacement at a 20° departure angle



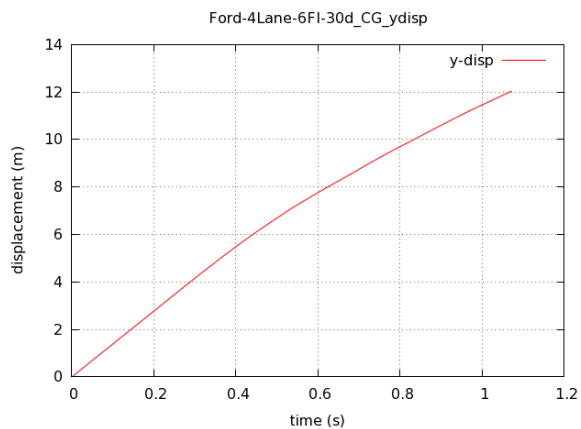
Traversal velocity at a 20° departure angle



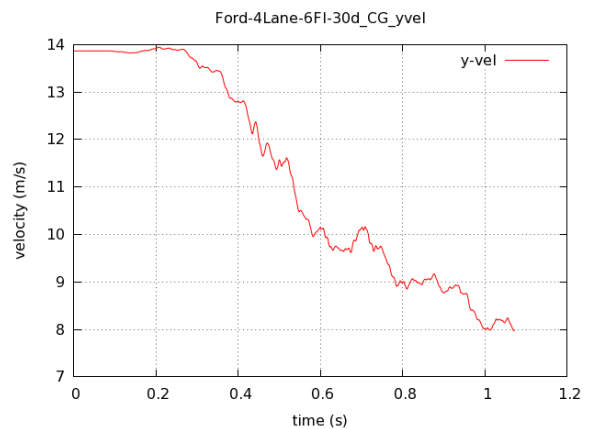
Traversal displacement at a 25° departure angle



Traversal velocity at a 25° departure angle

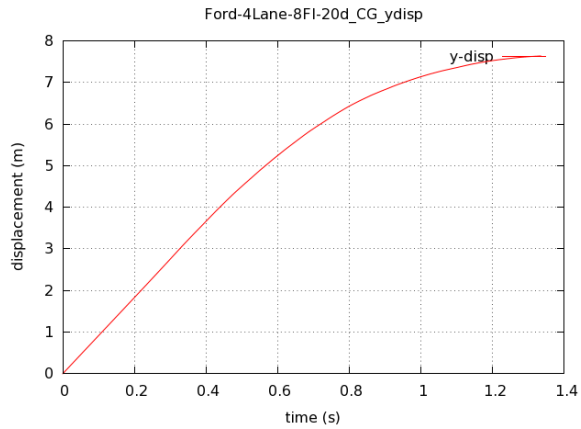


Traversal displacement at a 30° departure angle

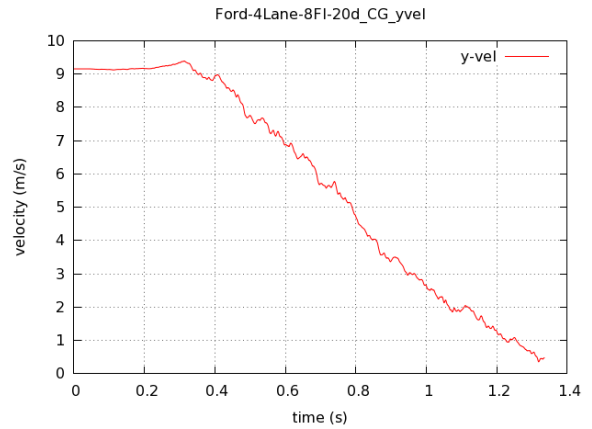


Traversal velocity at a 30° departure angle

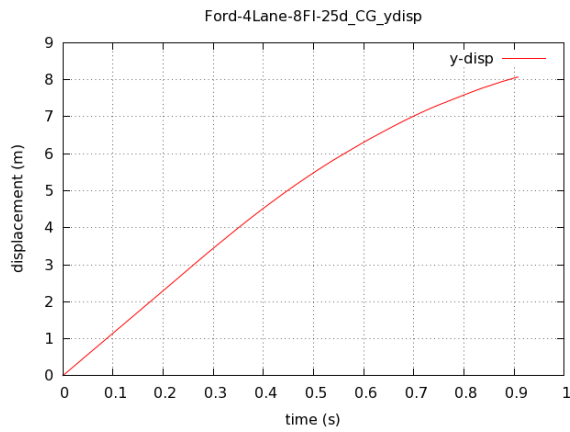
Fig. A.8: Front-side impacts by a Ford F250 on the CMB placed at 6 ft from the median centerline on the outer 6:1 slope of a four-lane freeway



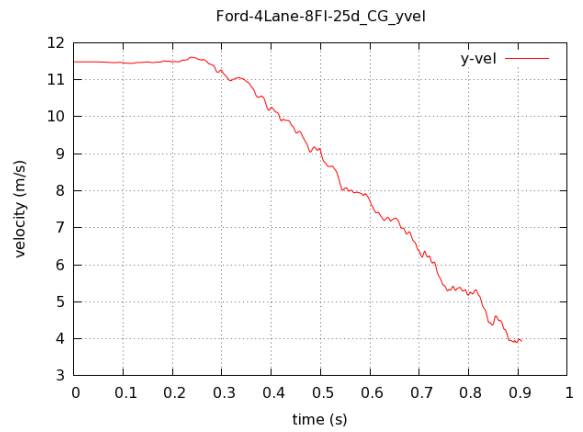
Traversal displacement at a 20° departure angle



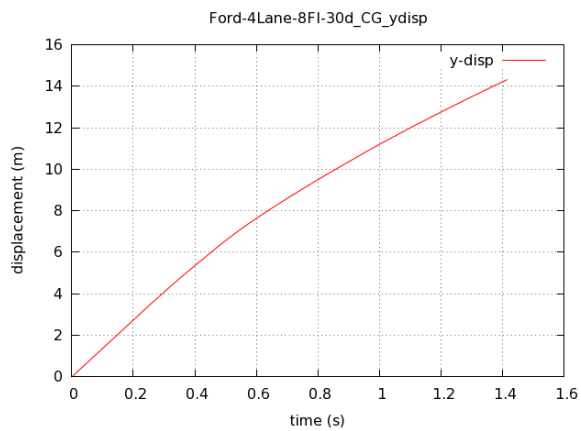
Traversal velocity at a 20° departure angle



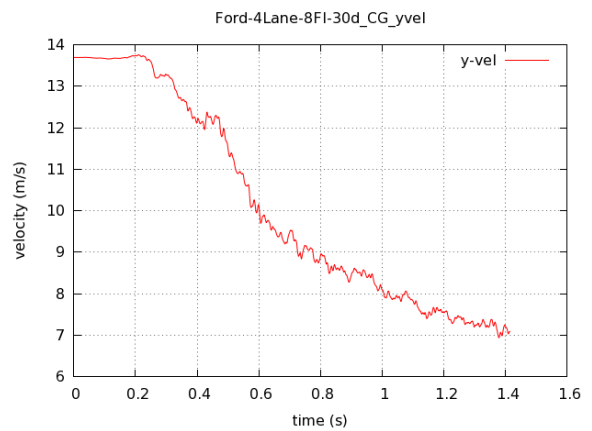
Traversal displacement at a 25° departure angle



Traversal velocity at a 25° departure angle

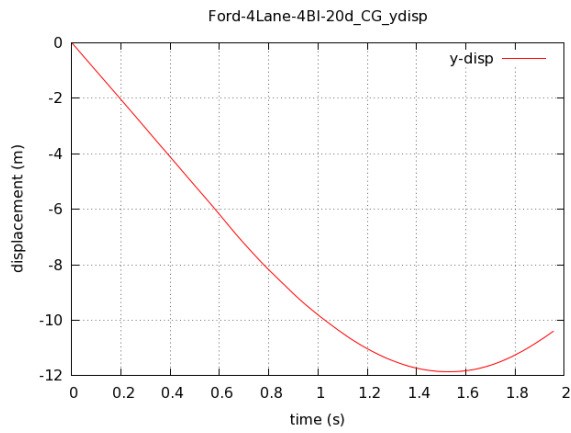


Traversal displacement at a 30° departure angle

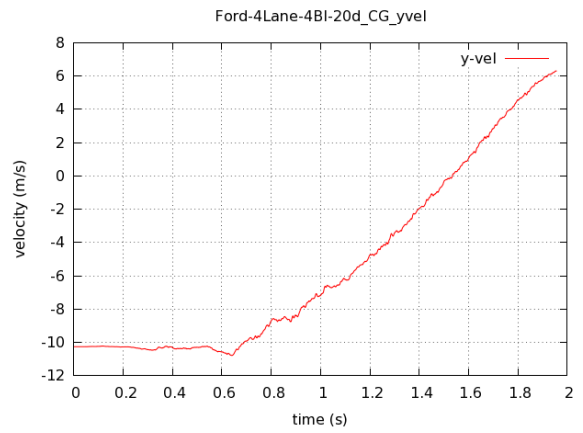


Traversal velocity at a 30° departure angle

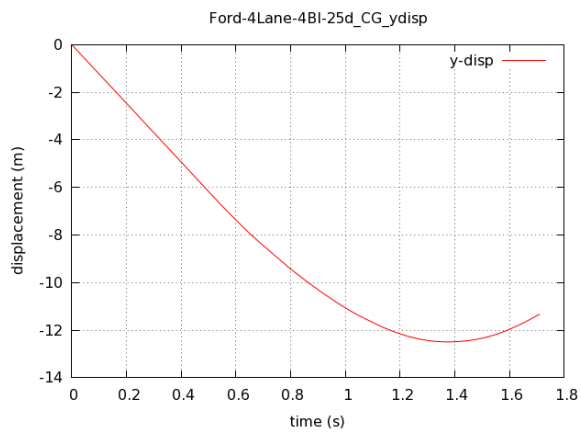
Fig. A.9: Front-side impacts by a Ford F250 on the CMB placed at 8 ft from the median centerline on the outer 6:1 slope of a four-lane freeway



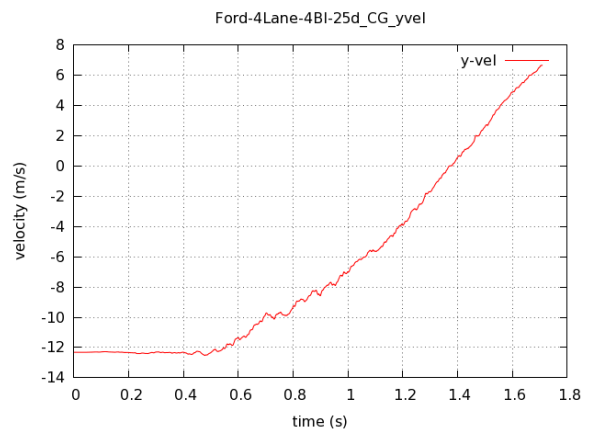
Traversal displacement at a 20° departure angle



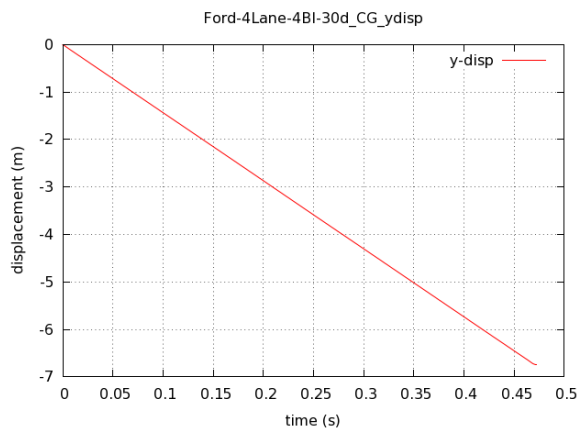
Traversal velocity at a 20° departure angle



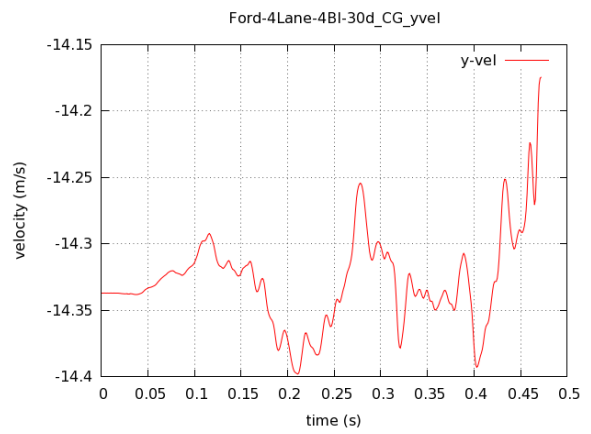
Traversal displacement at a 25° departure angle



Traversal velocity at a 25° departure angle

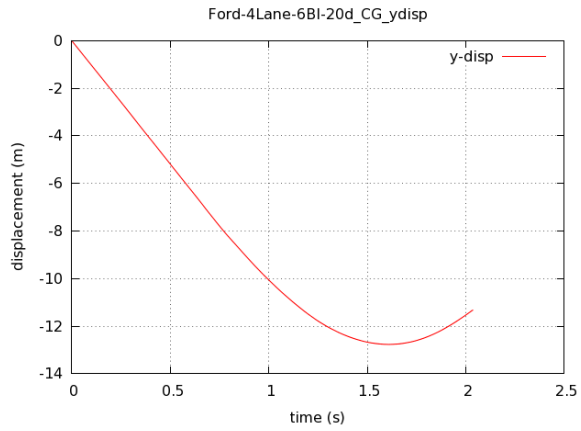


Traversal displacement at a 30° departure angle

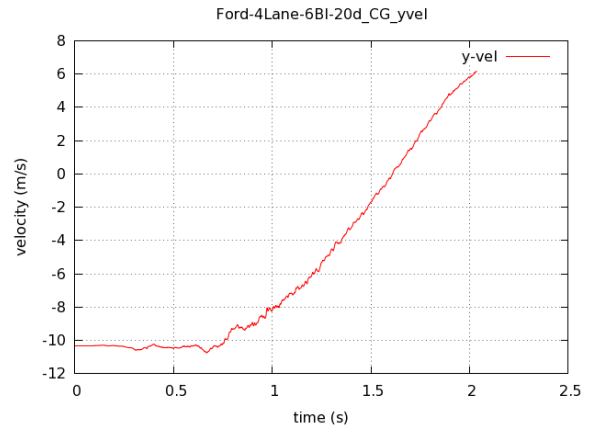


Traversal velocity at a 30° departure angle

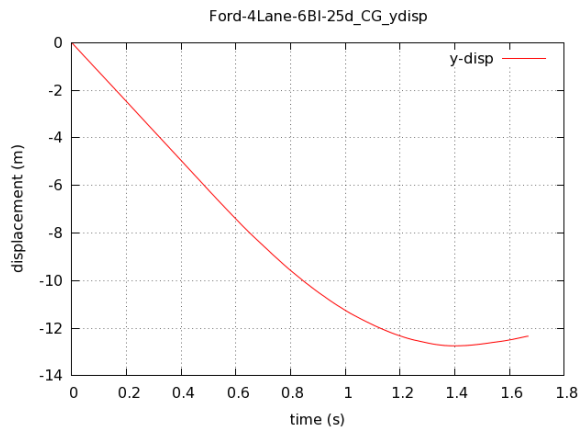
Fig. A.10: Backside impacts by a Ford F250 on the CMB placed at 4 ft from the median centerline on the outer 6:1 slope of a four-lane freeway



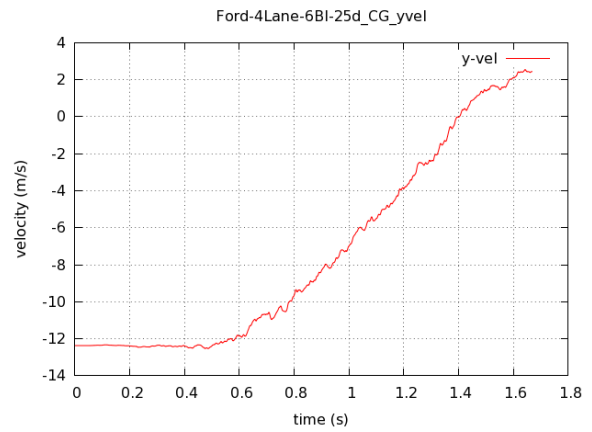
Traversal displacement at a 20° departure angle



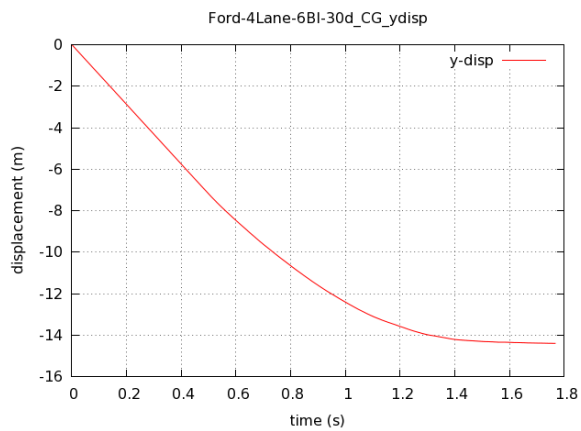
Traversal velocity at a 20° departure angle



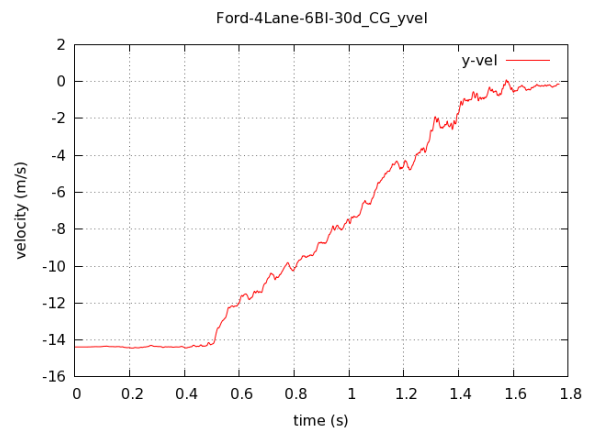
Traversal displacement at a 25° departure angle



Traversal velocity at a 25° departure angle

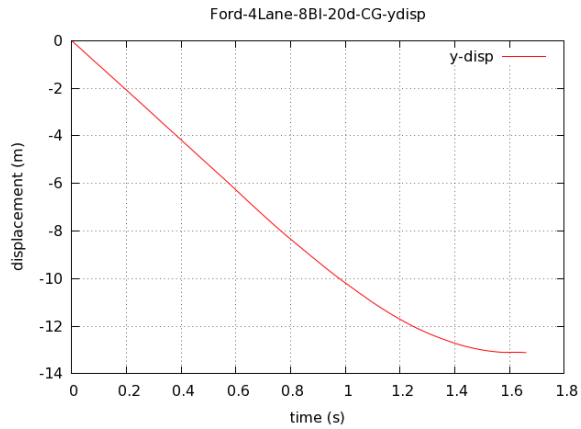


Traversal displacement at a 30° departure angle

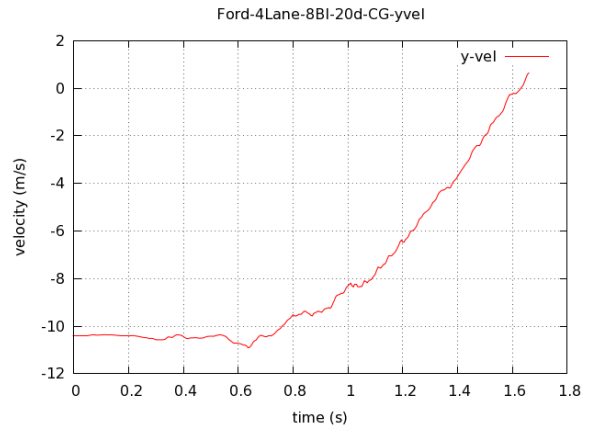


Traversal velocity at a 30° departure angle

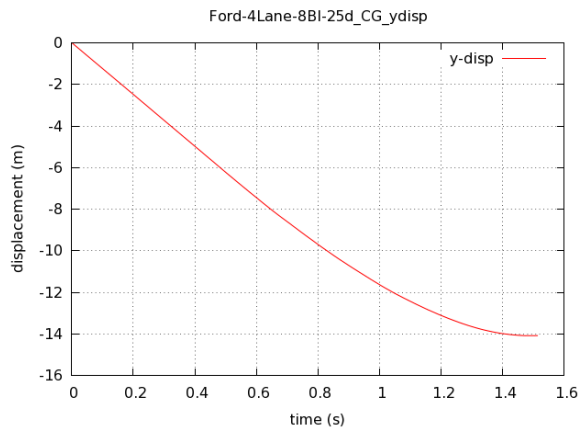
Fig. A.11: Backside impacts by a Ford F250 on the CMB placed at 6 ft from the median centerline on the outer 6:1 slope of a four-lane freeway



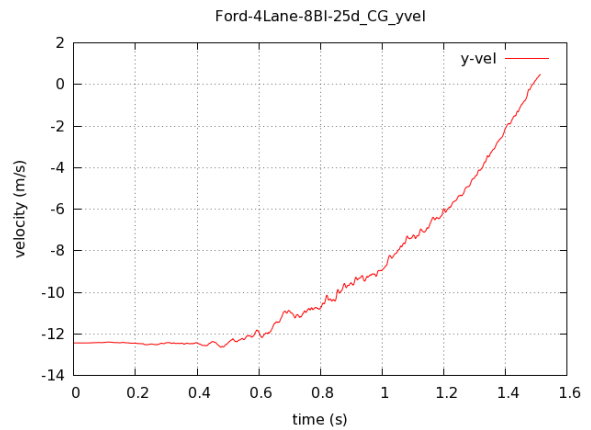
Traversal displacement at a 20° departure angle



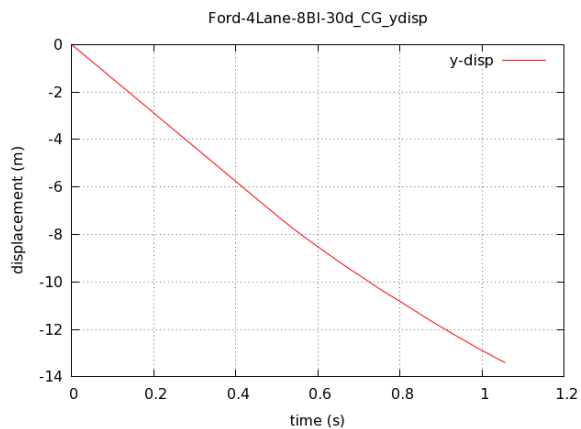
Traversal velocity at a 20° departure angle



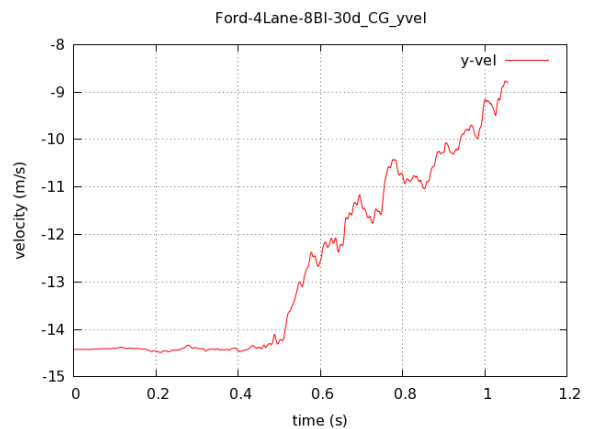
Traversal displacement at a 25° departure angle



Traversal velocity at a 25° departure angle

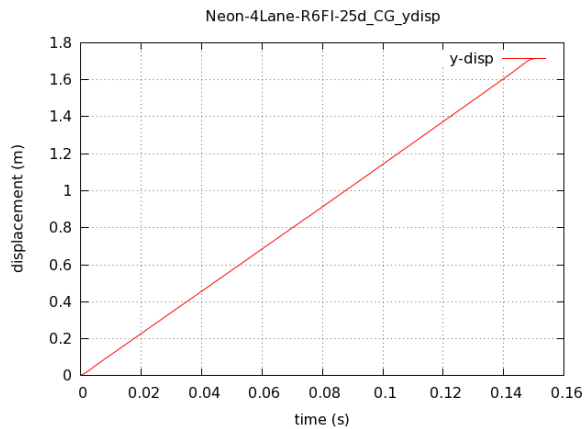


Traversal displacement at a 30° departure angle

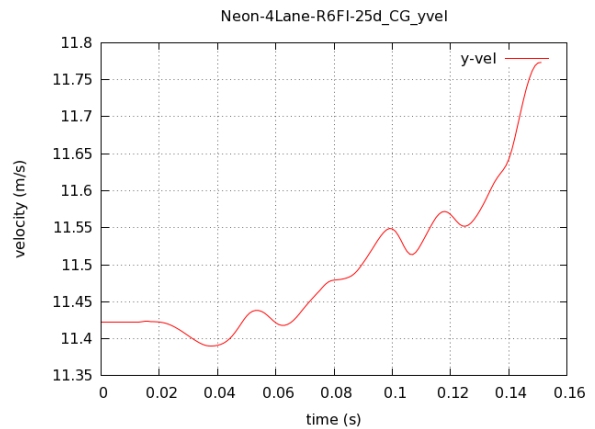


Traversal velocity at a 30° departure angle

Fig. A.12: Backside impacts by a Ford F250 on the CMB placed at 8 ft from the median centerline on the outer 6:1 slope of a four-lane freeway

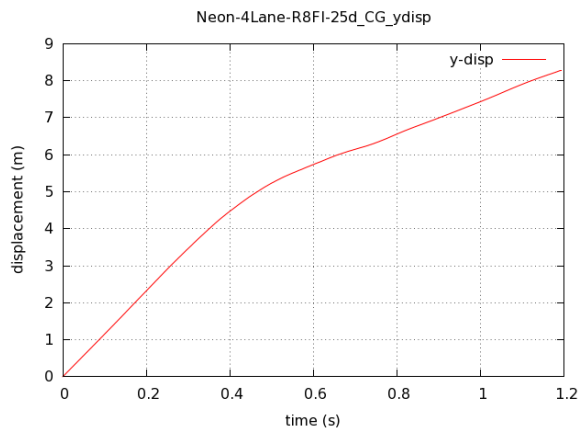


Traversal displacement at a 25° departure angle

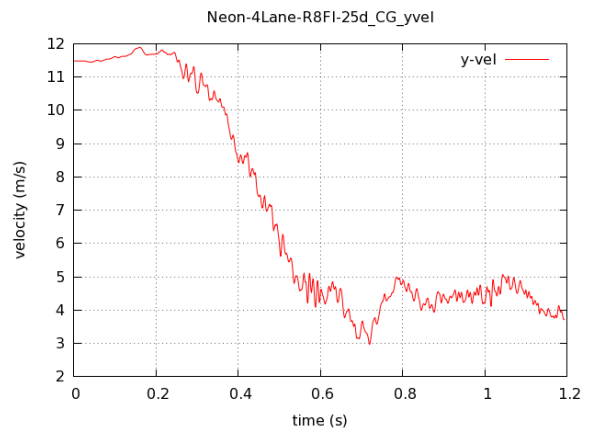


Traversal velocity at a 25° departure angle

Fig. A.13: Front-side impact by a Dodge Neon on the retrofit CMB placed at 6 ft from the median centerline on the outer 6:1 slope of a four-lane freeway

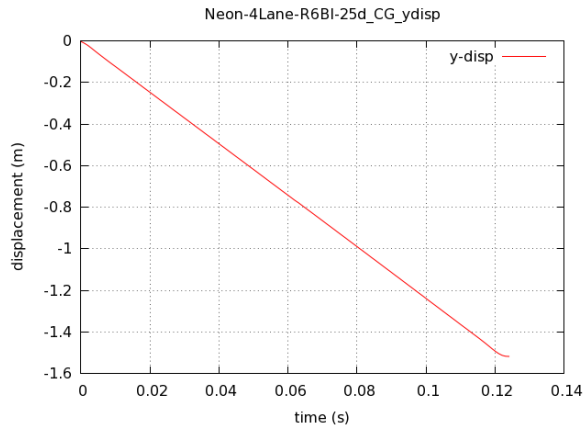


Traversal displacement at a 25° departure angle

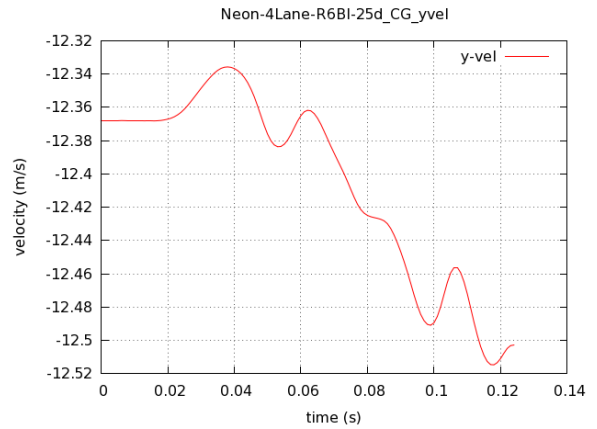


Traversal velocity at a 25° departure angle

Fig. A.14: Front-side impact by a Dodge Neon on the retrofit CMB placed at 8 ft from the median centerline on the outer 6:1 slope of a four-lane freeway

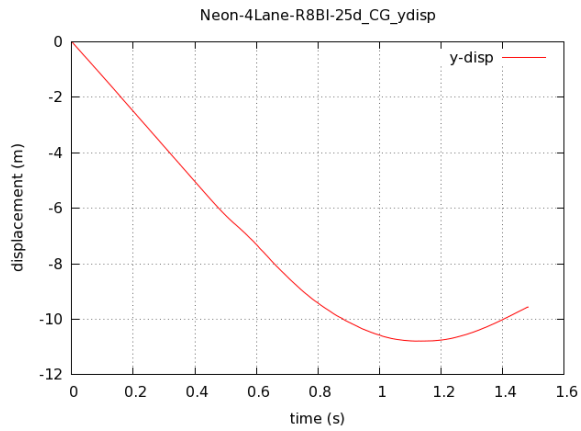


Traversal displacement at a 25° departure angle

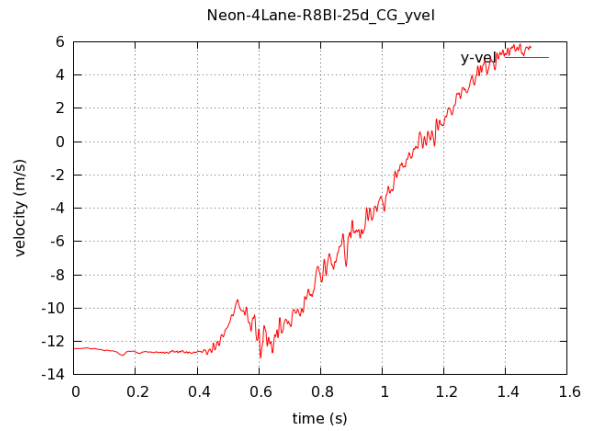


Traversal velocity at a 25° departure angle

Fig. A.15: Backside impact by a Dodge Neon on the retrofit CMB placed at 6 ft from the median centerline on the outer 6:1 slope of a four-lane freeway

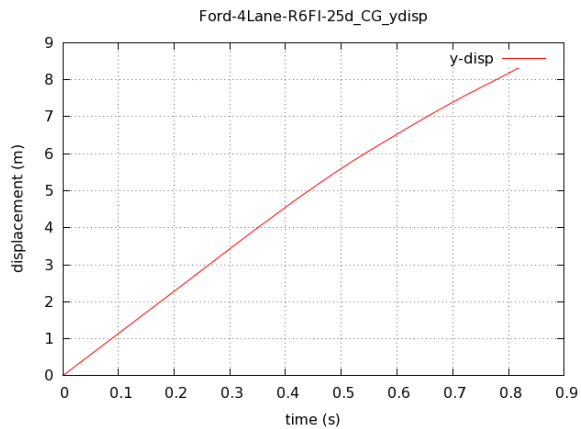


Traversal displacement at a 25° departure angle

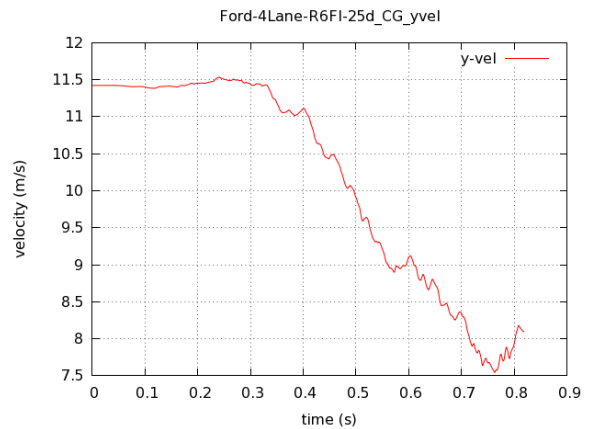


Traversal velocity at a 25° departure angle

Fig. A.16: Backside impact by a Dodge Neon on the retrofit CMB placed at 8 ft from the median centerline on the outer 6:1 slope of a four-lane freeway

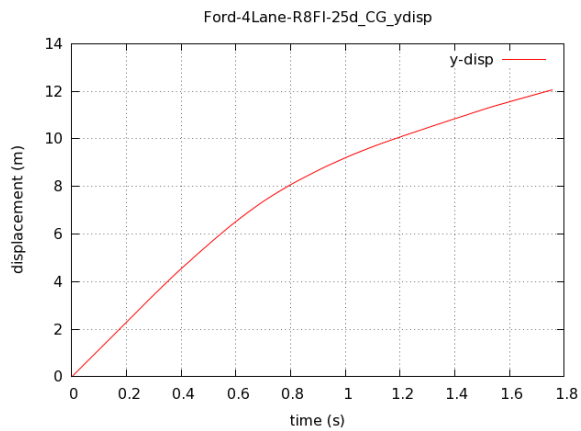


Traversal displacement at a 25° departure angle

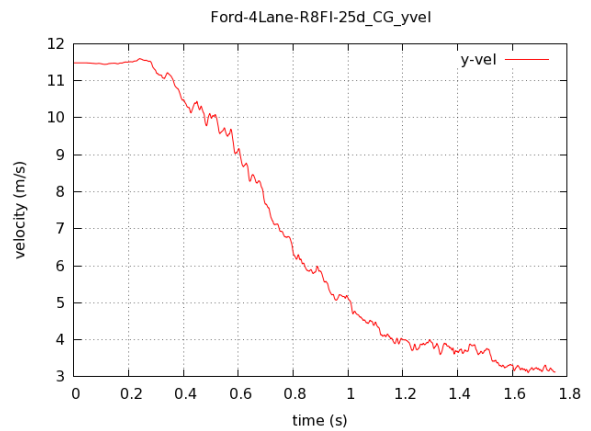


Traversal velocity at a 25° departure angle

Fig. A.17: Front-side impact by a Ford F250 on the retrofit CMB placed at 6 ft from the median centerline on the outer 6:1 slope of a four-lane freeway

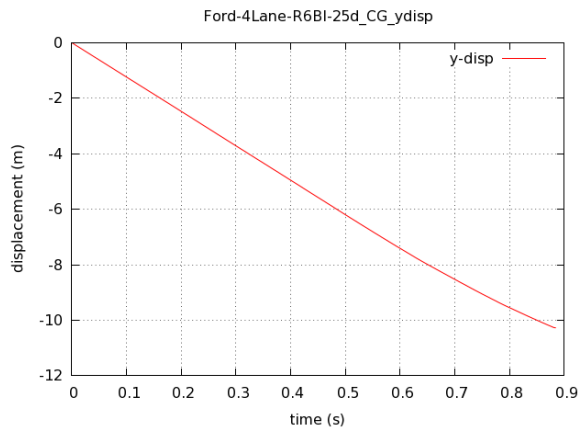


Traversal displacement at a 25° departure angle

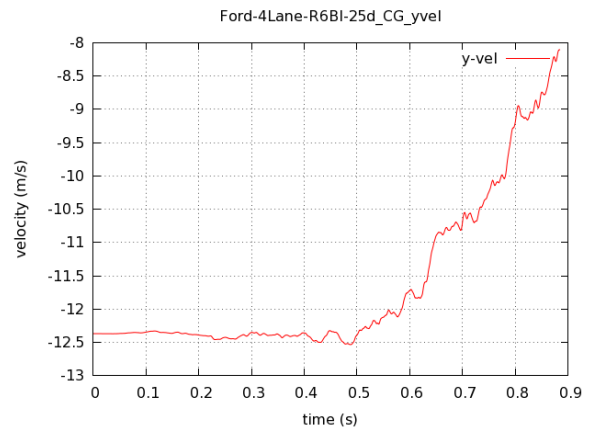


Traversal velocity at a 25° departure angle

Fig. A.18: Front-side impact by a Ford F250 on the retrofit CMB placed at 8 ft from the median centerline on the outer 6:1 slope of a four-lane freeway

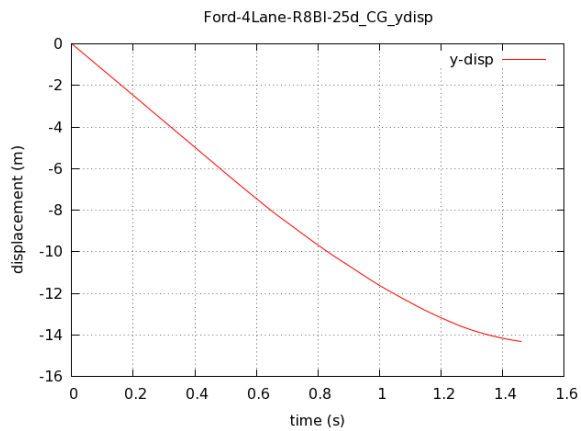


Traversal displacement at a 25° departure angle

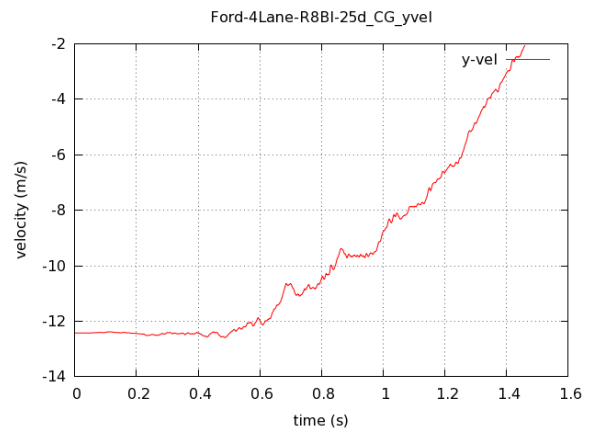


Traversal velocity at a 25° departure angle

Fig. A.19: Backside impact by a Ford F250 on the retrofit CMB placed at 6 ft from the median centerline on the outer 6:1 slope of a four-lane freeway

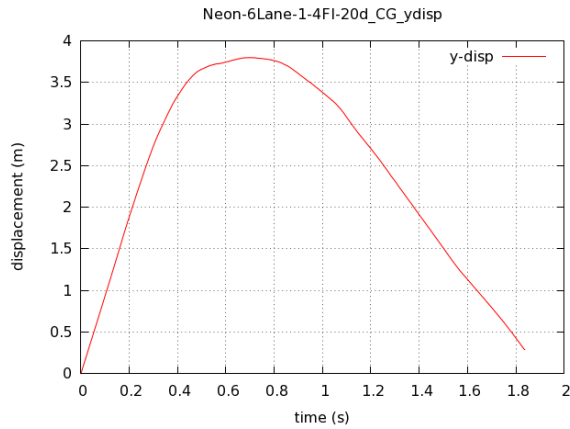


Traversal displacement at a 25° departure angle

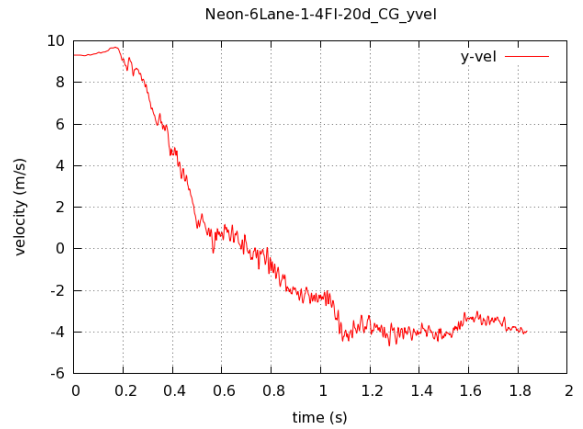


Traversal velocity at a 25° departure angle

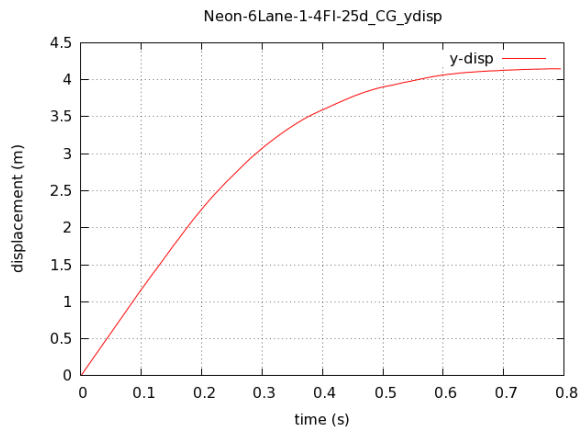
Fig. A.20: Backside impact by a Ford F250 on the retrofit CMB placed at 8 ft from the median centerline on the outer 6:1 slope of a four-lane freeway



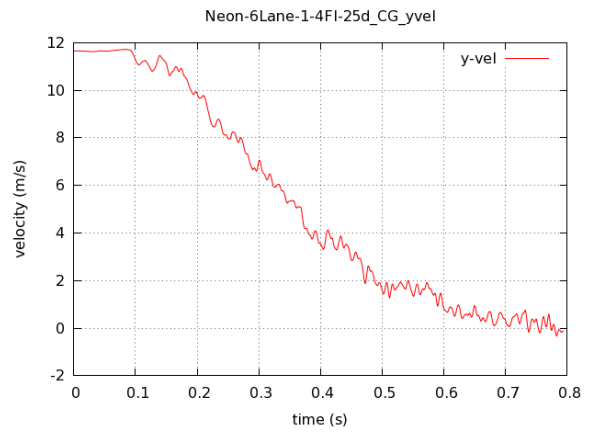
Traversal displacement at a 20° departure angle



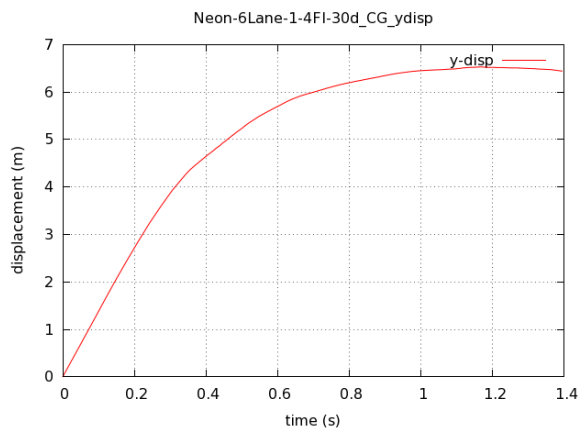
Traversal velocity at a 20° departure angle



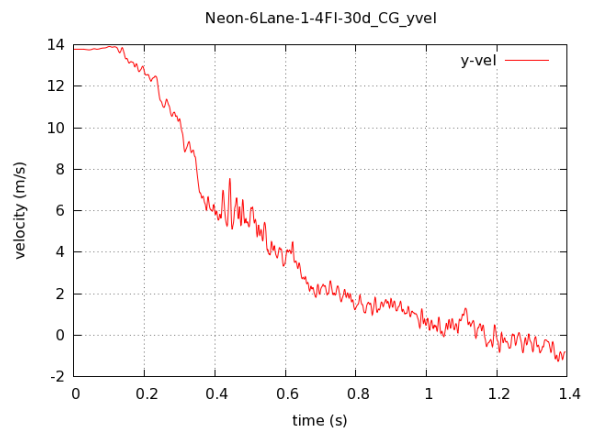
Traversal displacement at a 25° departure angle



Traversal velocity at a 25° departure angle

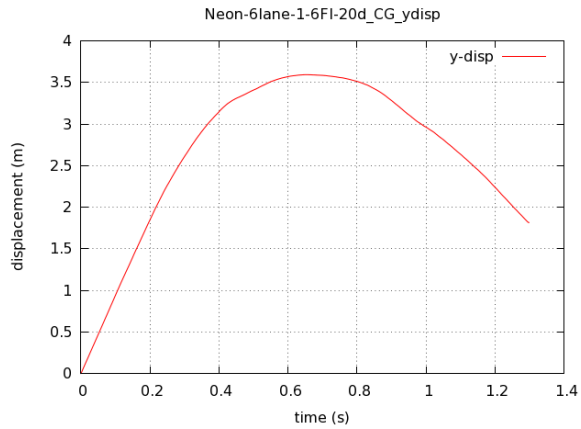


Traversal displacement at a 30° departure angle

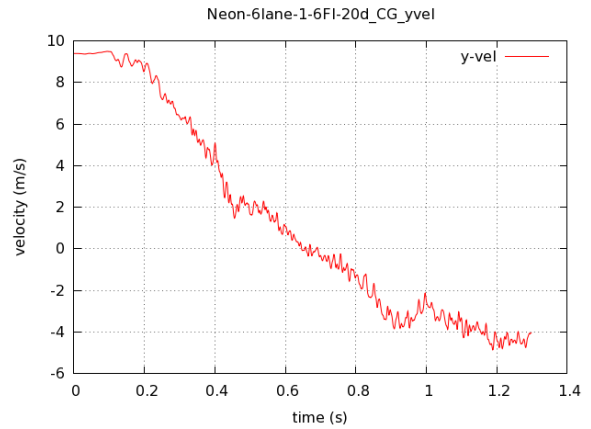


Traversal velocity at a 30° departure angle

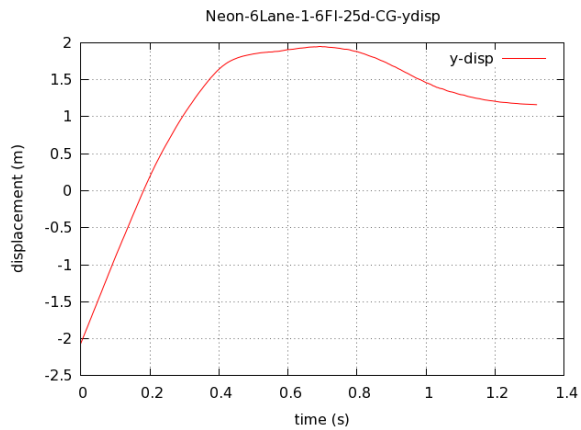
Fig. A.21: Front-side impacts by a Dodge Neon on the CMB placed at 4 ft from the median centerline on the outer 6:1 slope of a six-lane freeway



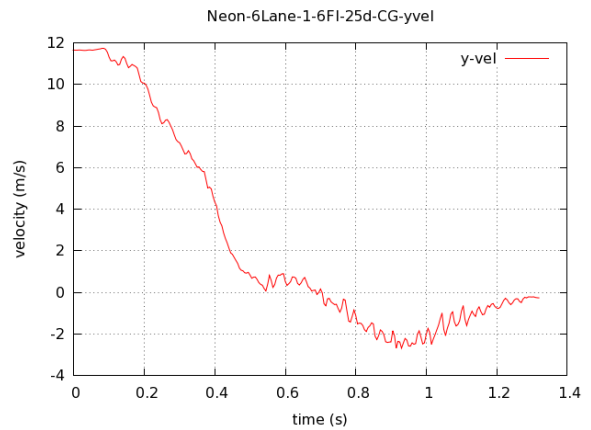
Traversal displacement at a 20° departure angle



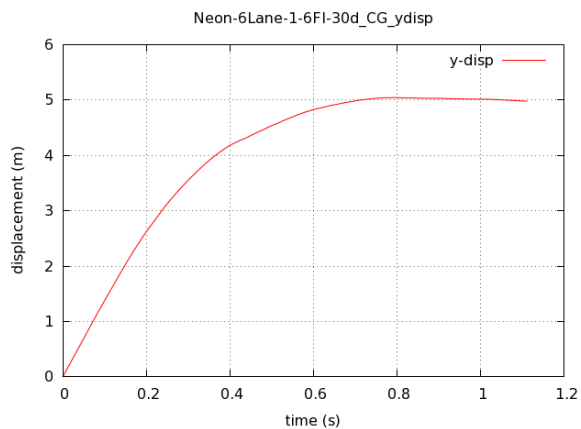
Traversal velocity at a 20° departure angle



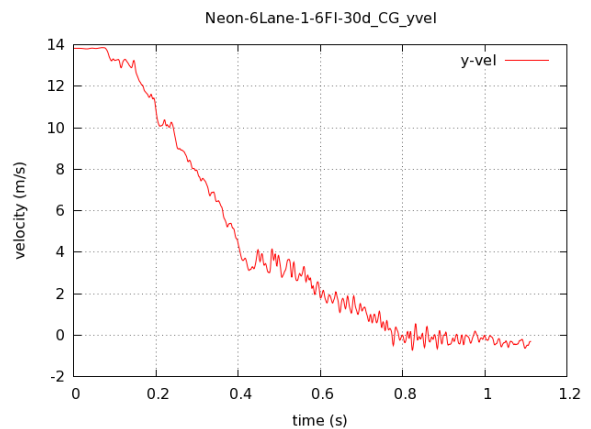
Traversal displacement at a 25° departure angle



Traversal velocity at a 25° departure angle

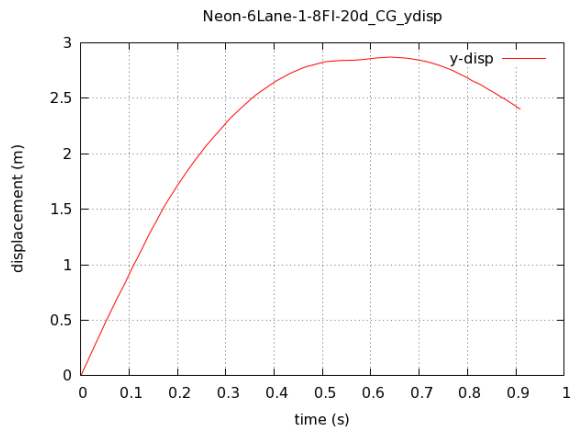


Traversal displacement at a 30° departure angle

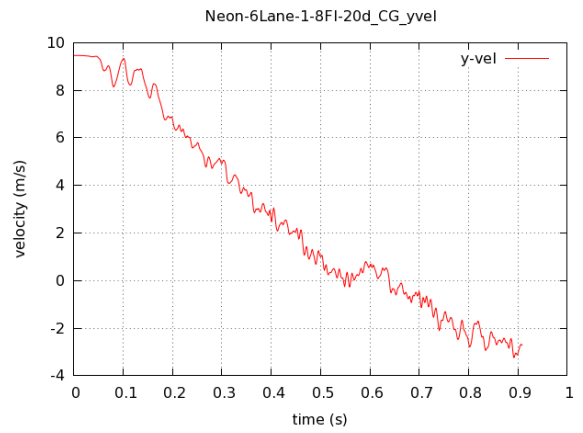


Traversal velocity at a 30° departure angle

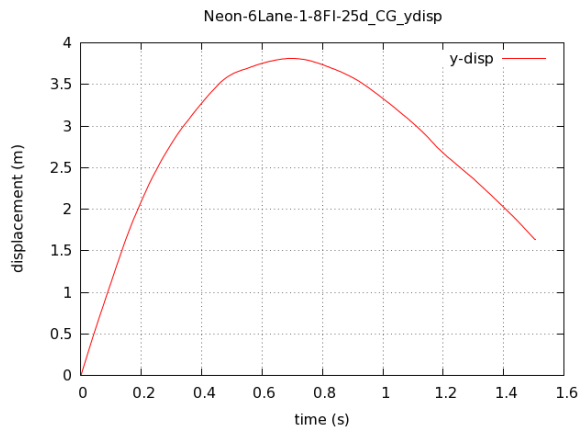
Fig. A.22: Front-side impacts by a Dodge Neon on the CMB placed at 6 ft from the median centerline on the outer 6:1 slope of a six-lane freeway



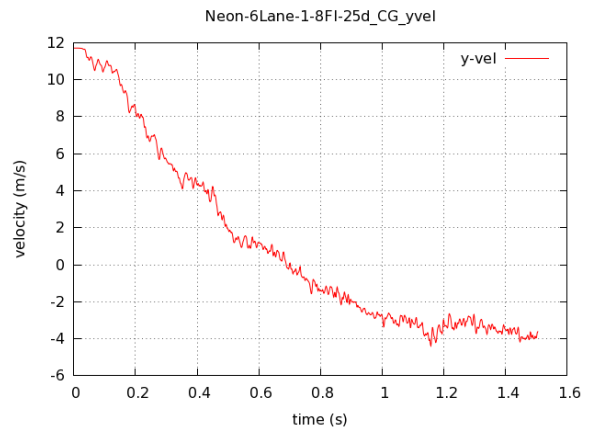
Traversal displacement at a 20° departure angle



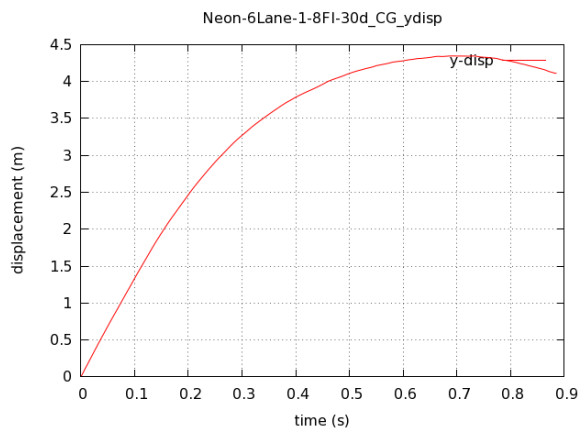
Traversal velocity at a 20° departure angle



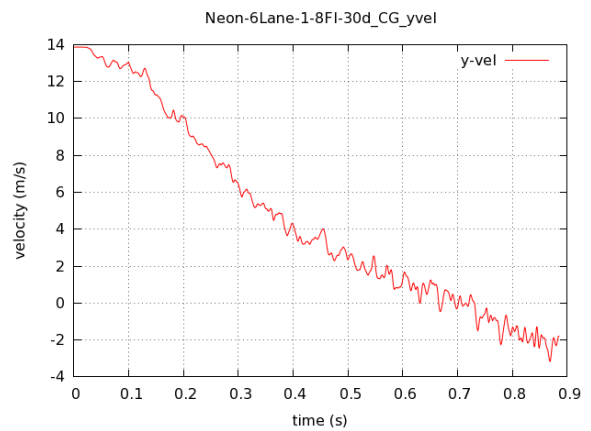
Traversal displacement at a 25° departure angle



Traversal velocity at a 25° departure angle

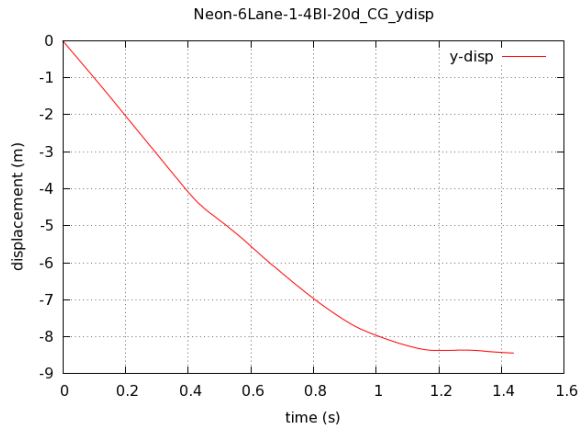


Traversal displacement at a 30° departure angle

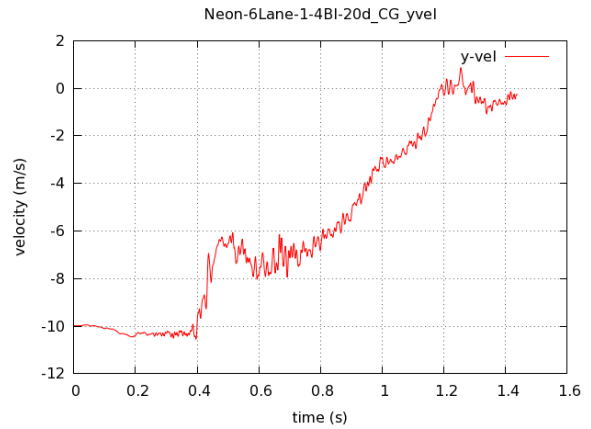


Traversal velocity at a 30° departure angle

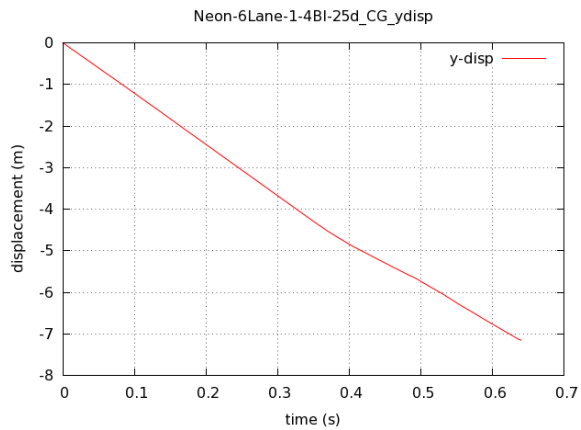
Fig. A.23: Front-side impacts by a Dodge Neon on the CMB placed at 8 ft from the median centerline on the outer 6:1 slope of a six-lane freeway



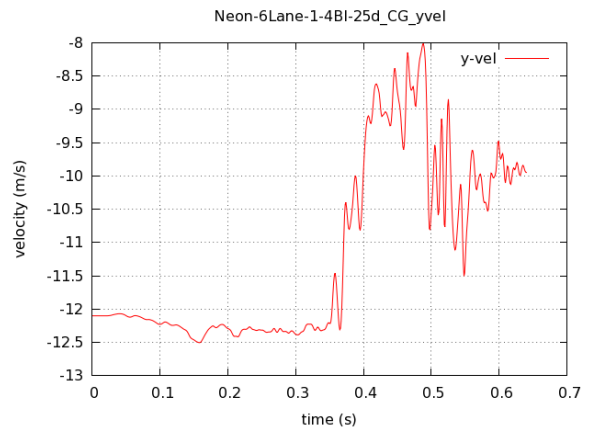
Traversal displacement at a 20° departure angle



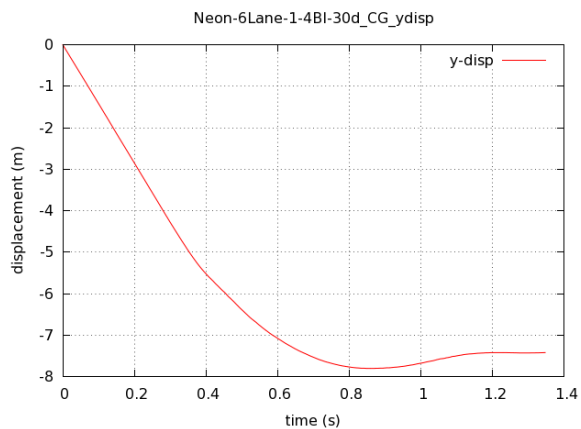
Traversal velocity at a 20° departure angle



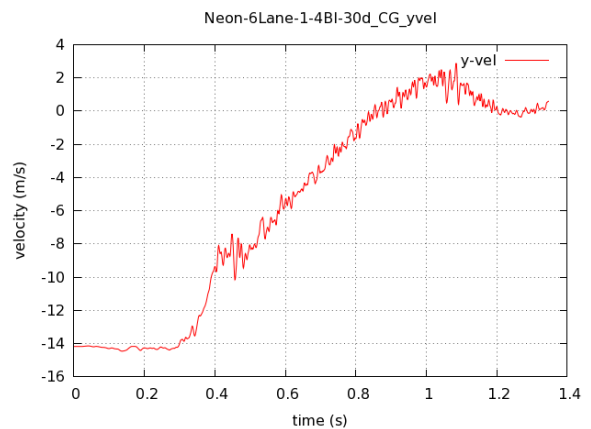
Traversal displacement at a 25° departure angle



Traversal velocity at a 25° departure angle

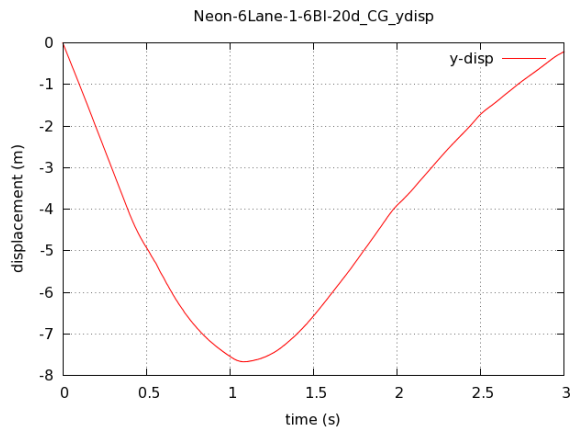


Traversal displacement at a 30° departure angle

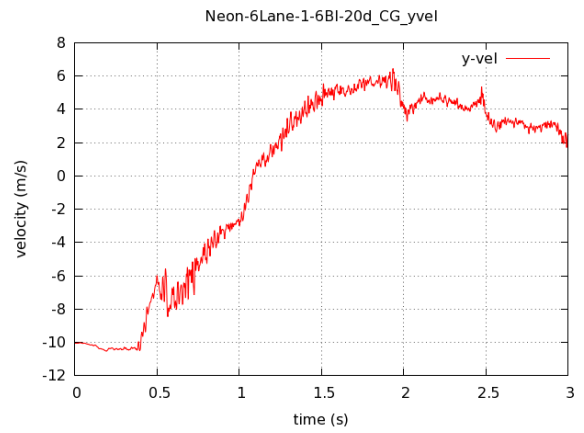


Traversal velocity at a 30° departure angle

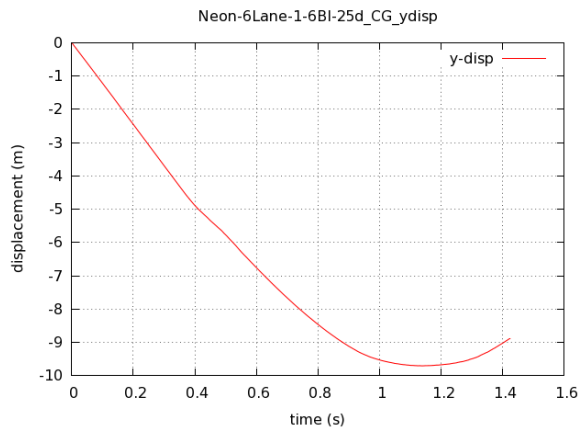
Fig. A.24: Backside impacts by a Dodge Neon on the CMB placed at 4 ft from the median centerline on the outer 6:1 slope of a six-lane freeway



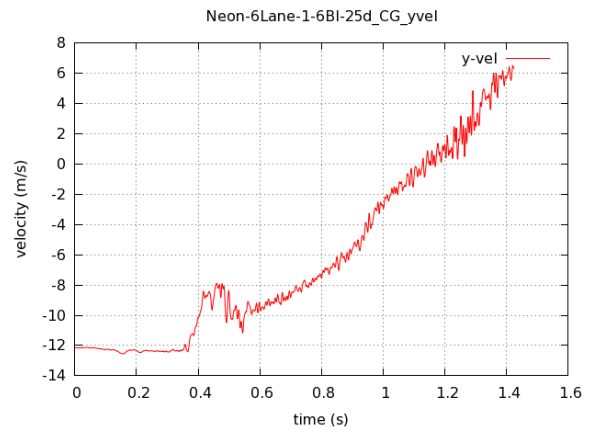
Traversal displacement at a 20° departure angle



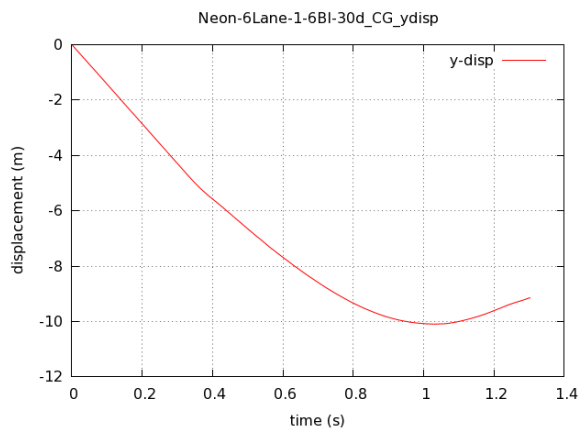
Traversal velocity at a 20° departure angle



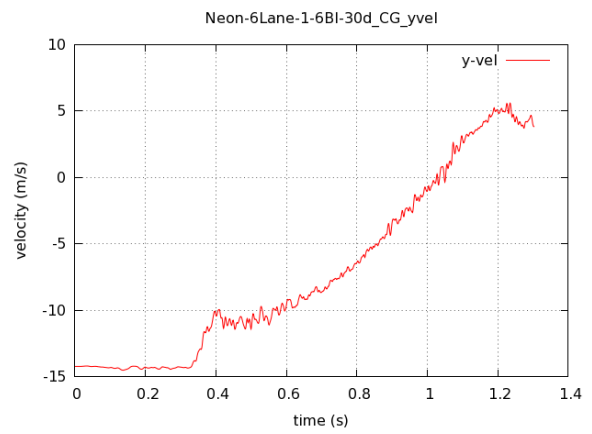
Traversal displacement at a 25° departure angle



Traversal velocity at a 25° departure angle

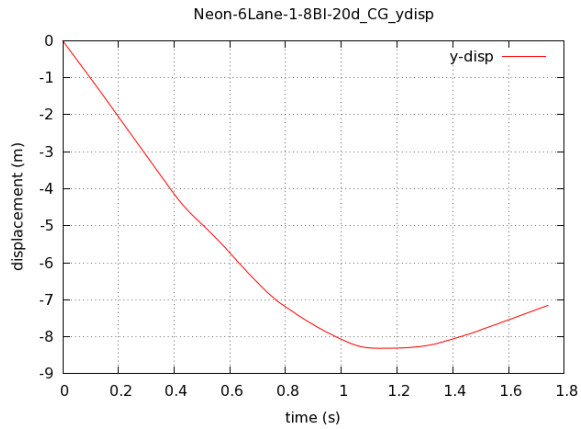


Traversal displacement at a 30° departure angle

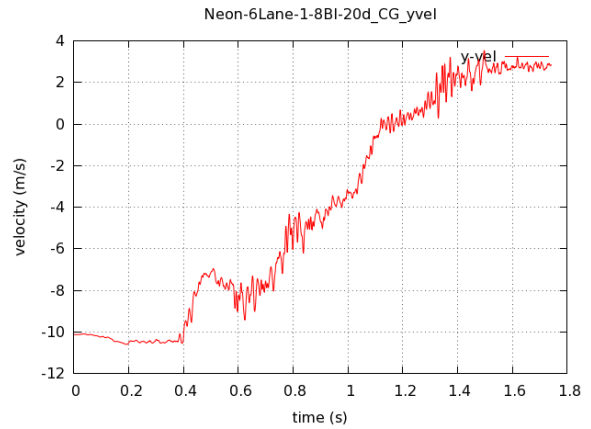


Traversal velocity at a 30° departure angle

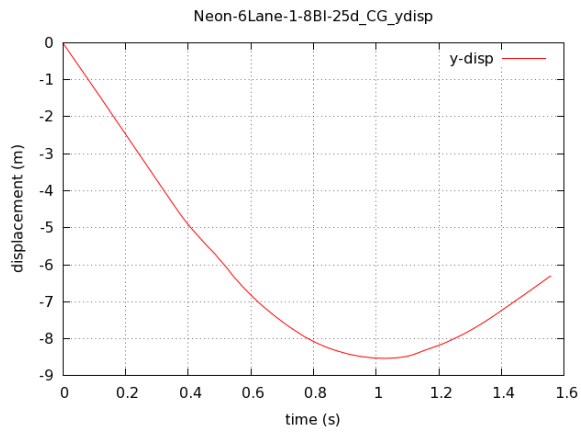
Fig. A.25: Backside impacts by a Dodge Neon on the CMB placed at 6 ft from the median centerline on the outer 6:1 slope of a six-lane freeway



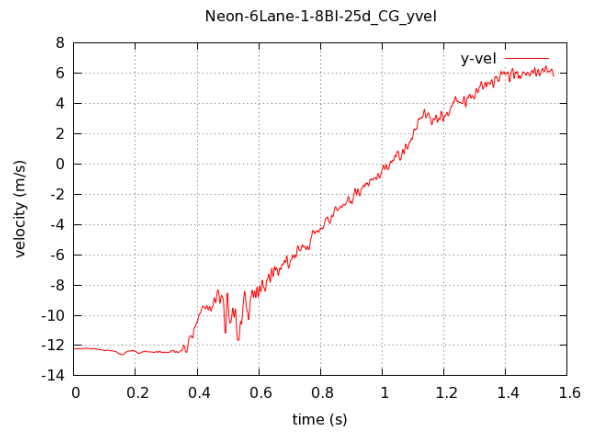
Traversal displacement at a 20° departure angle



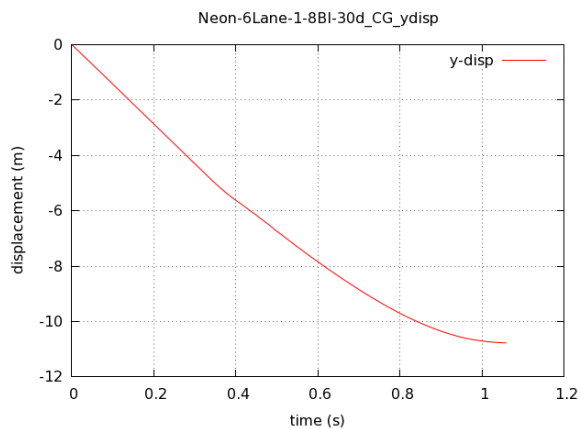
Traversal velocity at a 20° departure angle



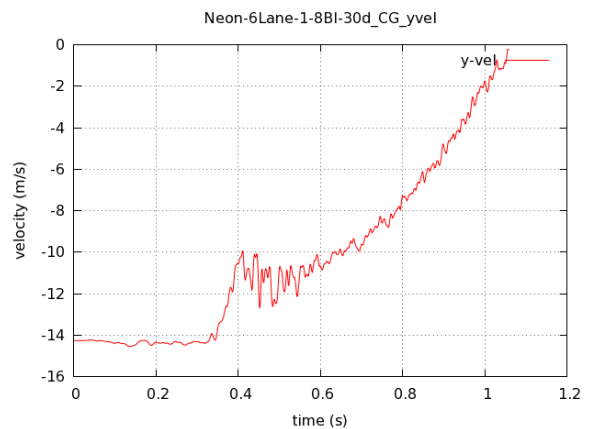
Traversal displacement at a 25° departure angle



Traversal velocity at a 25° departure angle

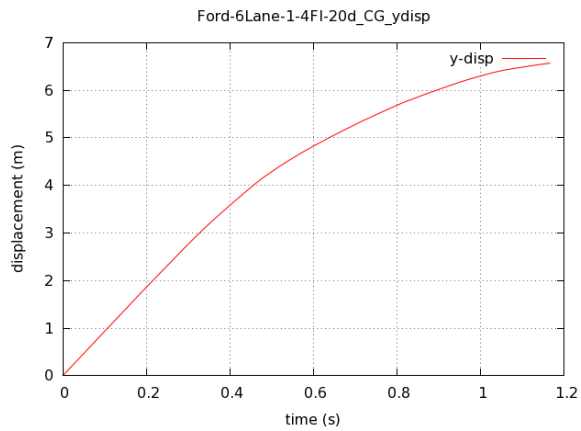


Traversal displacement at a 30° departure angle

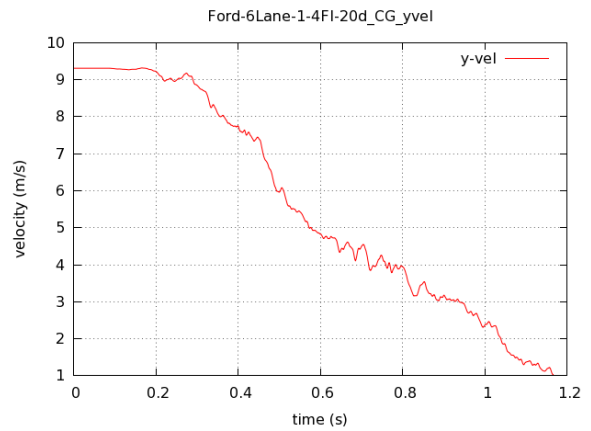


Traversal velocity at a 30° departure angle

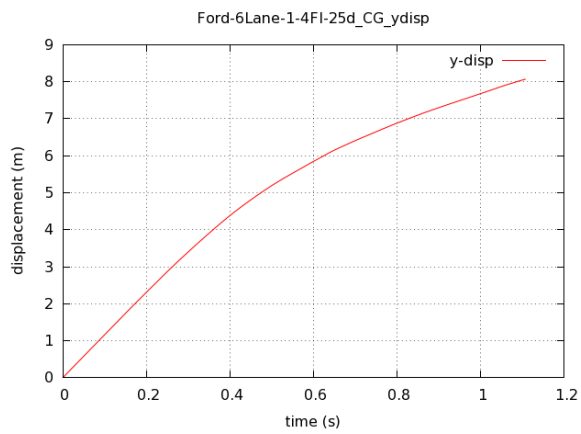
Fig. A.26: Backside impacts by a Dodge Neon on the CMB placed at 8 ft from the median centerline on the outer 6:1 slope of a six-lane freeway



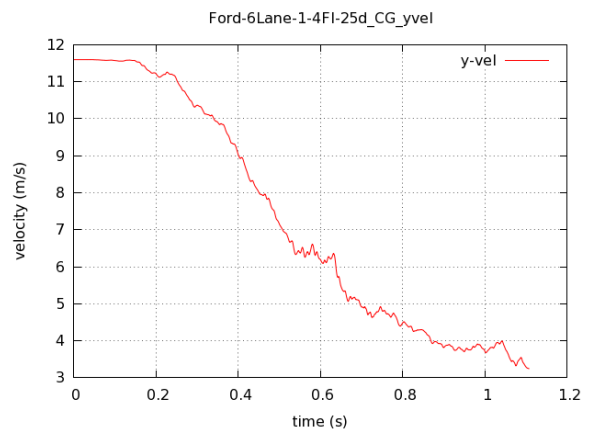
Traversal displacement at a 20° departure angle



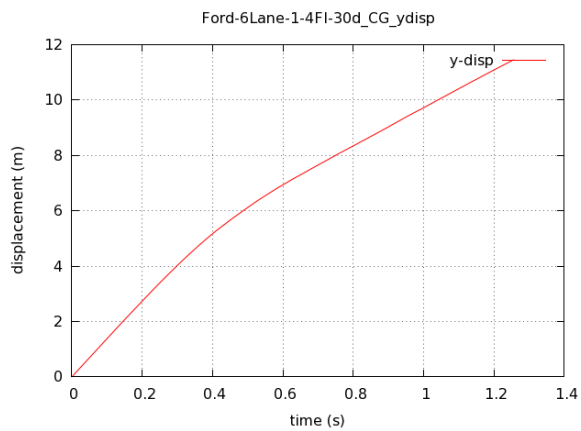
Traversal velocity at a 20° departure angle



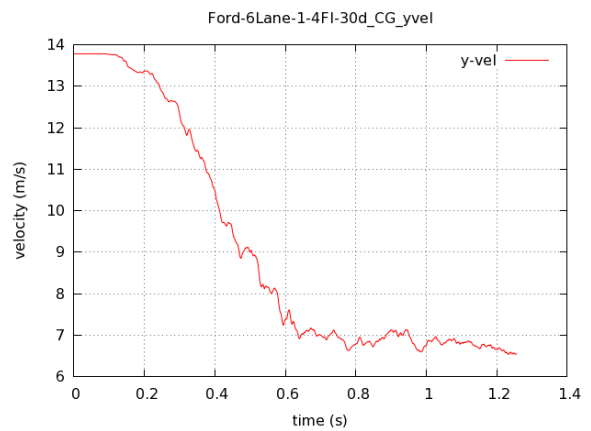
Traversal displacement at a 25° departure angle



Traversal velocity at a 25° departure angle

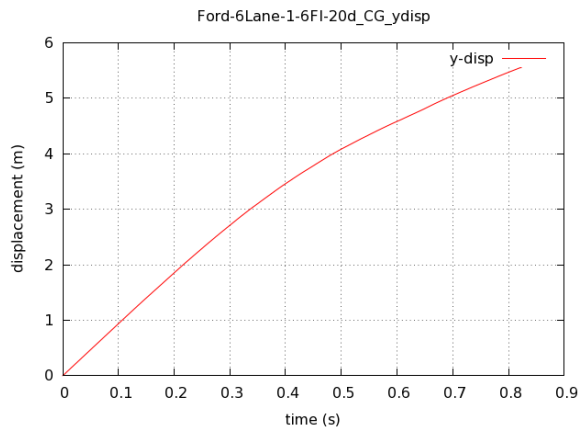


Traversal displacement at a 30° departure angle

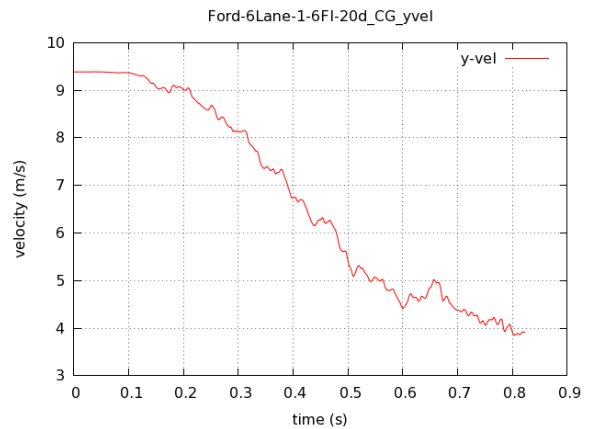


Traversal velocity at a 30° departure angle

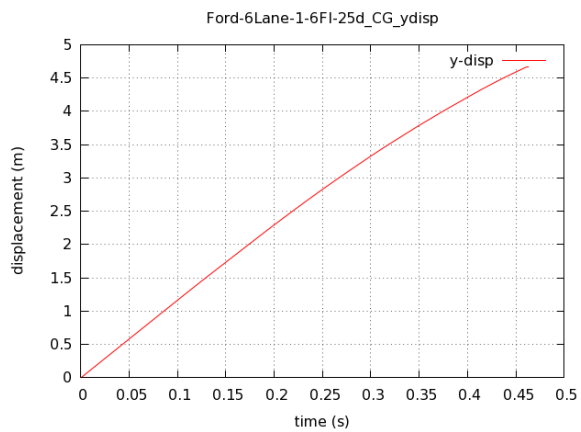
Fig. A.27: Front-side impacts by a Ford F250 on the CMB placed at 4 ft from the median centerline on the outer 6:1 slope of a six-lane freeway



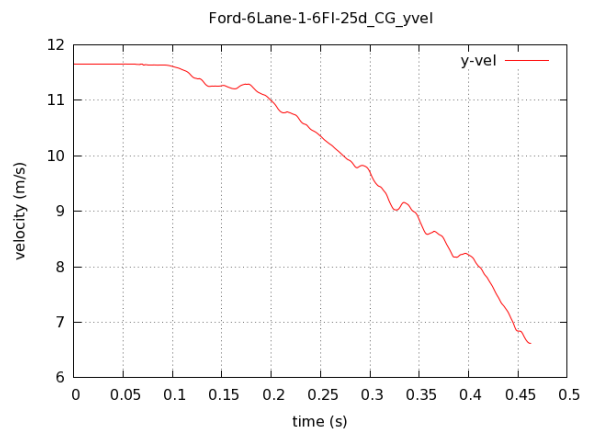
Traversal displacement at a 20° departure angle



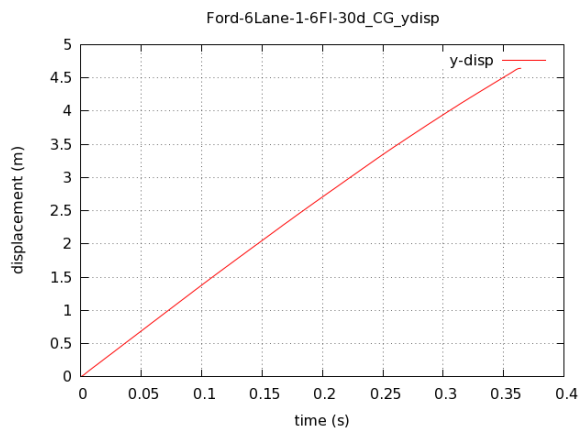
Traversal velocity at a 20° departure angle



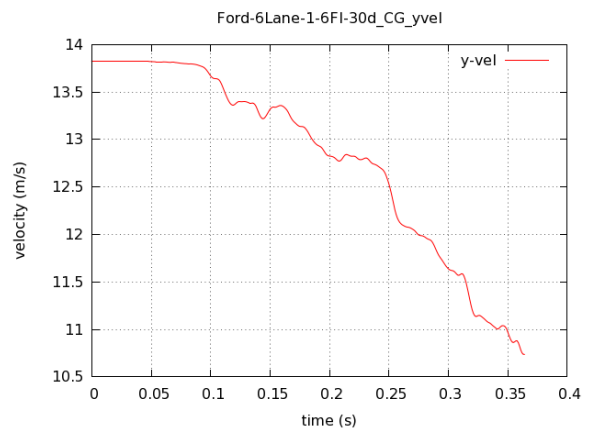
Traversal displacement at a 25° departure angle



Traversal velocity at a 25° departure angle

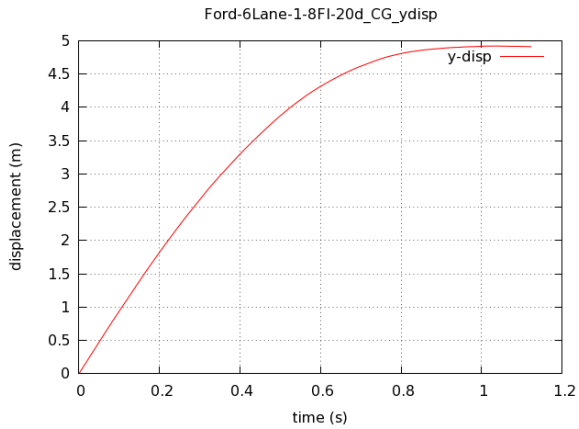


Traversal displacement at a 30° departure angle

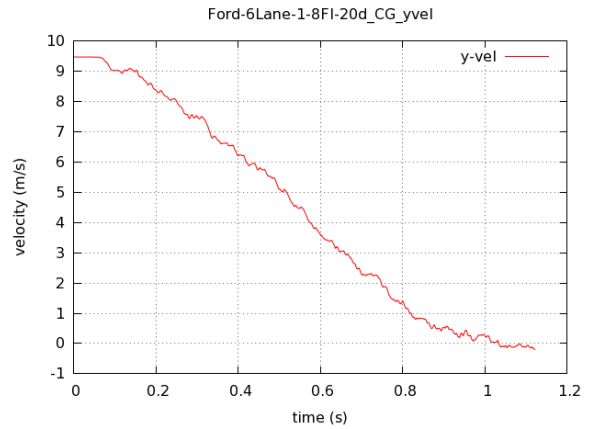


Traversal velocity at a 30° departure angle

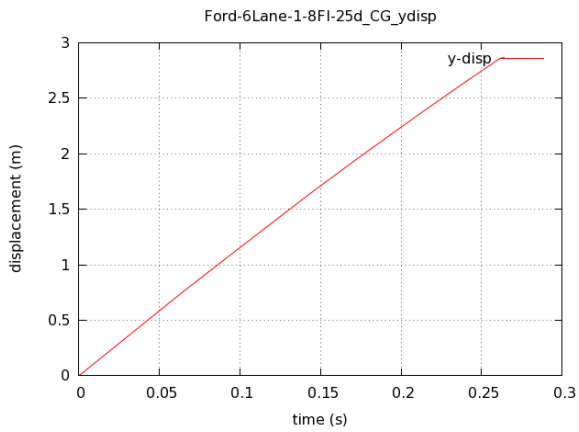
Fig. A.28: Front-side impacts by a Ford F250 on the CMB placed at 6 ft from the median centerline on the outer 6:1 slope of a six-lane freeway



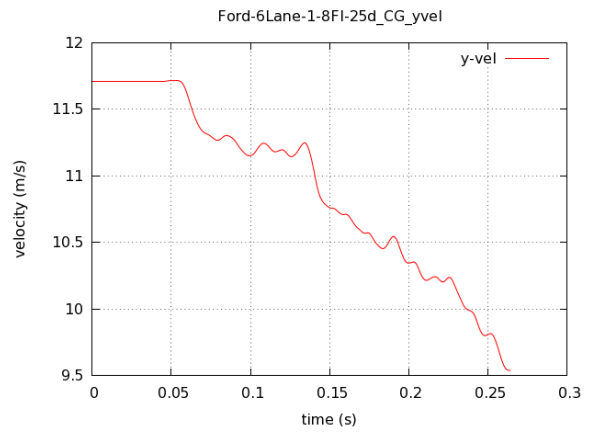
Traversal displacement at a 20° departure angle



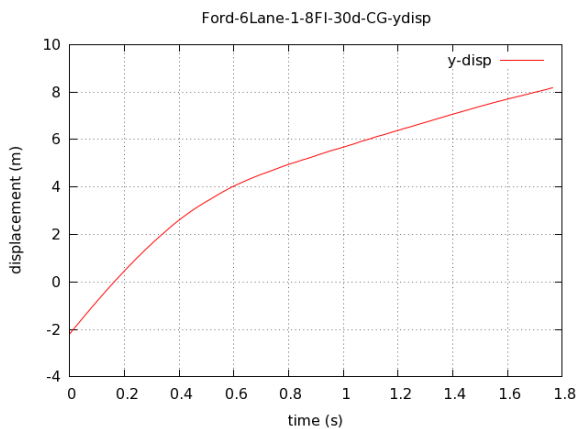
Traversal velocity at a 20° departure angle



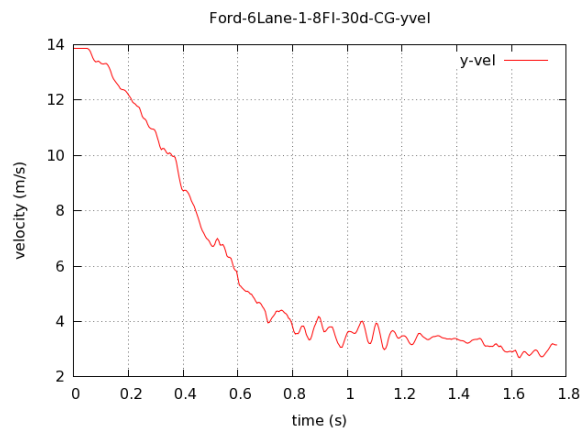
Traversal displacement at a 25° departure angle



Traversal velocity at a 25° departure angle

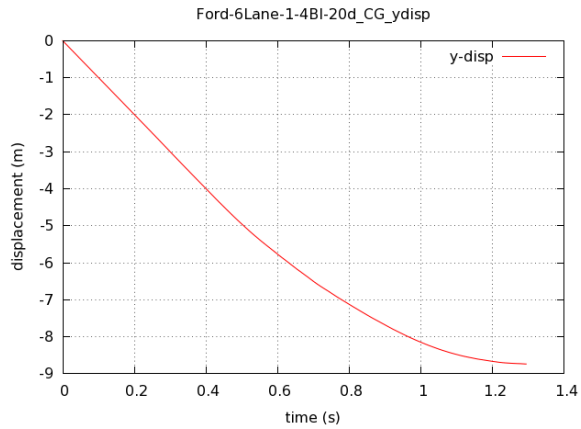


Traversal displacement at a 30° departure angle

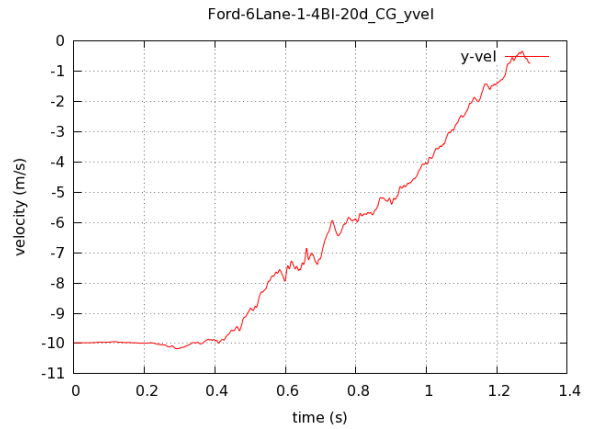


Traversal velocity at a 30° departure angle

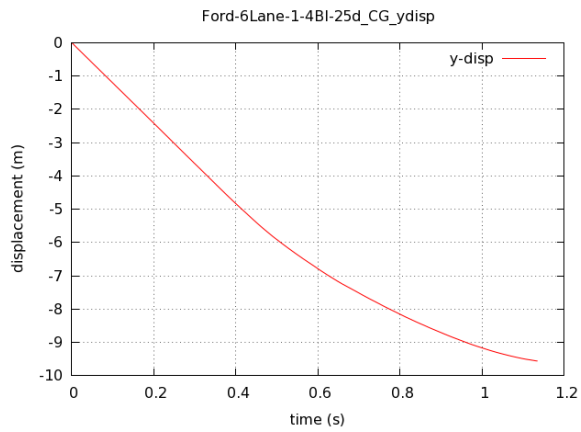
Fig. A.29: Front-side impacts by a Ford F250 on the CMB placed at 8 ft from the median centerline on the outer 6:1 slope of a six-lane freeway



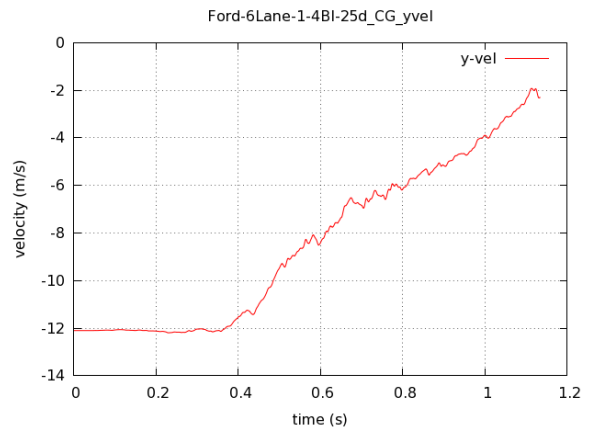
Traversal displacement at a 20° departure angle



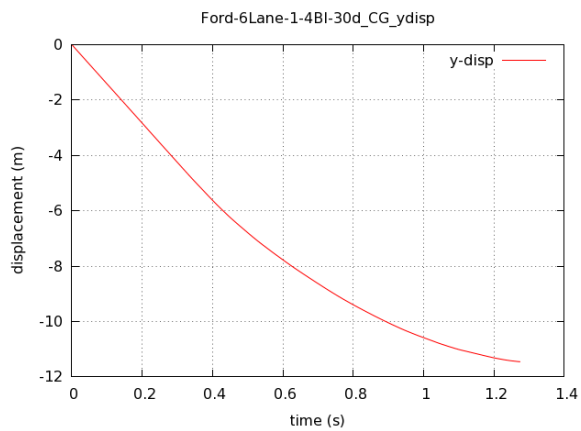
Traversal velocity at a 20° departure angle



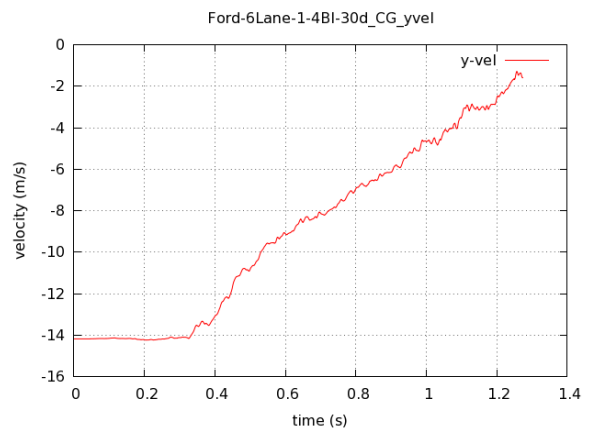
Traversal displacement at a 25° departure angle



Traversal velocity at a 25° departure angle

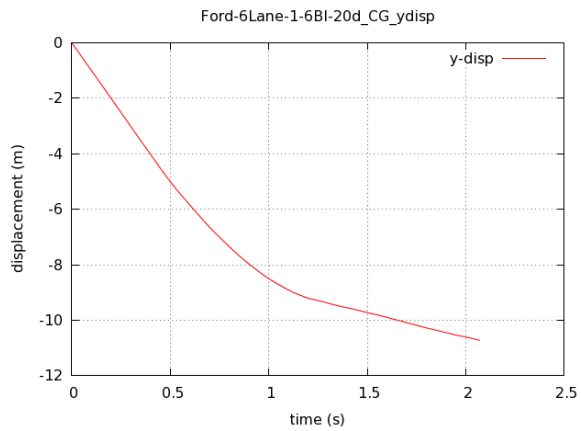


Traversal displacement at a 30° departure angle

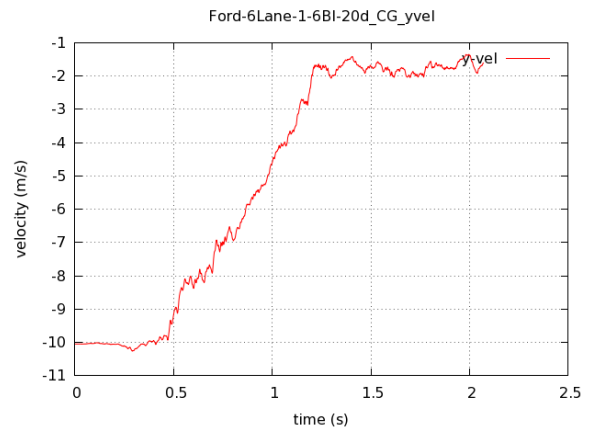


Traversal velocity at a 30° departure angle

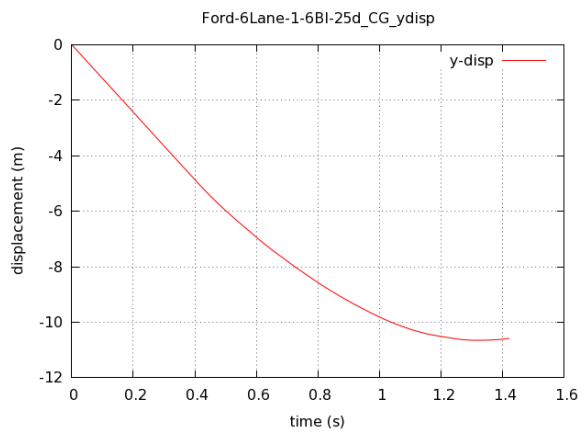
Fig. A.30: Backside impacts by a Ford F250 on the CMB placed at 4 ft from the median centerline on the outer 6:1 slope of a six-lane freeway



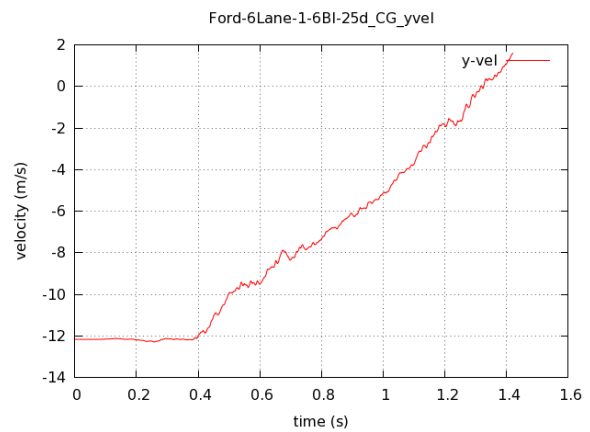
Traversal displacement at a 20° departure angle



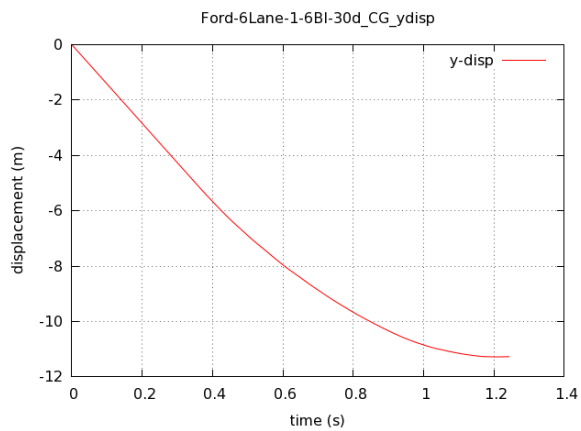
Traversal velocity at a 20° departure angle



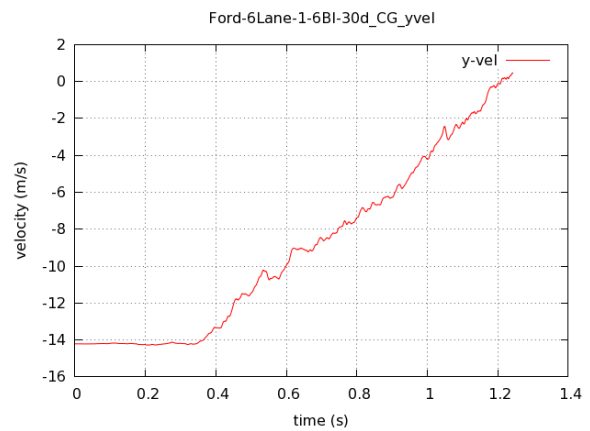
Traversal displacement at a 25° departure angle



Traversal velocity at a 25° departure angle

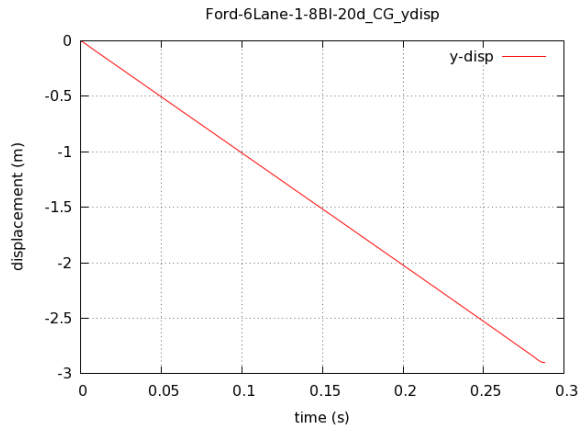


Traversal displacement at a 30° departure angle

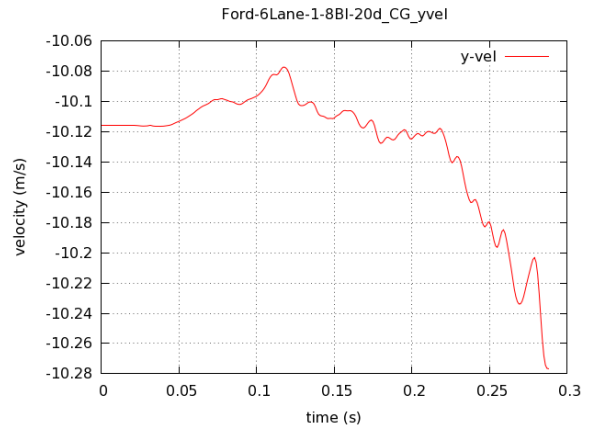


Traversal velocity at a 30° departure angle

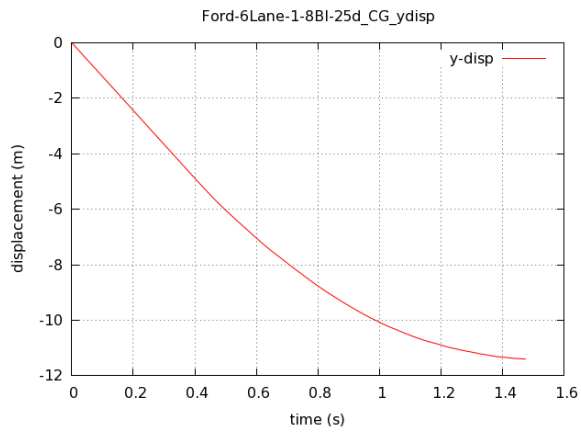
Fig. A.31: Backside impacts by a Ford F250 on the CMB placed at 6 ft from the median centerline on the outer 6:1 slope of a six-lane freeway



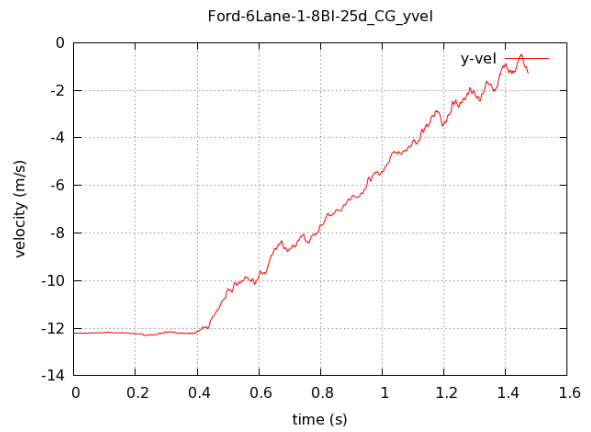
Traversal displacement at a 20° departure angle



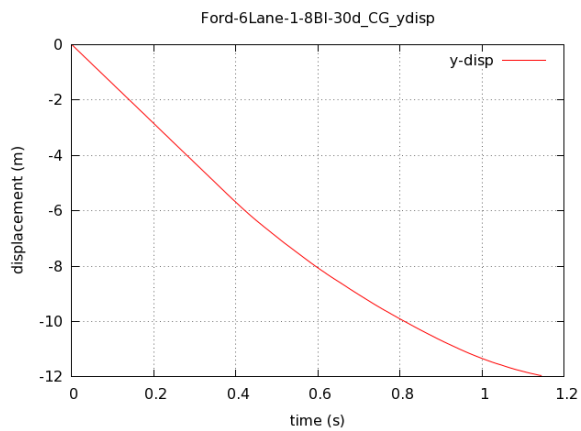
Traversal velocity at a 20° departure angle



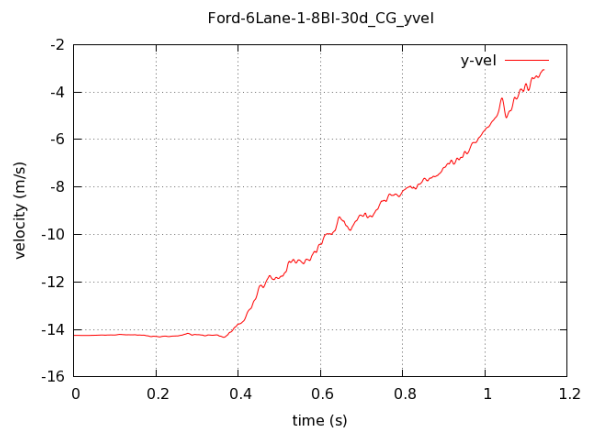
Traversal displacement at a 25° departure angle



Traversal velocity at a 25° departure angle

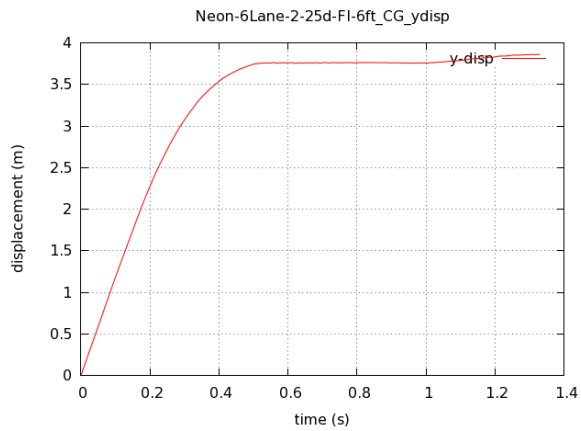


Traversal displacement at a 30° departure angle

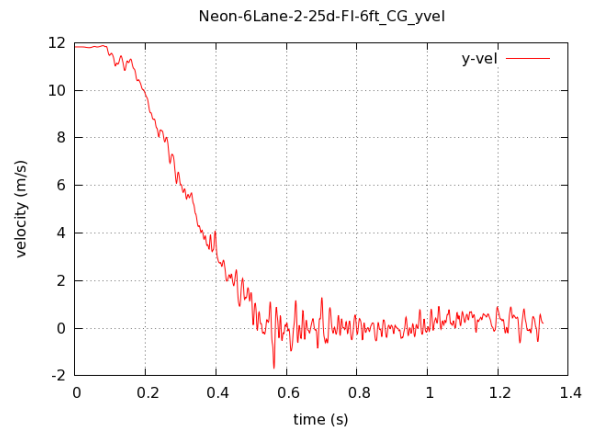


Traversal velocity at a 30° departure angle

Fig. A.32: Backside impacts by a Ford F250 on the CMB placed at 8 ft from the median centerline on the outer 6:1 slope of a six-lane freeway

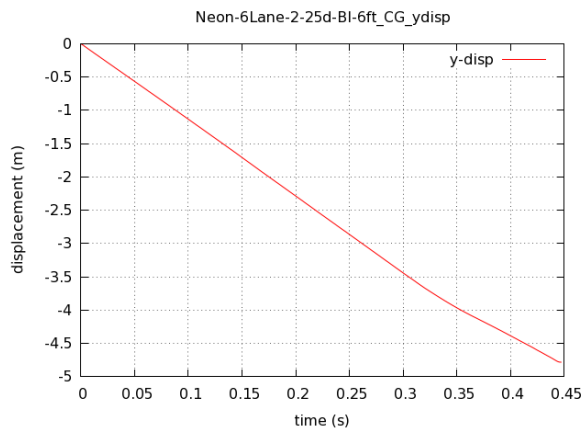


Traversal displacement at a 25° departure angle

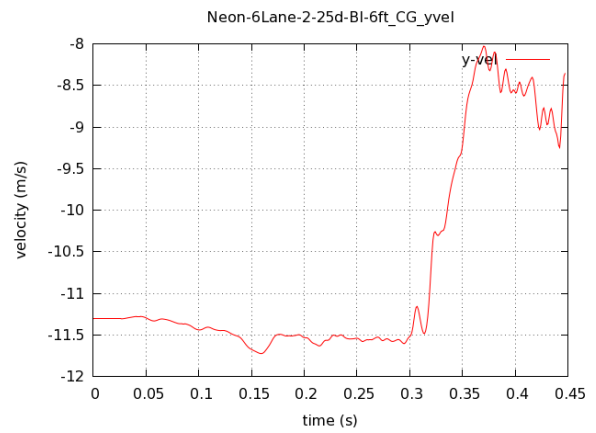


Traversal velocity at a 25° departure angle

Fig. A.33: Front-side impact by a Dodge Neon on the CMB placed at 6 ft from the median centerline on the inner 4:1 slope of a six-lane freeway

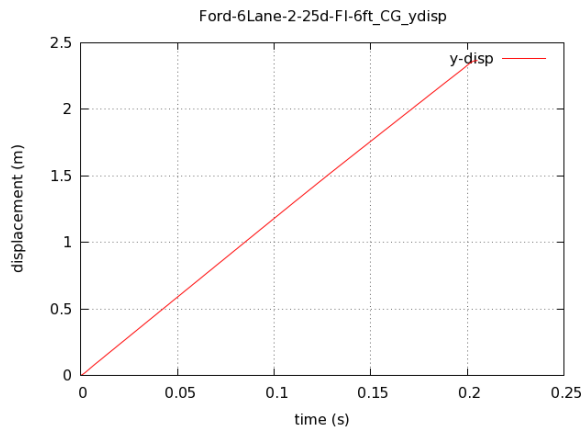


Traversal displacement at a 25° departure angle

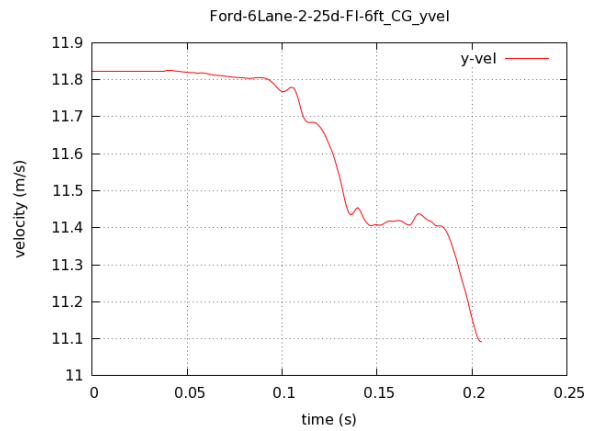


Traversal velocity at a 25° departure angle

Fig. A.34: Backside impact by a Dodge Neon on the CMB placed at 6 ft from the median centerline on the inner 4:1 slope of a six-lane freeway

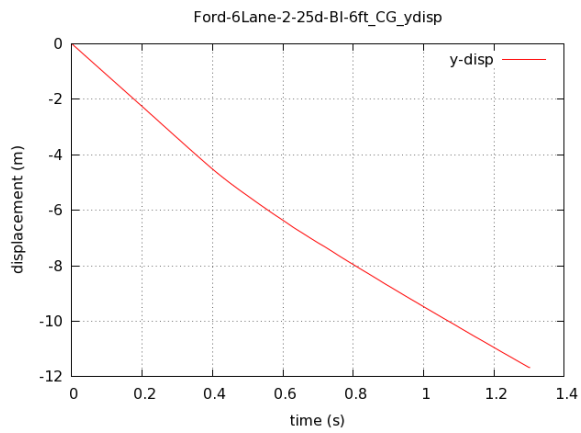


Traversal displacement at a 25° departure angle

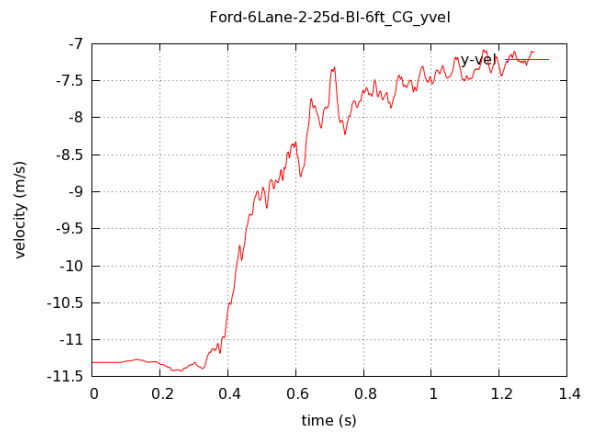


Traversal velocity at a 25° departure angle

Fig. A.35: Front-side impact by a Ford F250 on the CMB placed at 6 ft from the median centerline on the inner 4:1 slope of a six-lane freeway



Traversal displacement at a 25° departure angle



Traversal velocity at a 25° departure angle

Fig. A.36: Backside impact by a Ford F250 on the CMB placed at 6 ft from the median centerline on the inner 4:1 slope of a six-lane freeway